

**CHAPTER III**

RESULTS  
**AND**  
DISCUSSION

### **3. RESULTS AND DISCUSSION**

This chapter includes the results of the different investigations, and their discussion. In this respect, humic materials are separated, purified and characterized. The samples of humic materials comprise: soil humic acid (SHA), Ismailia canal humic acid (ICHA) and its fractions; gray HA (GHA) and brown HA (BHA); humin (Hn) and peat fulvic acid.

The sorption and complexation characteristics of humin, humic acid and fulvic acid were identified by studying the essential parameters, which include the effect of shaking time, the weight or concentration of humic material, the metal ion concentration and the effect of some competing cations.

#### **3.1 Characterization of Humic Materials:**

The characterization of humic materials by different methods has provided valuable information on the nature and characterization of humic substances. In this concern, the elemental composition was determined by ultimate analysis, the carboxylate capacities were determined by acid–base titration. The spectroscopic characteristics were studied by infrared and UV-visible spectroscopies.

##### **3.1.1 Ultimate analysis:**

Ultimate analysis is one of the most essential characteristics, which can be used to establish the nature and source of humic substances. Ultimate analysis of humic materials does not provide an absolute molecular formula since most humic preparations are mixtures of many components, but it does provide general compositional information. As more highly refined humic substances are produced, the ultimate analysis data will become more important in establishing the molecular formula information, the processing efficiency, the purity of humic preparations and understanding the geochemistry of these substances.

The elemental composition of the investigated humic substances is shown in Table (3.1). It is clear from the table that the major elements in humic substances are carbon and oxygen. Fulvic acid has lower carbon (C) but higher oxygen (O) content, while humin has higher C and lower O than humic acid. The data indicate that the humic materials have nearly identical elemental composition.

The simplest way to display information about the elemental composition of humic substances is to use atomic ratios. In table (3.2) the atomic ratios for the investigated humic materials are listed. The O/C ratios of humic acid samples cluster around 0.6 while fulvic acid has a higher ratio (0.7) and humin has a lower ratio (~0.5). The obtained ratios are almost similar to those reported <sup>[74]</sup> with slightly higher ratios for humic acid samples, which indicate a higher carbohydrate content. The H/C ratios are clustered around 1.0 for humic and fulvic acid samples. The ratio in case of humin is higher (1.3), which indicates a lower degree of unsaturation and a higher aliphatic character in humin than in both humic and fulvic acids. The obtained atomic ratios of hydrogen to carbon agree with that published previously <sup>[74]</sup>.

### **3.1.2 Protonation capacity and $pK_a$ of the carboxylate groups:**

The best method for determining the acidic properties of humic materials is the potentiometric titration. The carboxylate capacity and the  $pK_a$  values provide a good way of comparing the strength and ionization of humic substances. The humic substances are polyelectrolytic compounds with different functional groups, which can donate electrons to form complexes.

Moreover the carboxylate groups are the most important functional groups in humic substances because they form the strongest complex with metal ions. In this concern, direct titration of humic materials, under investigation, were performed, and the carboxylate capacities (cation exchange capacities) were determined from the

**Table (3.2):** The atomic ratios of the investigated humic materials.

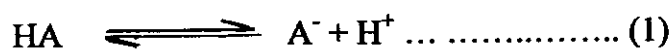
Sample	O/C	H/C
ICHA	0.56	1.12
BHA	0.61	1.16
GHA	0.61	1.02
SHA	0.60	1.13
PFA	0.70	1.01
Hn	0.46	1.31

maxima of the first derivatives of the titration curves, which allowed to calculate the  $pK_a$  values of these groups. The  $pK_a$  values were found to be dependent on the degree of ionization ( $\alpha$ ) of the carboxylate groups. Figs (3.1-3.6) give the potentiometric titration curves of the investigated samples. The curves have two inflections and, in general, they are similar to those obtained from weak acids. The plots of the first derivatives of the titration curves are shown in figures (3.7-3.12). The two maxima of each curve indicate two different kinds of ionizing functional groups.

This phenomenon has been explained<sup>[104]</sup> by the presence of two carboxylate groups; the stronger acid group is located ortho to phenolic groups on aromatic rings, while all the other carboxylate fall in the second, weaker group. The first maxima occur at (4.00, 3.79, 4.62, 7.14, 4.32 and 0.97 meq OH / g for PFA, ICHA, BHA, GHA, SHA and humin, respectively. The total carboxylate capacities are calculated from the second maxima to be 6.00, 6.60, 7.75, 12.96, 6.97 and 5.81 meq OH/g for PFA, ICHA, BHA, GHA, SHA and humin, respectively. The first maxima occur at pH's 3.90, 5.34, 3.60, 5.30, 5.62 and 4.83 for PFA, ICHA, BHA, GHA, SHA and humin, respectively, while the second maxima occur at pH's 8.90, 9.06, 8.54, 9.58, 8.88 and 8.63, for PFA, ICHA, BHA, GHA, SHA and humin, respectively.

The carboxylate capacities of humic materials have a wide range of values depending on the source as well as the separation and purification methods of the samples. To determine the  $pK_a$  values of the samples, the following analysis is given:-

The dissociation of an acidic functional group (HA) from the humic material proceeds as:



so, the ionization constant (K) is:

$$K = [A^-][H^+] / [HA] \dots \dots \dots (2)$$

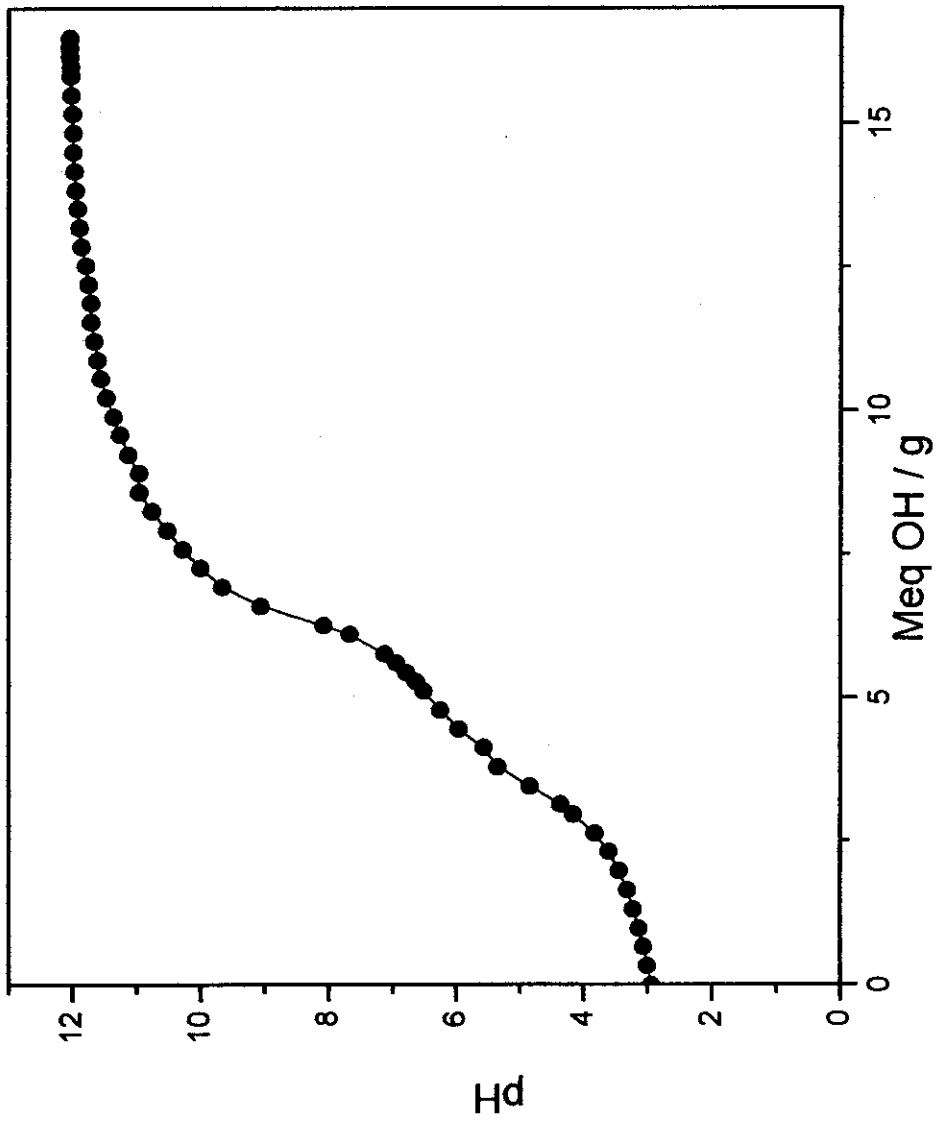


Fig. (3.1): Titration curve of Ismailia Canal humic acid.

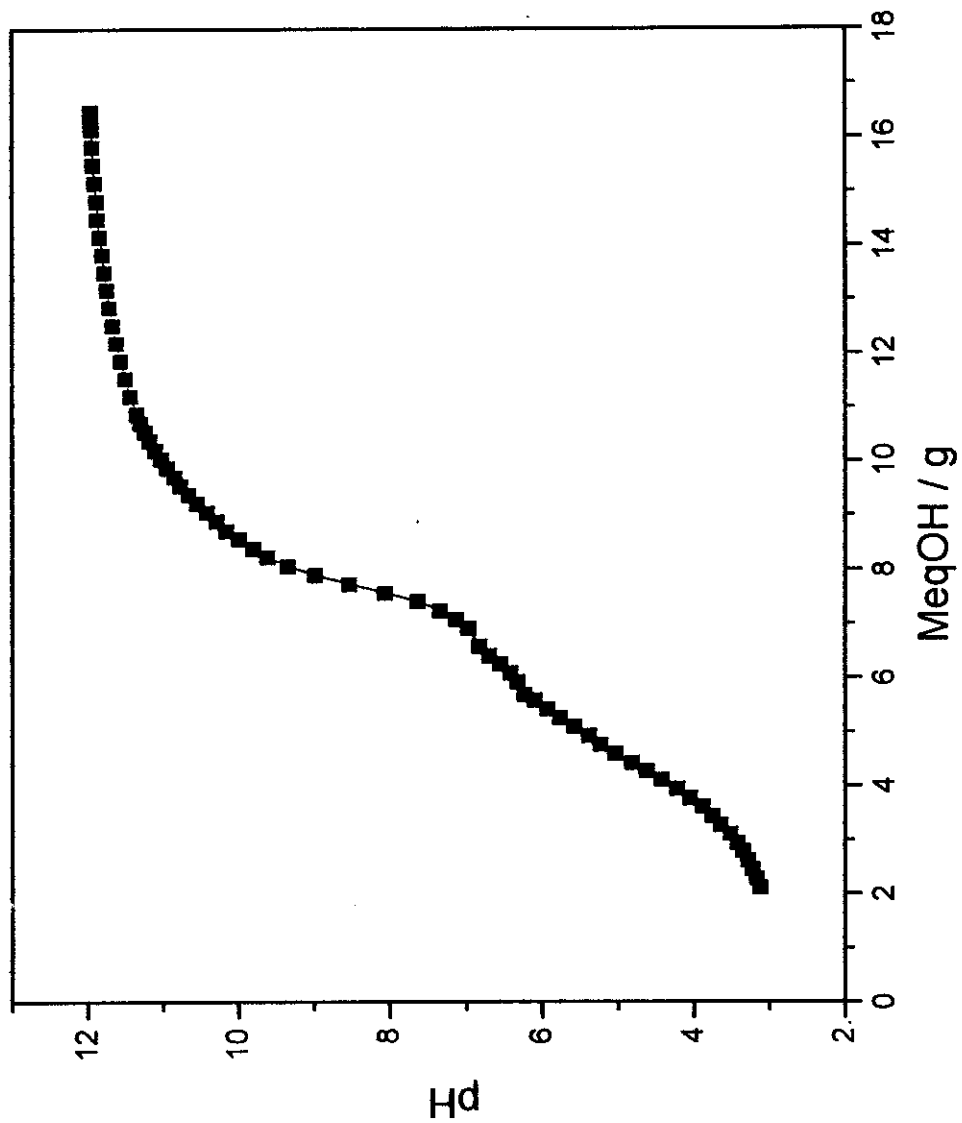


Fig. (3.2): Titration curve of brown humic acid.

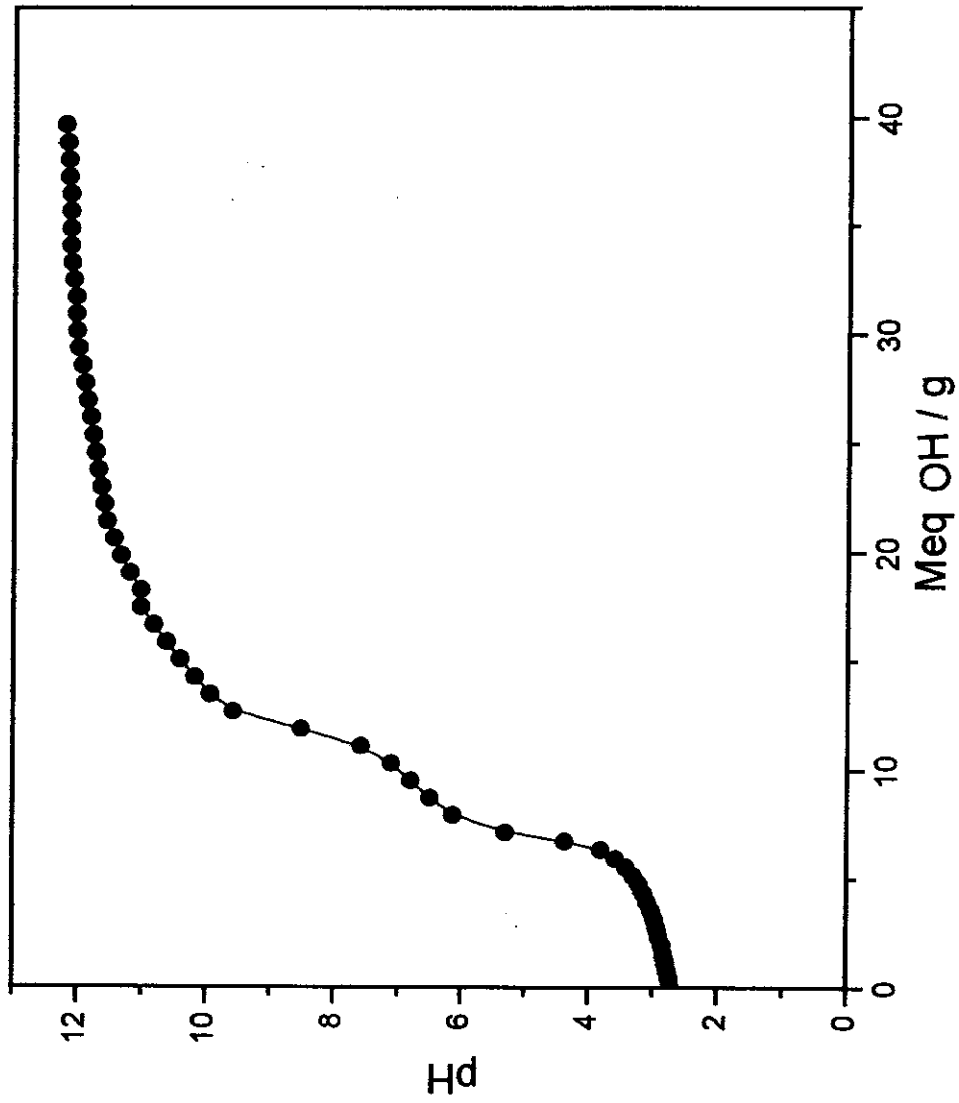


Fig (3.3): Titration curve of gray humic acid.



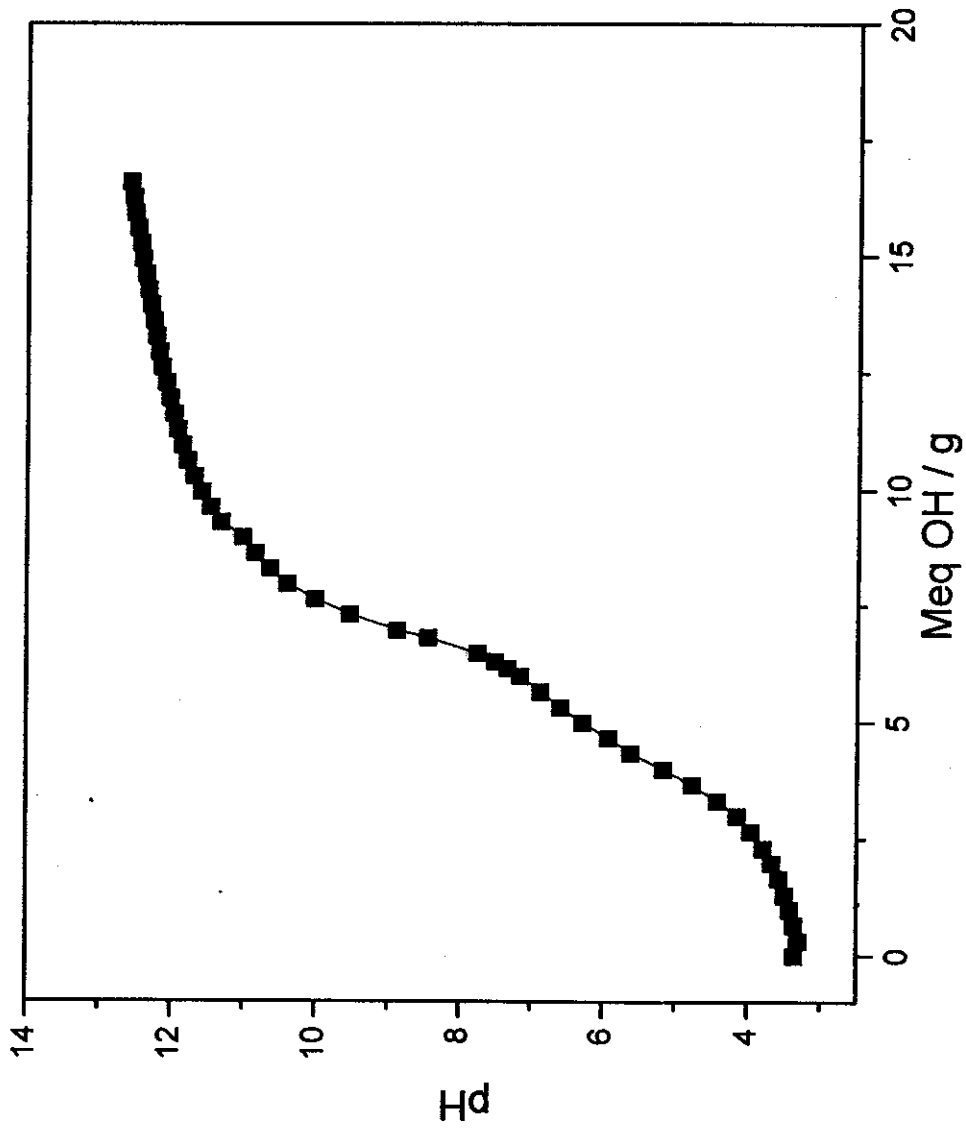


Fig (3.4): Titration curve of soil humic acid.

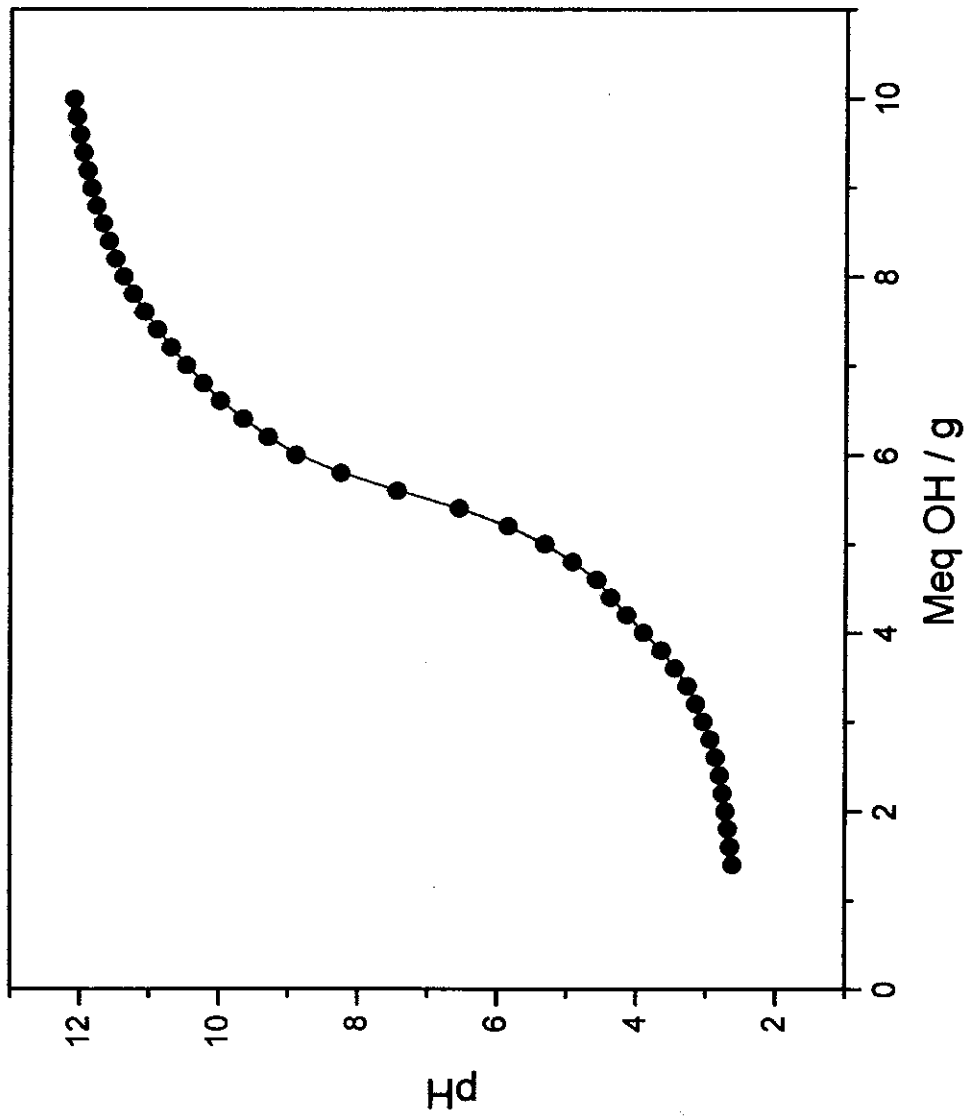


Fig (3.5 ): Titration curve of peat fulvic acid

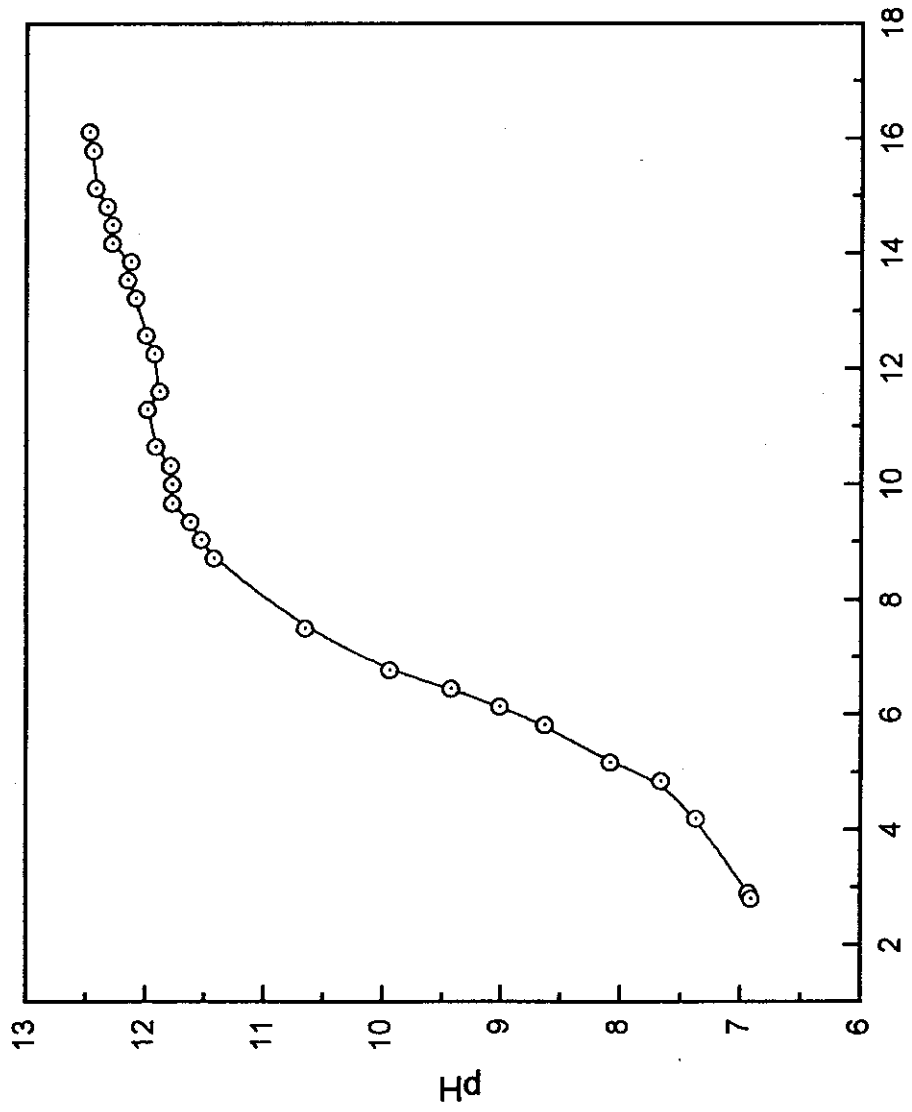


Fig ( 3.6 ) : Titration curve of humin.

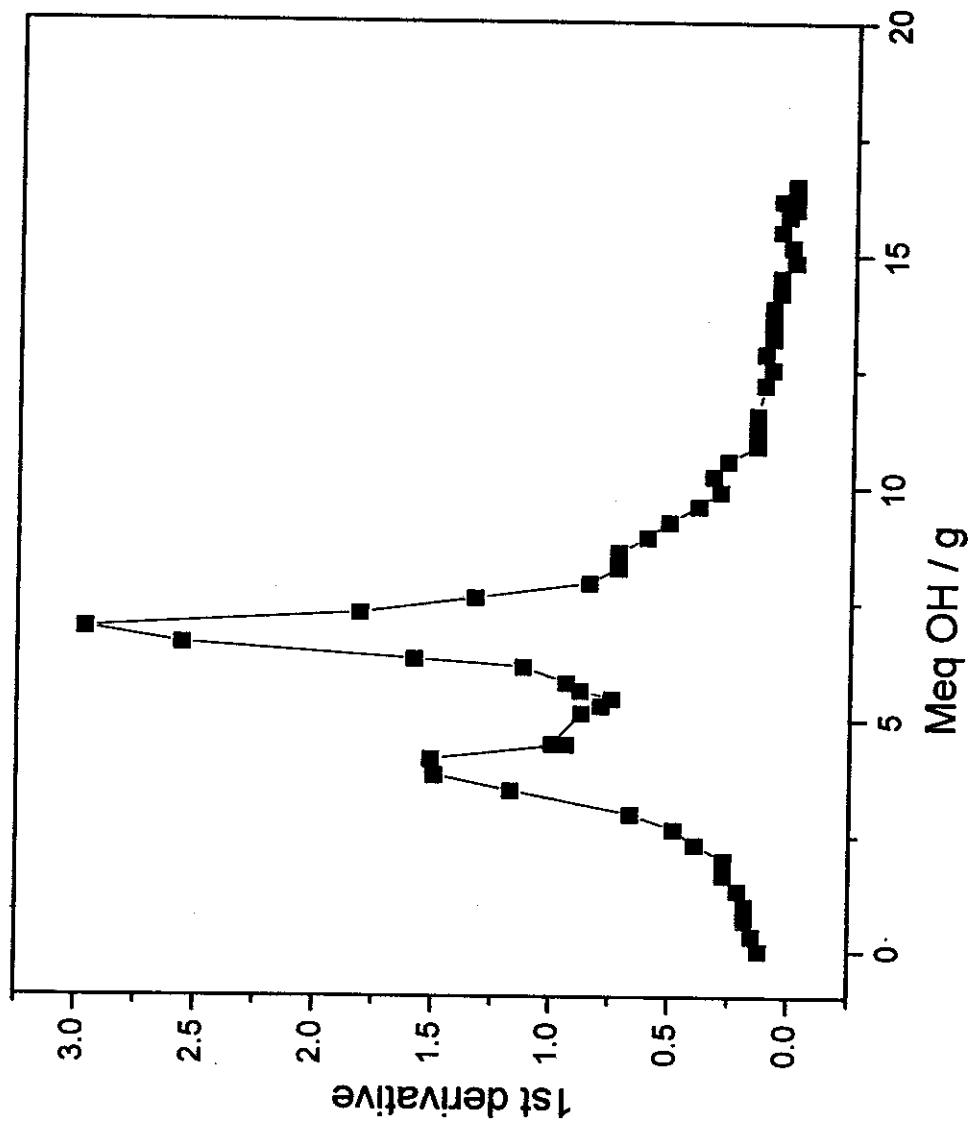


Fig (3.7): Derivative curve of Ismailia canal humic acid.

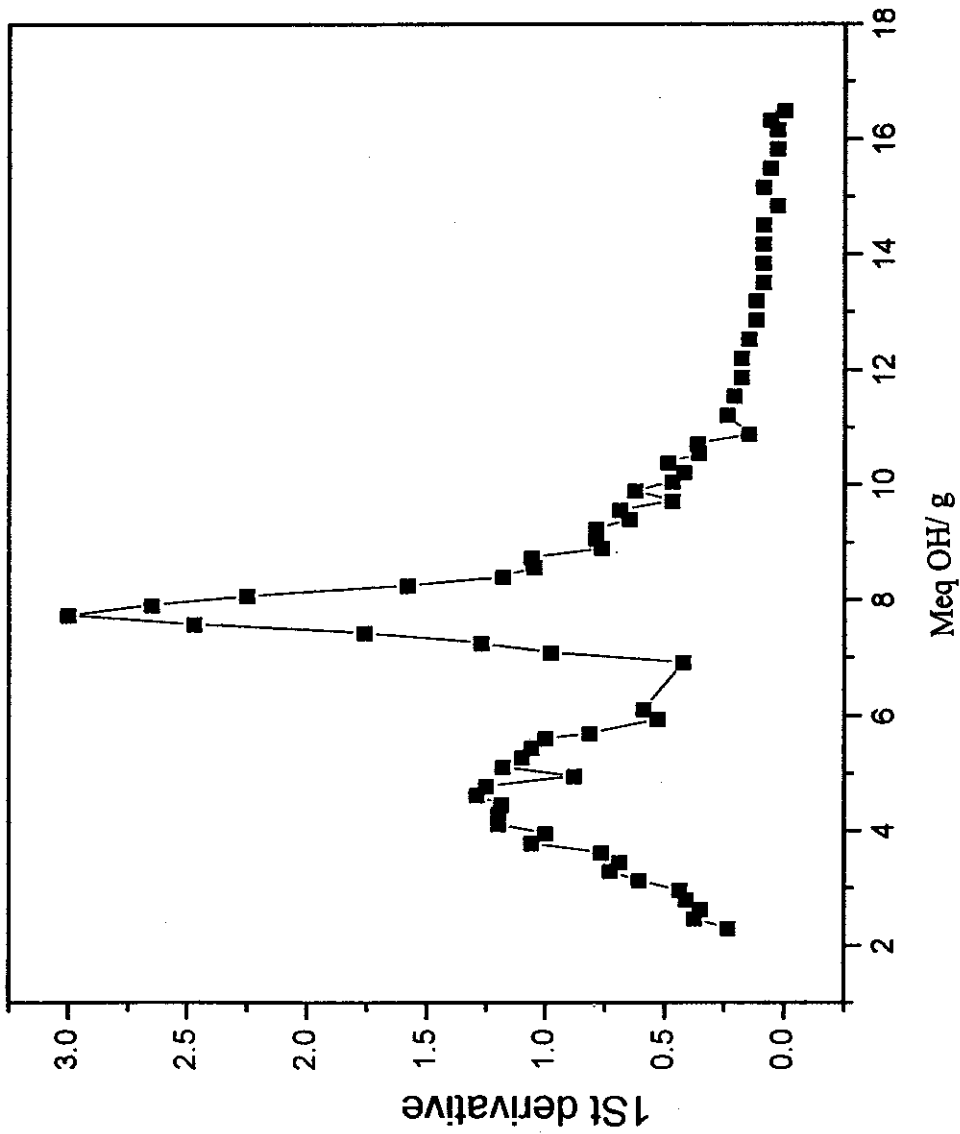


Fig (3.8): Derivative curve of brown humic acid.

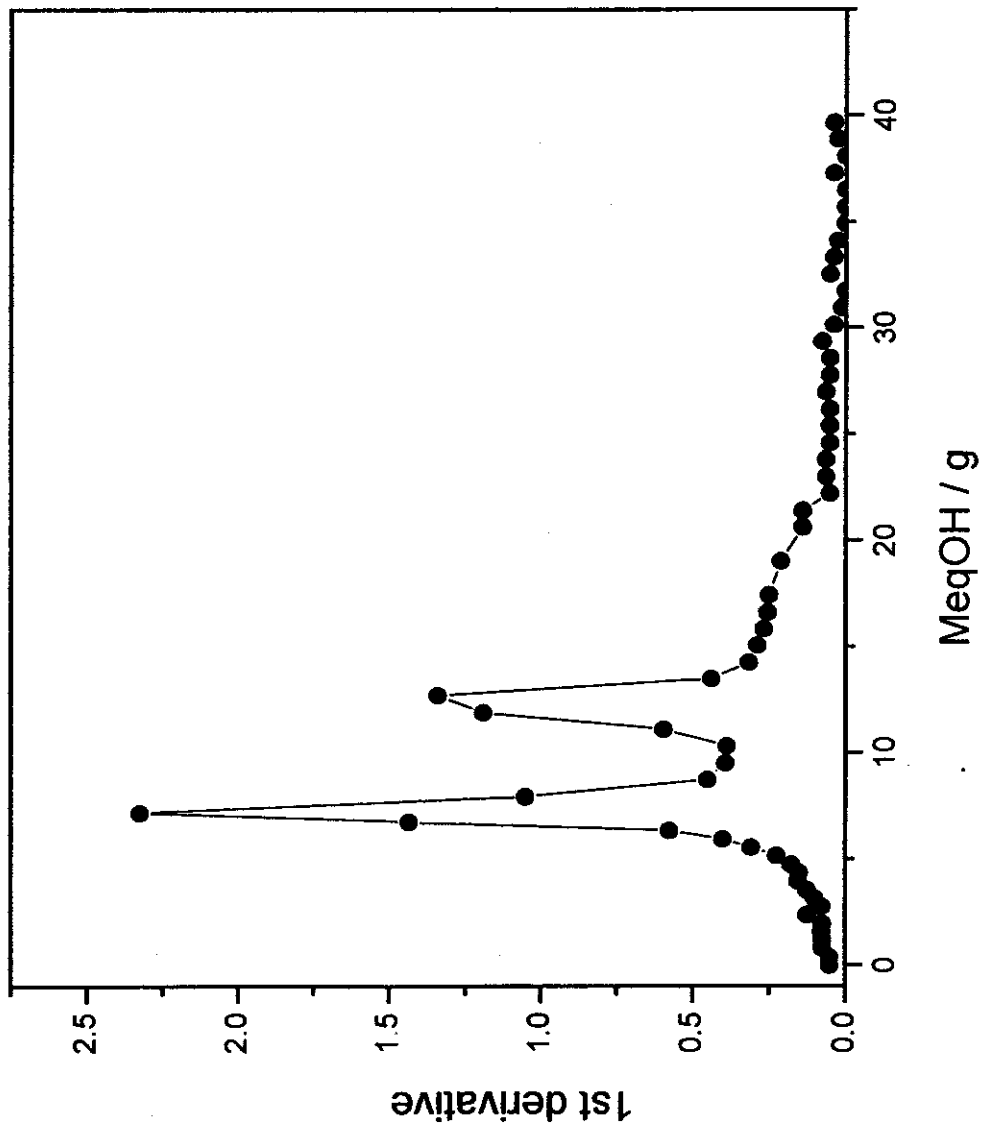


Fig. (3.9): Derivative Curve of gray humic acid.

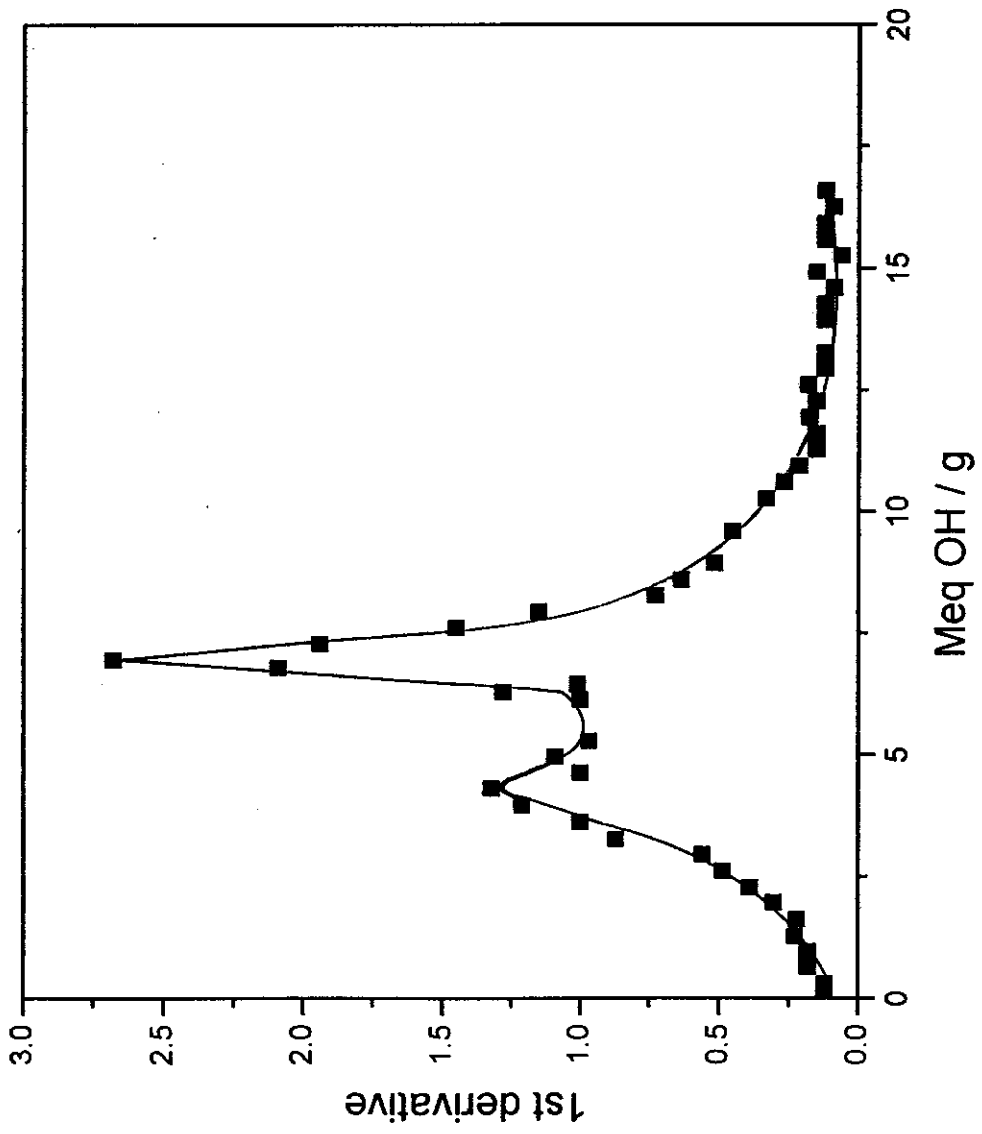


Fig. (3.10): Derivative curve of soil humic acid

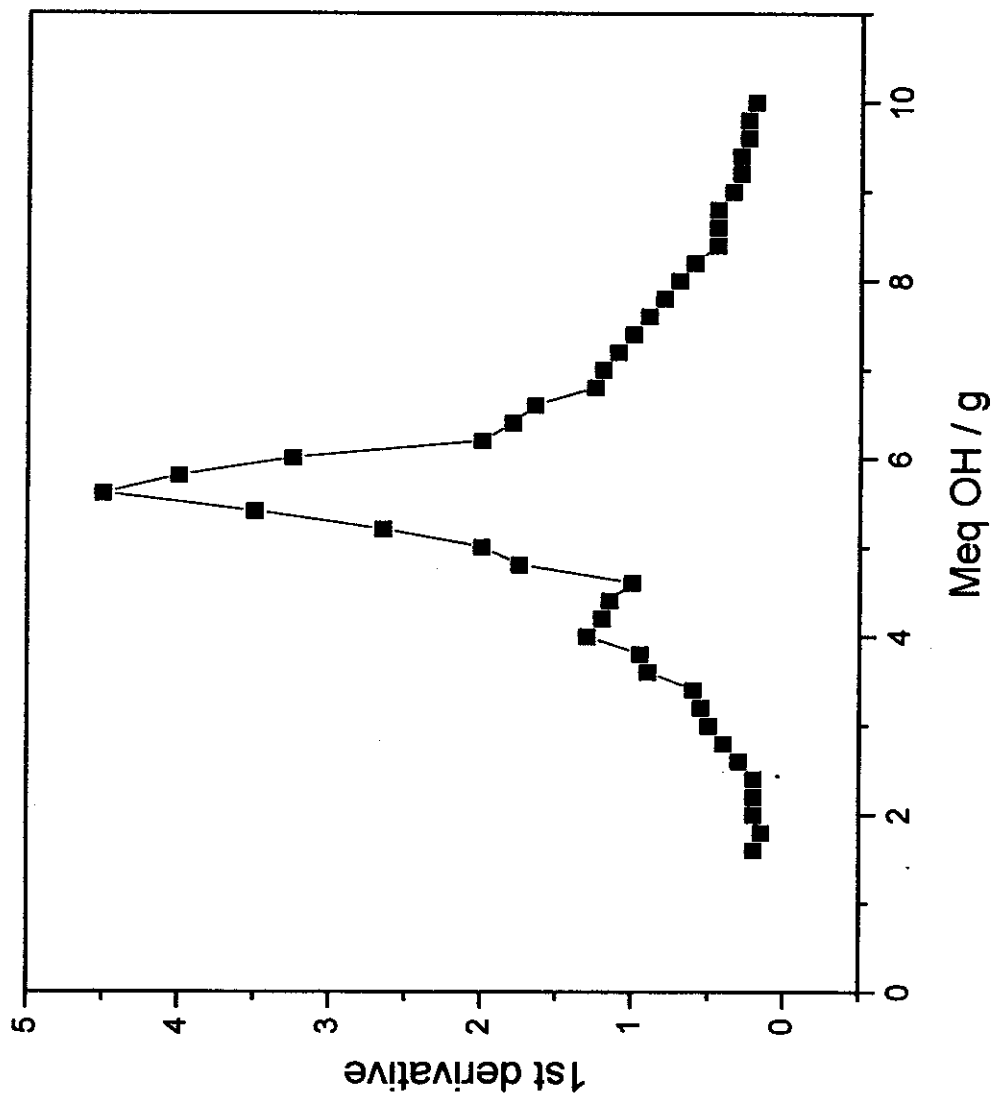


Fig (3.11): Derivative curve of peat fulvic acid



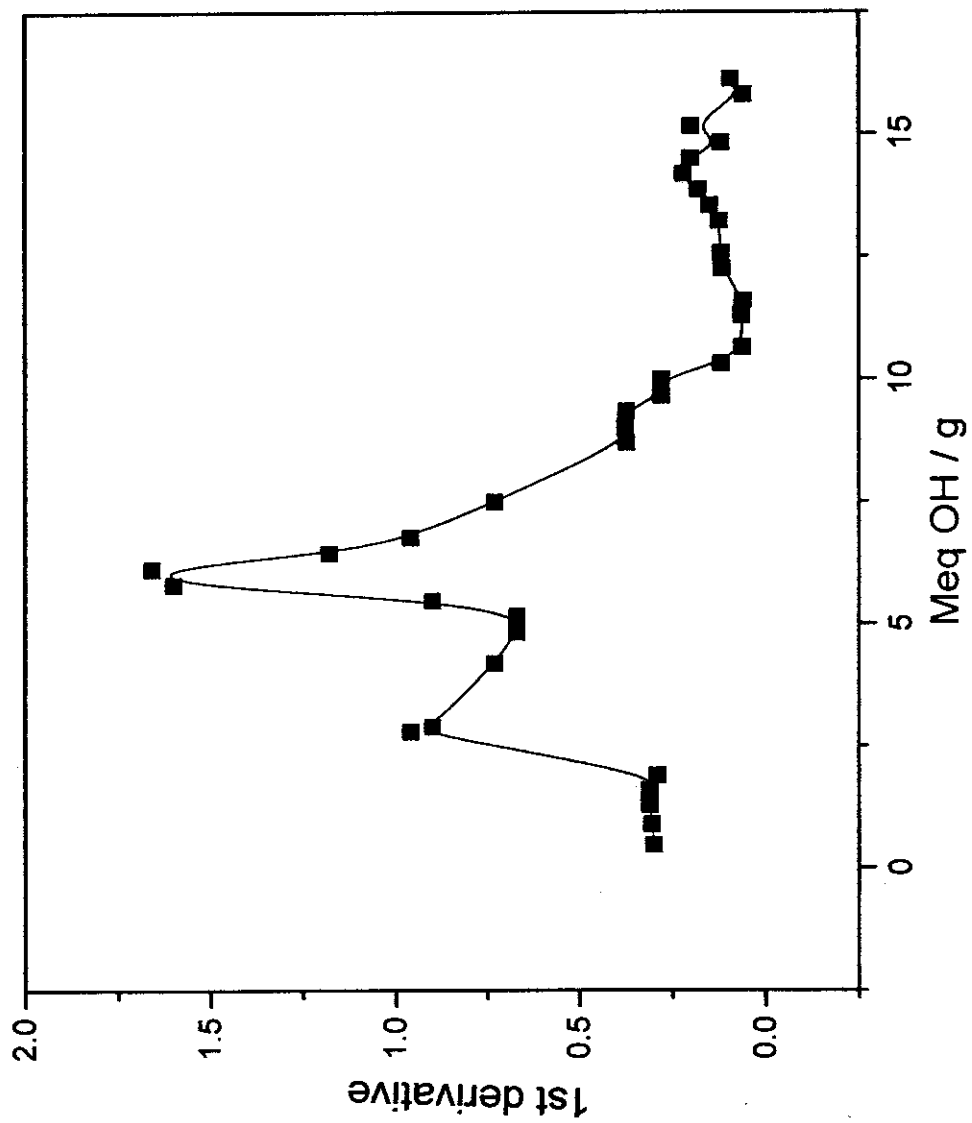


Fig (3.12): Derivative curve of humin.

By using this equation, the ionization constant can be determined from the titration data which provide estimates for (A<sup>-</sup>) and (HA) at any given pH. By applying the negative logarithm on equation (2):

$$pK = -\log [A^-][H^+]/[HA] \quad \dots\dots\dots(3)$$

$$pK = pH - \log [A^-] / [HA] \quad \dots\dots\dots(4)$$

pK is equal to pH at half-neutralization; this is referred to as the pK<sub>a</sub> of the acidic group. The pK<sub>a</sub> values of the investigated samples were determined by application of the Henderson- Hasselbalch equation:-

$$pH = pK_a + n \log [\alpha / 1-\alpha ] \quad \dots\dots(5)$$

Where  $\alpha$  is the degree of ionization. The pK<sub>a</sub> and n are constants, for a given titration, depend on the concentration and ionic strength. A plot of pH versus  $\log [\alpha / (1-\alpha)]$  gives a straight line of slope n and intercept corresponds to pK<sub>a</sub>. Figures (3.13-3.18) represent the plot of pK<sub>a</sub> vs the degree of ionization ( $\alpha$ ) for humic materials investigated. It is observed that the titrated humic fractions display similar characteristics of polyelectrolyte in that the pK<sub>a</sub> value increases with increasing the degree of ionization of functional groups.

Henderson-Hasselblach plots (pH against  $\log \alpha/1-\alpha$ ) were traced, Figs.(3.19-24), to determine the pK<sub>a</sub> value at half neutralization from the intercept of the straight part (at zero value of  $\log \alpha / 1-\alpha$ ). For the values of pH in the range 4-6, the Henderson-Hasselbalch treatment is adequate with n = 1.22, 2.1, 1.85, 5.25, 2 and 1.1 for PFA, ICHA, BHA, GHA, SHA, and humin, respectively. At lower and higher values of  $\alpha$ , the curves flatten. The pK<sub>a</sub> values at  $\alpha = 0.5$  (50% ionization) were found to be 2.94, 4.63, 4.25, 3.81, 4.56 and 5.99 for PFA, ICHA, BHA, GHA, SHA and humin, respectively, (at ionic strength of 0.1 M in sodium perchlorate medium). The values of the total carboxylate capacity and pK<sub>a</sub> at half neutralization of the investigated samples are illustrated in Table (3.3). Comparing the total carboxylate capacities of the humic acid samples, it is clear that the values agree with the percentages of

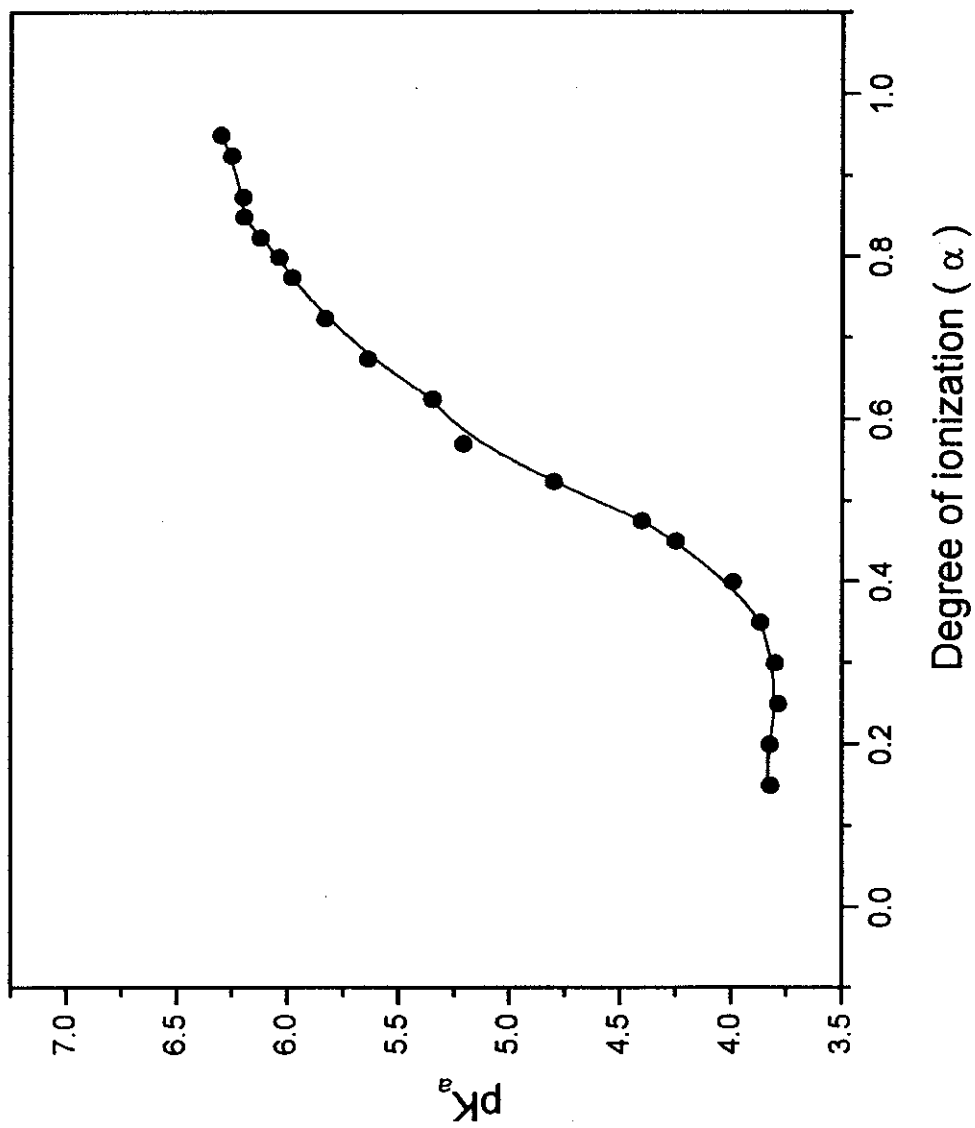


Fig. (3.13): Variation of  $pK_a$  with the degree of ionization of Ismailia canal humic acid.

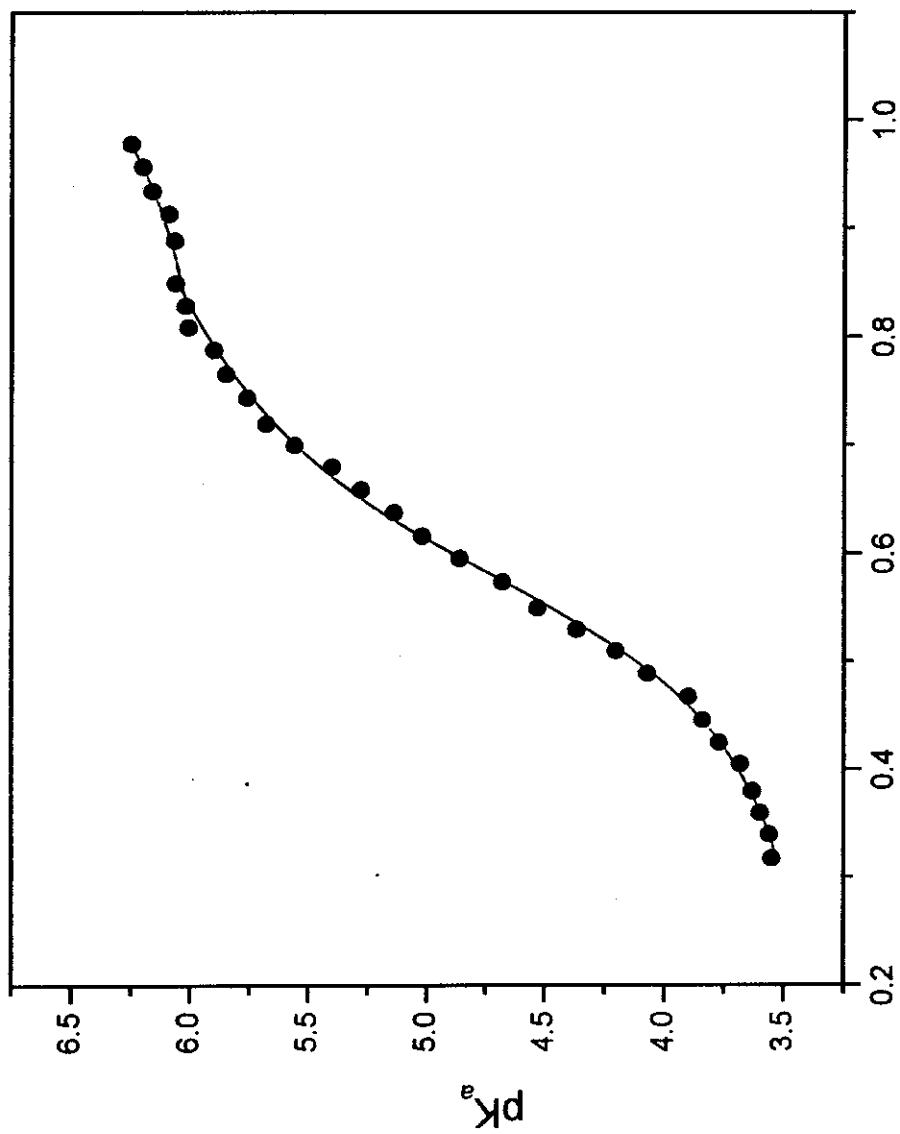


Fig. (3.14): Variation of  $pK_a$  with the degree of ionization of brown humic acid

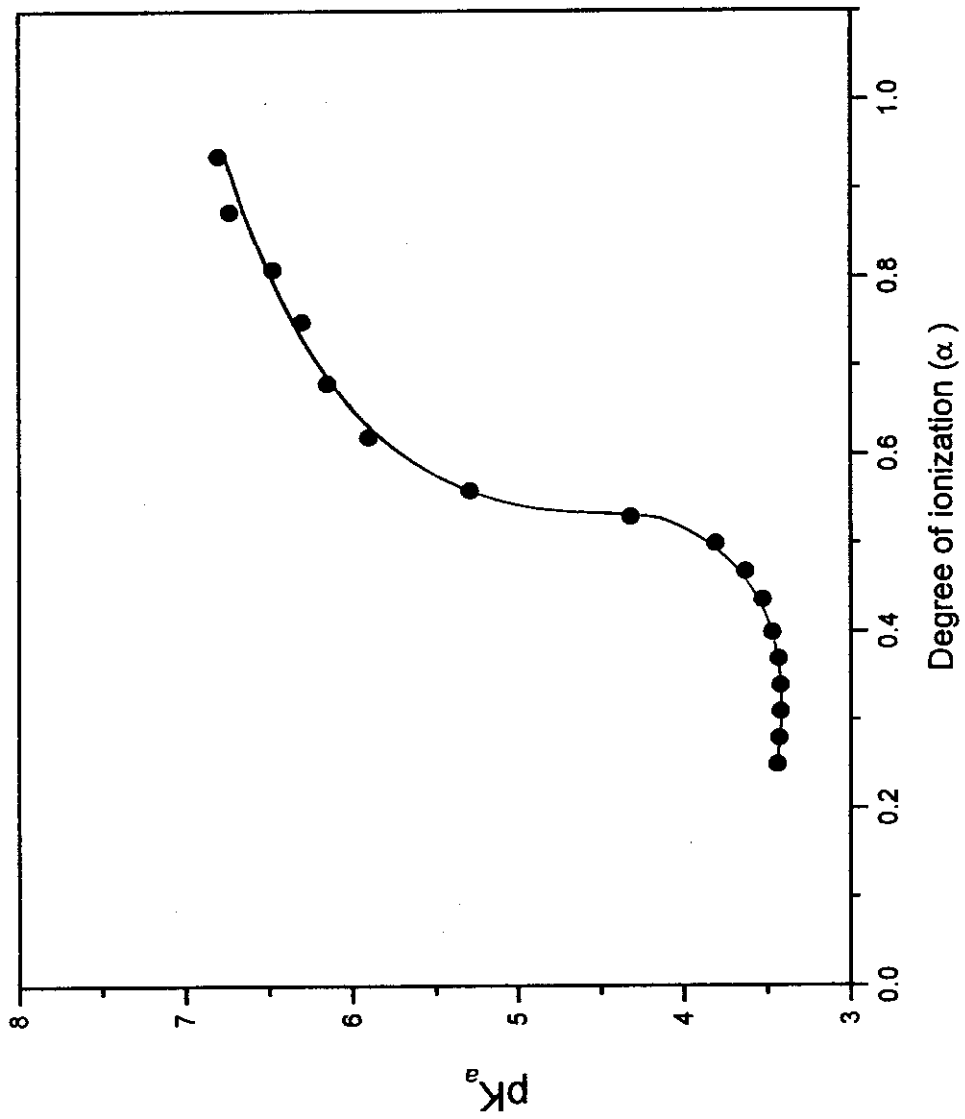


Fig. (3.15): Variation of  $pK_a$  with the degree of ionization of gray humic acid

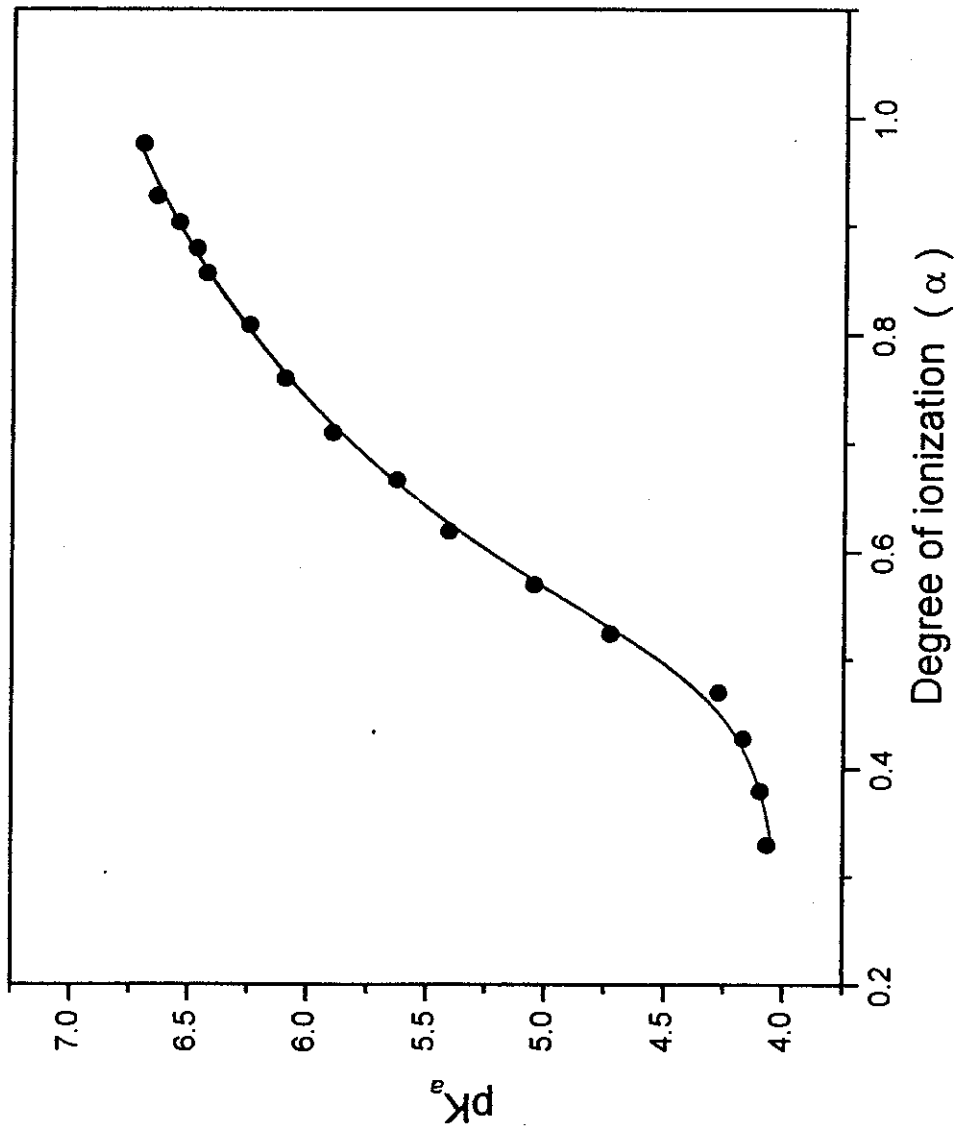


Fig. (3.16): Variation of  $pK_a$  with the degree of ionization of soil humic acid

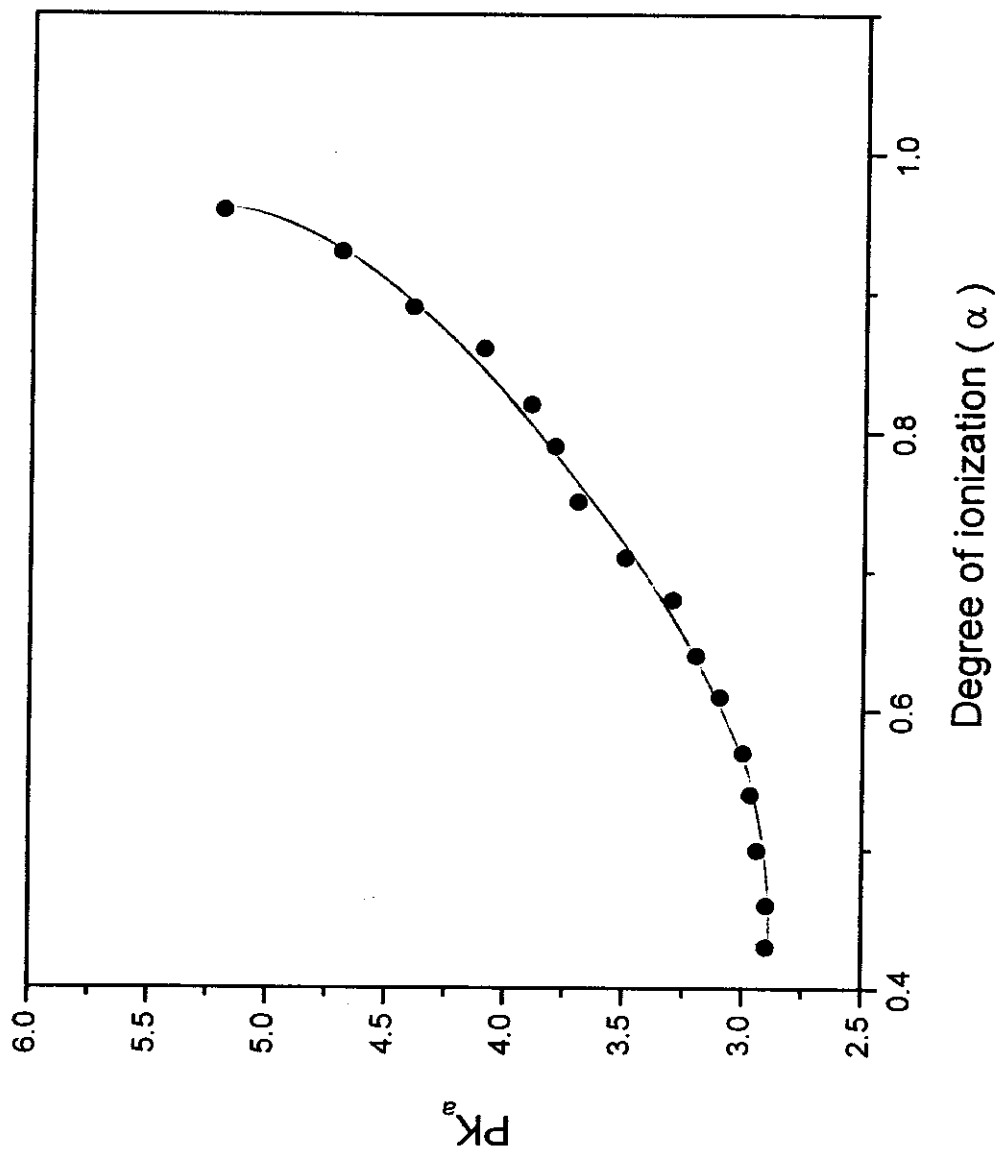


Fig. (3.17): Variation of  $pK_a$  with the degree of ionization of peat fulvic acid.

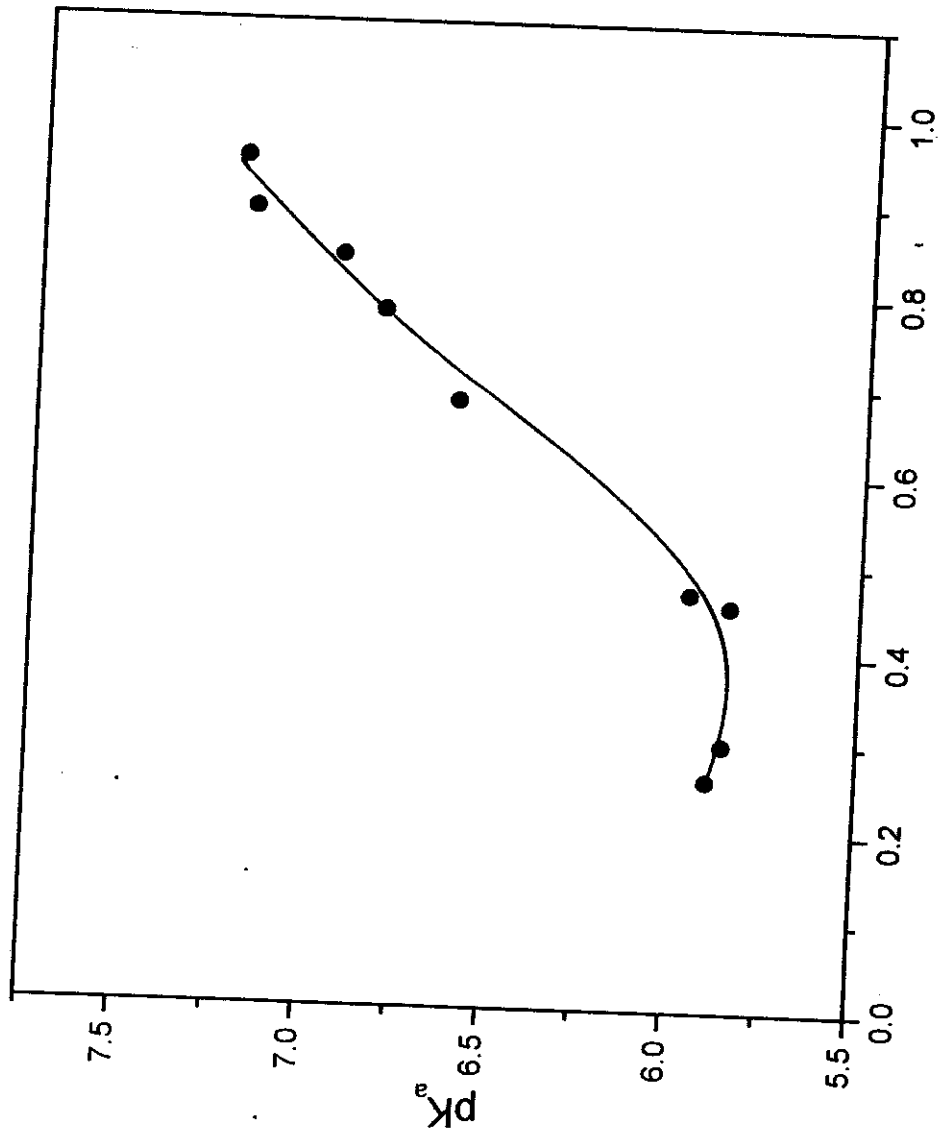


Fig. (3.18): Variation of  $pK_a$  with the degree of ionization of humin.



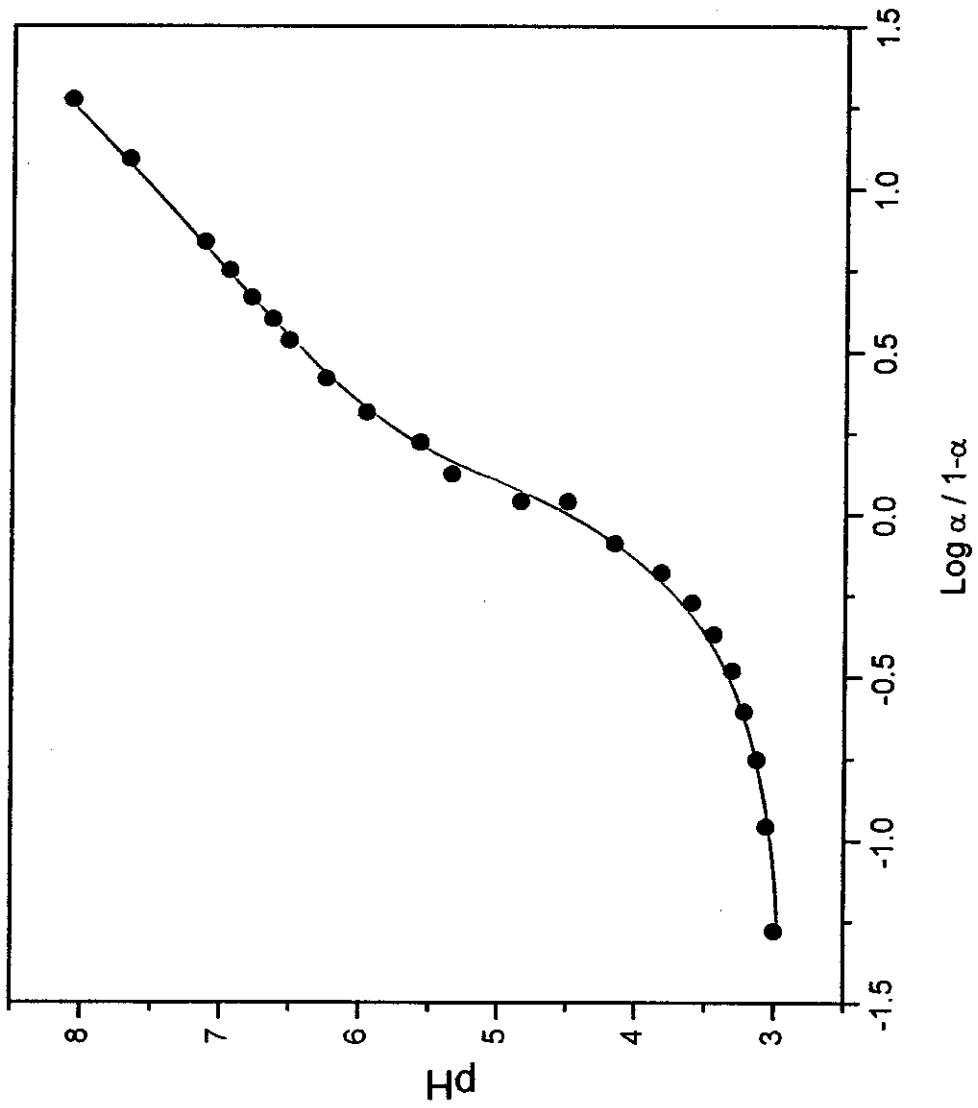


Fig. (3.19): Henderson - Hasselbalch plot of Ismailia canal humic acid.

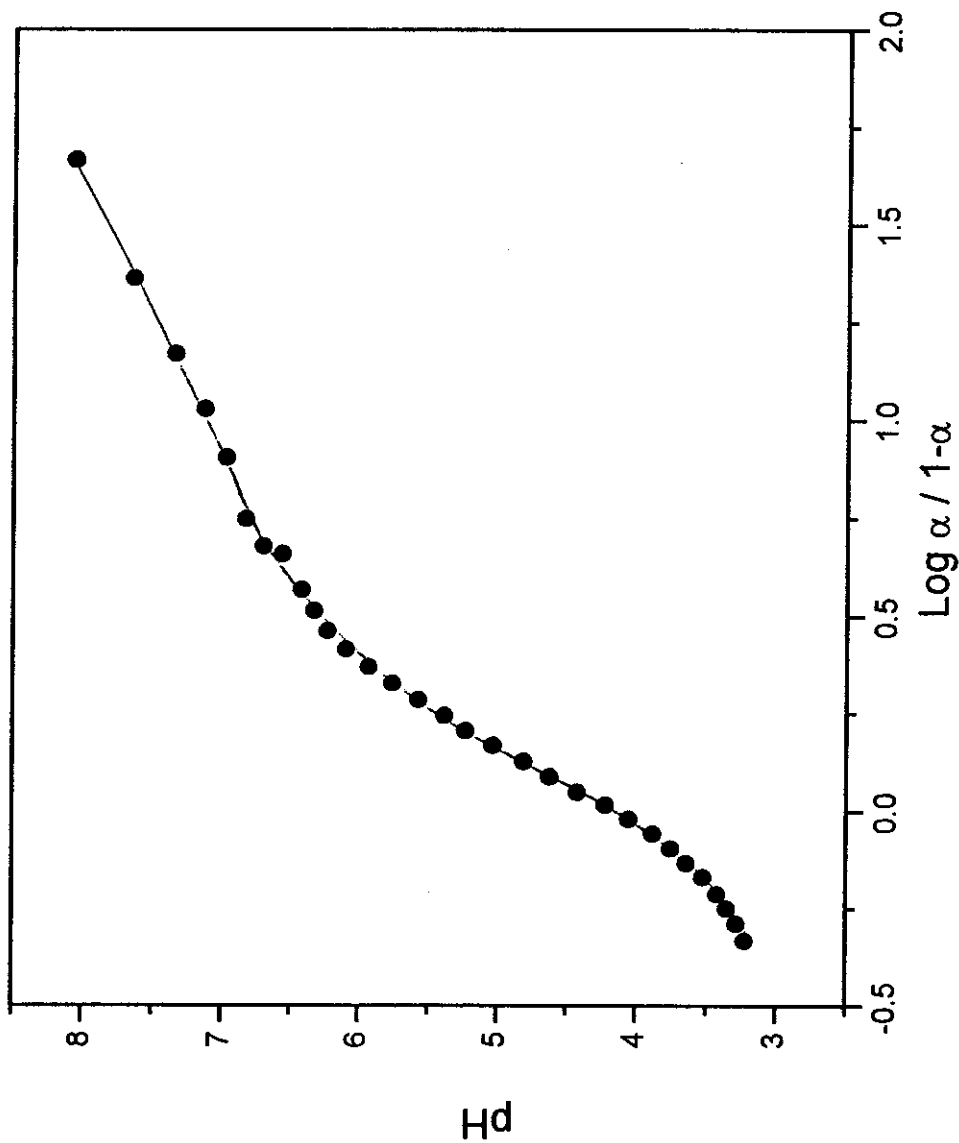


Fig. (3.20): Henderson - Hasselbalch plot of brown humic acid.

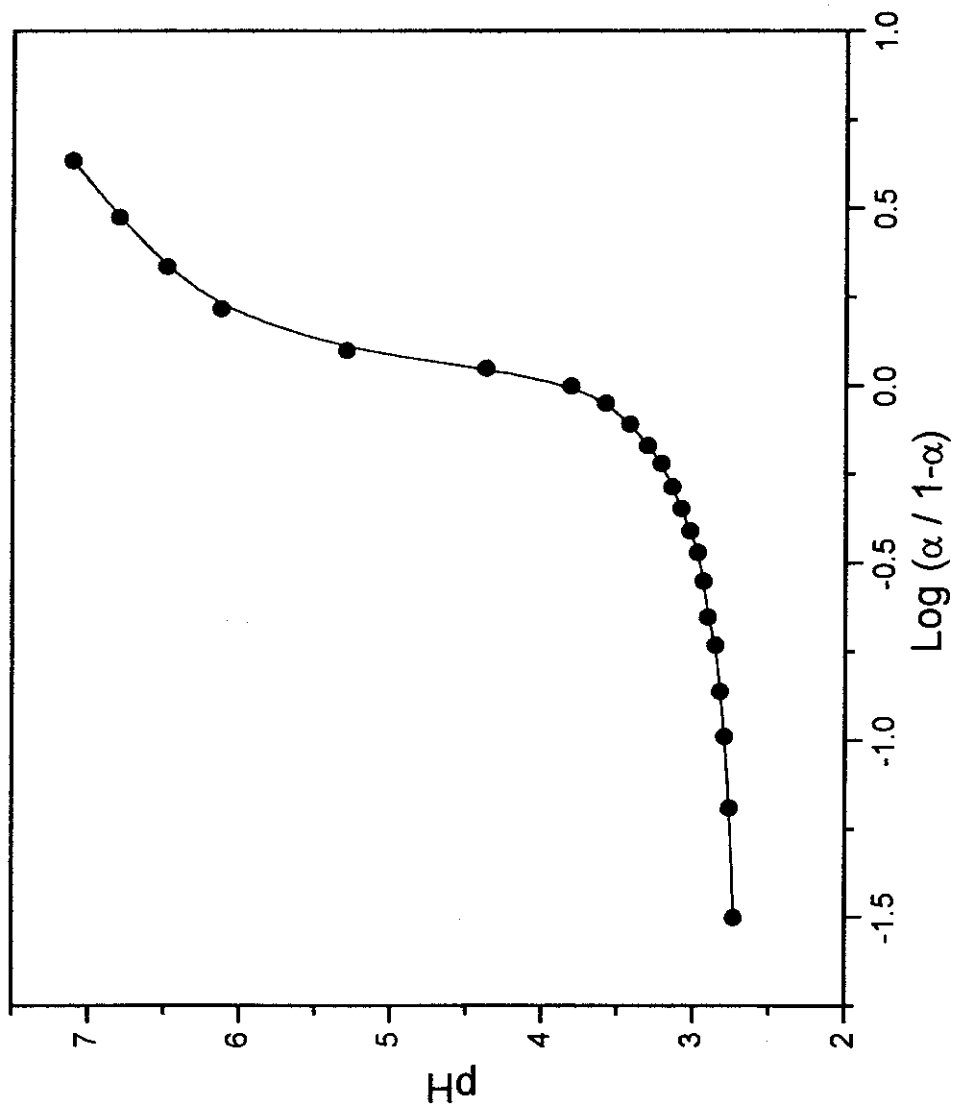


Fig (3.21): Henderson- Hasselbalch plot of gray humic acid.

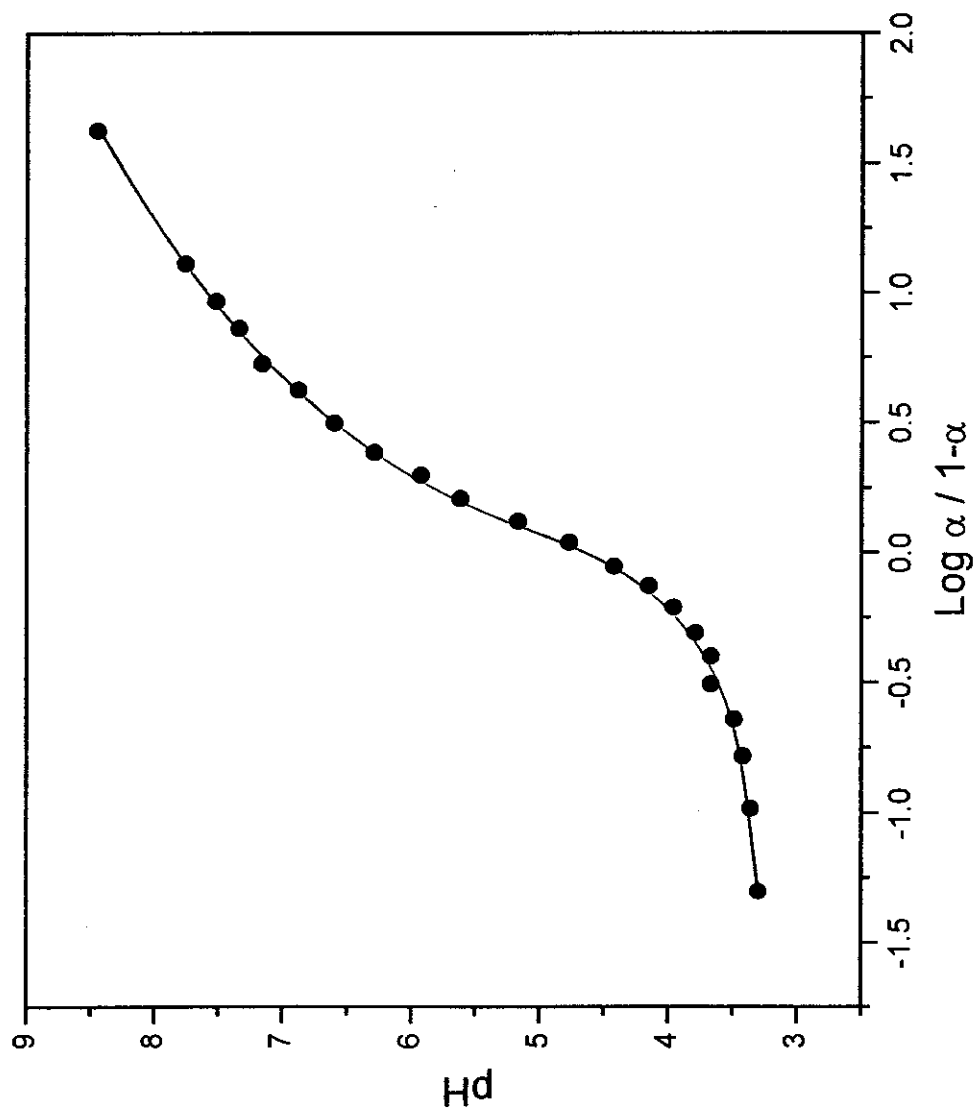


Fig. (3.22): Henderson - Hasselbalch plot of soil humic acid.

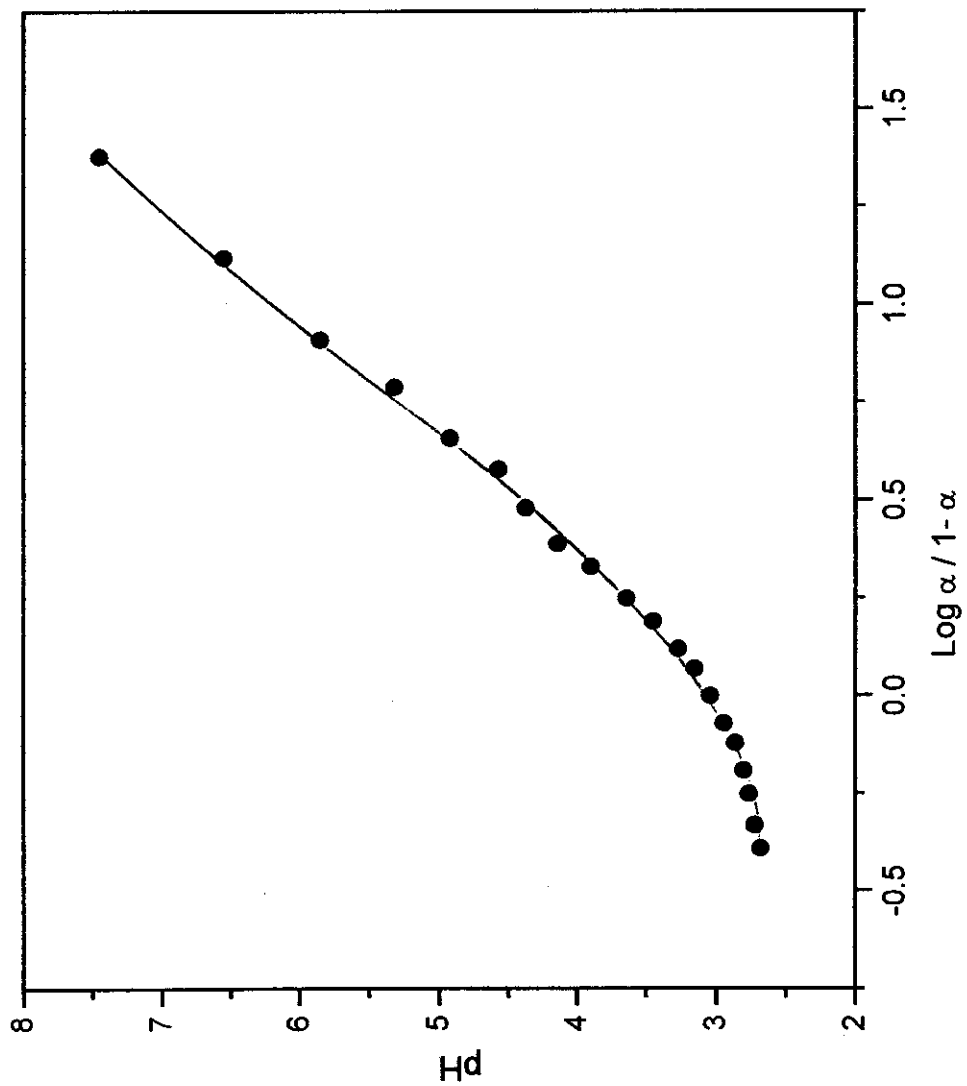


Fig. (3.23): Henderson - Hasselblach plot of peat fulvic acid.

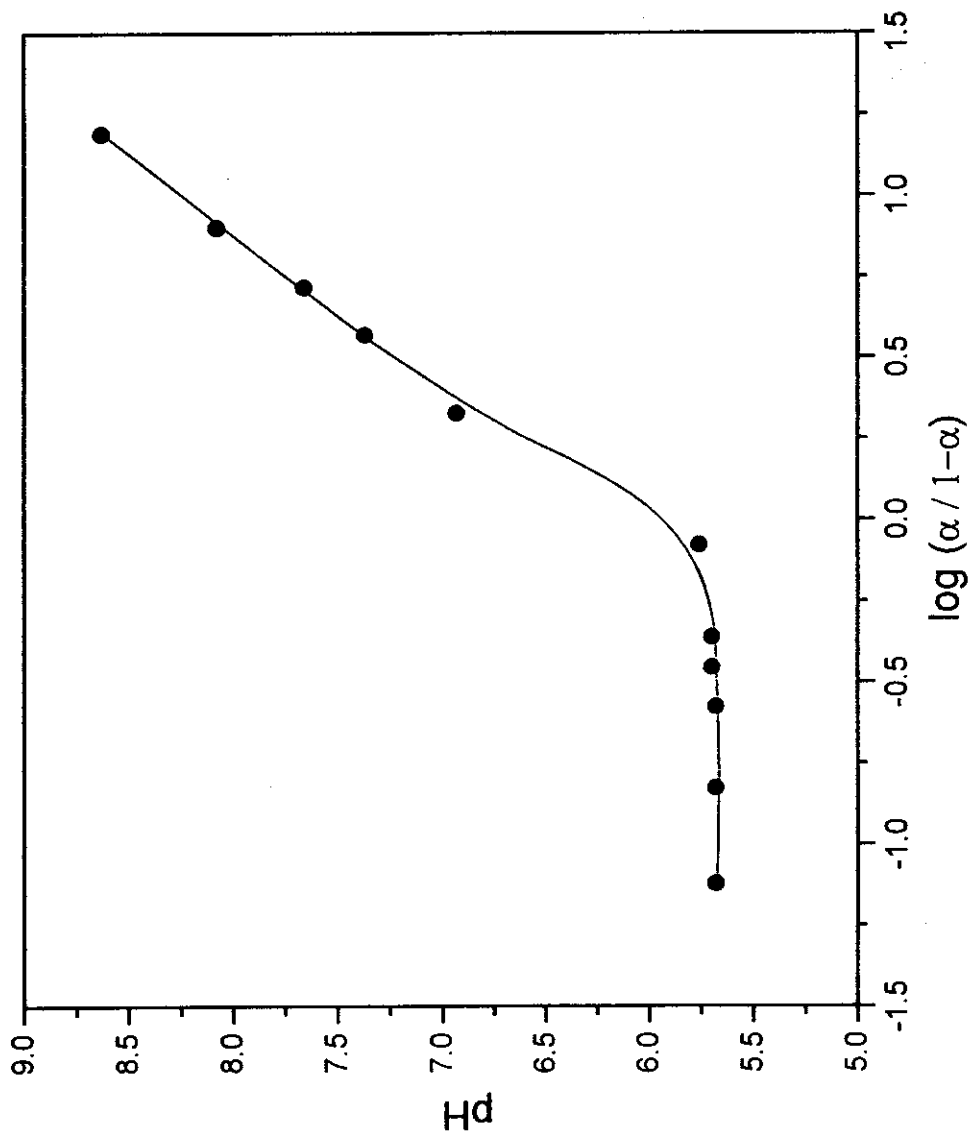


Fig (3.24): Henderson-Hasselbalch plot of humin.

**Table (3.3):** The total carboxylate capacities and the  $pK_a$  values at ( $\alpha=0.5$ ).

Sample	Total-COO <sup>-</sup> capacity, meq/g	$pK_a$ at ( $\alpha=0.5$ )
ICHA	6.6	4.63
BHA	7.75	4.25
GHA	12.96	3.81
SHA	6.97	4.56
PFA	6	2.94
Hn	5.81	5.99

oxygen (Table 3.3). The  $pK_a$  values provide a convenient way of comparing the strength of COOH groups. The lower the  $pK_a$ , the stronger is the acidic group. It is clear that GHA, which has the lowest  $pK_a$  value, has the highest carboxylate capacity. The comparison between humic acid samples and both fulvic acid and humin is not convenient since they are obtained from different sources.

### 3.1.3 Infrared spectroscopy:

The infrared spectra in the region  $4000\text{ cm}^{-1}$  to  $500\text{ cm}^{-1}$  of the investigated humic materials were found to have more or less similar spectra with a variety of bands that are diagnostic of specific molecular structure. The main absorption bands as indicated in Fig.(3.25) were found as the following:

- The absorption around the region  $3400\text{ cm}^{-1}$ , which is clear in all the samples, is attributed to the OH stretching. The broadness of these bands is generally due to hydrogen bonding<sup>[112]</sup>.
- The bands in the region  $2920\text{-}2930\text{ cm}^{-1}$  are evident in the spectra of all samples. They are generally more pronounced in humic acids and humin than in fulvic acid. These bands, in addition to the little bands at  $2860\text{ cm}^{-1}$  which appear only in the spectra of ICHA, BHA, SHA and Hn, are attributed to the asymmetric and symmetric stretching vibrations, respectively, of aliphatic C-H bonds in methyl and / or methylene units<sup>[35]</sup>.
- The  $1720\text{ cm}^{-1}$  bands in ICHA, BHA, GHA, Hn and PFA are generally attributed to the C=O stretching vibration, due mainly to carboxyl groups<sup>[113]</sup>.
- The bands in the region  $1600\text{-}1650\text{ cm}^{-1}$  has been assigned to aromatic C=C "double bonds" conjugated with C=O and / or COO<sup>-</sup><sup>[40]</sup>.
- The bands in the region  $1380\text{-}1440\text{ cm}^{-1}$  have been attributed to the bonding vibration of aliphatic C-H groups<sup>[40]</sup>.



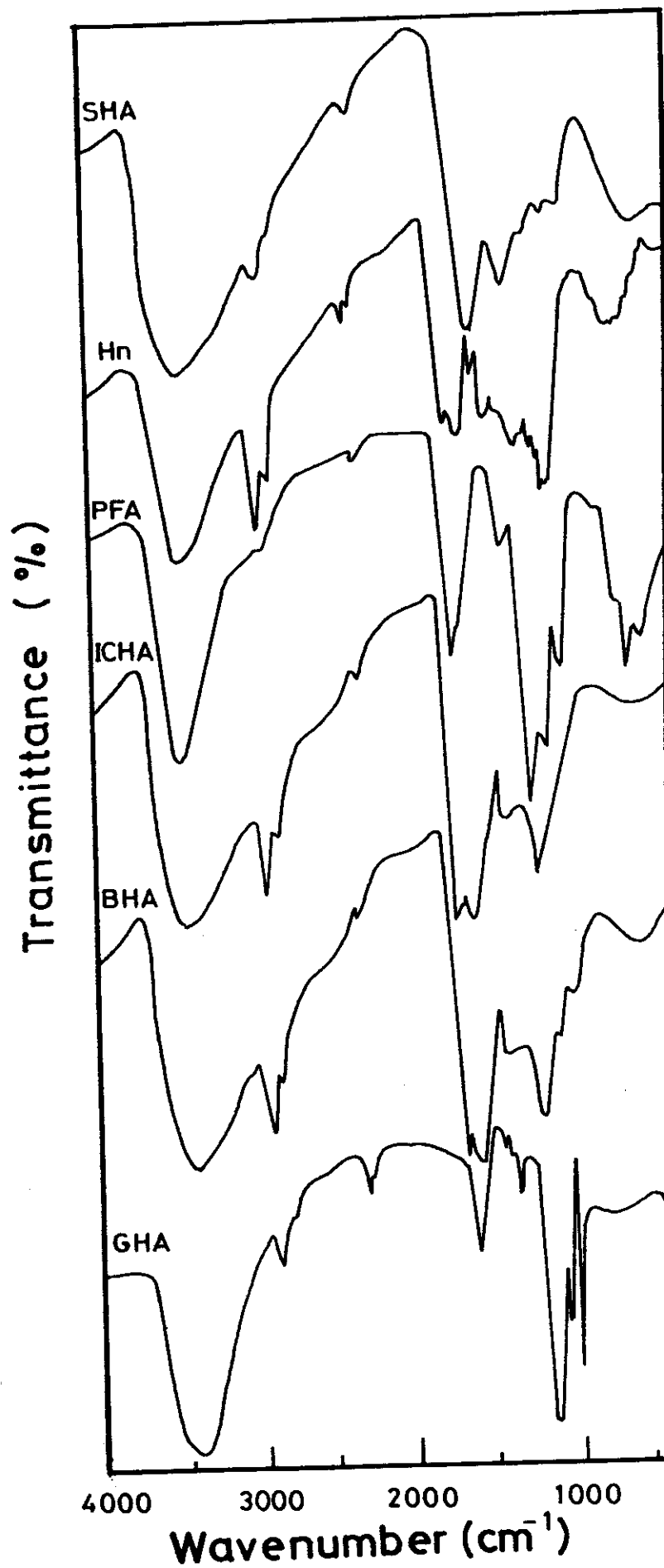


Fig.(3.25): The infrared spectra of the investigated humic materials.

-The bands, appear in ICHA, BHA and SHA, in the region 1200-1280  $\text{cm}^{-1}$  are assigned to C-O stretching and OH deformation of COOH<sup>[114]</sup>.

-The band at 1182  $\text{cm}^{-1}$  appears in GHA, which has the highest value of ash percent is probably due to silicate impurities. The absorption at 1040  $\text{cm}^{-1}$  is typical of the C-O stretching of carbohydrates.

### 3.1.4 Ultraviolet and visible spectroscopy:

The ultraviolet and visible (UV-visible) regions are generally, considered together since both correspond to electronic transitions within the absorbing species. Although the UV-visible absorption spectra of humic and fulvic acids do not provide much detailed information on their chemical structure, but it has other useful applications, such as the estimation of the degree of humification using the  $E_4 / E_6$  ratios:

The  $E_4 / E_6$  ratio is the ratio of the absorbancies of dilute aqueous humic or fulvic acid solutions at 465 and 665 nm.

It has been observed that  $E_4/E_6$  ratio is related to the degree of condensation of the aromatic carbon network, the ratio of carbon in aromatic "nuclei" to carbon in aliphatic side chains, total carbon content and molecular weight. The magnitude of  $E_4/E_6$  ratio is inversely proportional to the degree of condensation or the molecular weight, as observed by chen et al.<sup>[65]</sup> i.e., the high  $E_4 / E_6$  ratio indicates a smaller molecule which contains less carbon, but more oxygen and – COOH groups. The values of  $E_4/E_6$  ratio for the humic and fulvic acid samples are shown in Table (3.4). It is clear from the table that PFA and SHA have higher  $E_4/E_6$  ratio than the other fractions. Comparing the deduced results of  $E_4/E_6$  ratio with that of elemental composition, potentiometric titration and IR spectra of the investigated humic materials indicate that they are in good agreement with each other.

Table (3.4): E<sub>4</sub>/E<sub>6</sub> ratio of humic and fulvic acids.

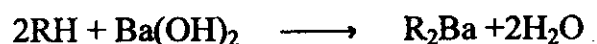
Sample	Absorbance ratio		E <sub>4</sub> /E <sub>6</sub>
	465nm	665nm	
ICHA	1.1	0.270	4.07
BHA	1.63	0.405	4.02
SHA	0.446	0.077	5.79
PFA	0.45	0.075	6

### 3.1.5 Functional group analysis

The common oxygen-containing functional groups were determined by the wet chemical methods.

#### 1) Total acidity (COOH plus phenolic- and / or Enolic-OH):

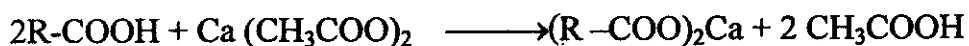
The total acidity of (ICHA) was determined by the barium hydroxide method. The barium hydroxide  $\text{Ba}(\text{OH})_2$  approach is an indirect potentiometric method in that it is based on release of  $\text{H}^+$  from acidic groups. The sample is allowed to react with excess  $\text{Ba}(\text{OH})_2$ , then, the unused reagent is titrated with standard acid. The overall reaction is:



Where R is the macromolecule and H is the proton of a COOH or acidic OH group. The total acidity of ICHA was found 855.5 cmole /Kg.

2) **Carboxyl groups:** The carboxyl groups were determined using the Ca-acetate method. This method is based on ion exchange and can be regarded as an indirect potentiometric titration approach.

The reaction is:



The acetic acid liberated during the reaction is titrated with a standardized NaOH solution. The value of COOH for ICHA was 495 cmole/ kg. This value may not be the exact value of COOH since the binding of  $\text{Ca}^+$  to humic acid may lead to release of  $\text{H}^+$  from sites other than a COOH group. Also, the removal of humic matter during filtration may be incomplete.

3) **Total OH:** The total OH was determined by acetylation method. In this method, acetylation is performed by acetic anhydride to form acetate esters. The total acetyl content and the OH content were found 23 and 676.5 respectively, in cmole/kg.

4) **Phenolic OH:** The amount of phenolic OH is calculated as the difference between total acidity and COOH (in cmole / Kg)

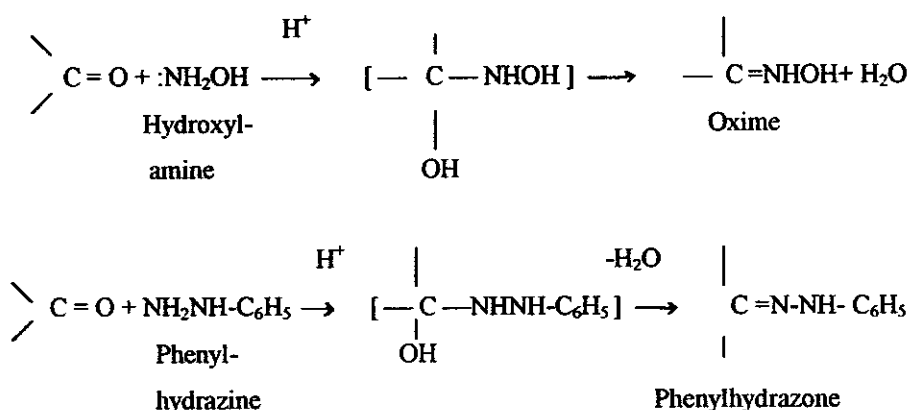
$$\text{Phenolic OH} = \text{total acidity} - \text{COOH} = 360.5 \text{ cmole /kg}$$

**Alcoholic OH:** The value of alcoholic OH groups is obtained from the difference between total OH and phenolic OH.

$$\text{Alcoholic OH} = \text{total OH} - \text{phenolic OH} = 316 \text{ cmole/Kg}$$

**Carbonyl C=O:** The method is based on the formation of derivatives by reaction with 0.25M 2-dimethyl amino ethanol and 0.4M hydroxyl ammonium chloride solution.

The typical reactions are as follows:



Figs. (3.26-3.29) show the potentiometric titration and the first derivative curve for the sample and blank respectively, which the end point was calculated. The carbonyl C=O content was found 793 cmole/kg.

These results (table 3.5) agree with what summarized by Schnitzer<sup>[61]</sup>, who found that the total acidities of the fulvic acids (ranging from 640 to 1420 cmole/kg) are unmistakably higher than those of the humic acids (from 560 to 860 cmole /kg). Both the COOH and acidic OH groups contribute to the acidic nature of these substances, with COOH being the most important. Of particular interest is the very high COOH content of fulvic acids.

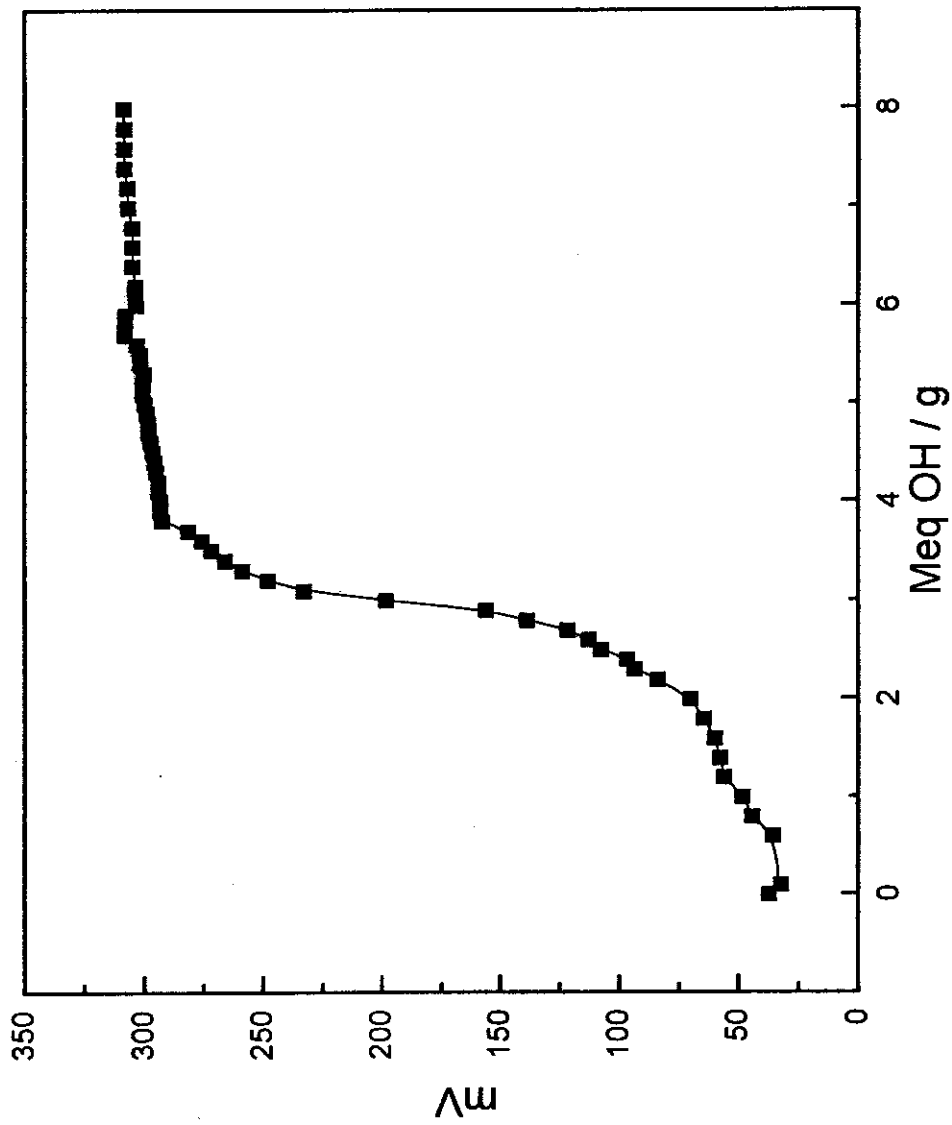


Fig.(3.26): Titration curve of sample.

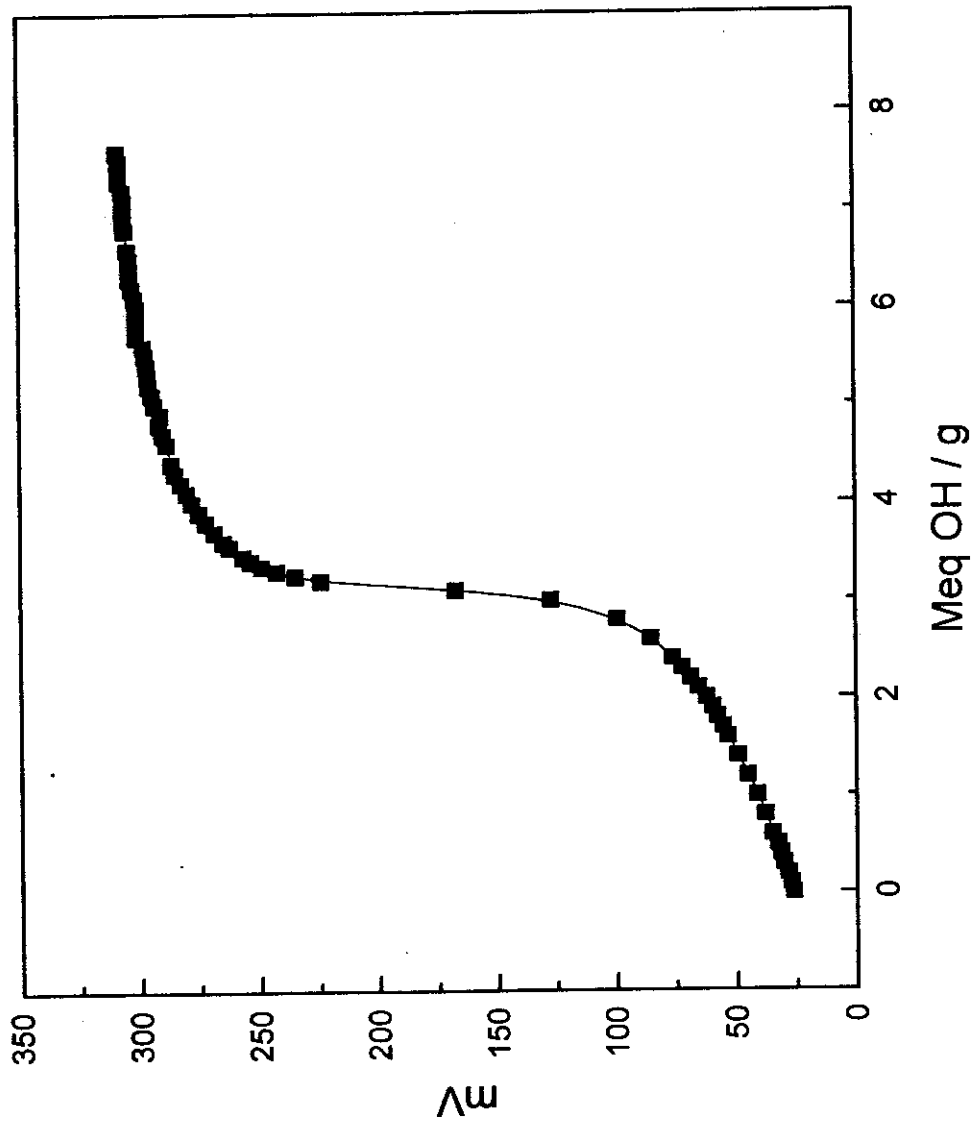


Fig (3.27): Titration curve of blank.

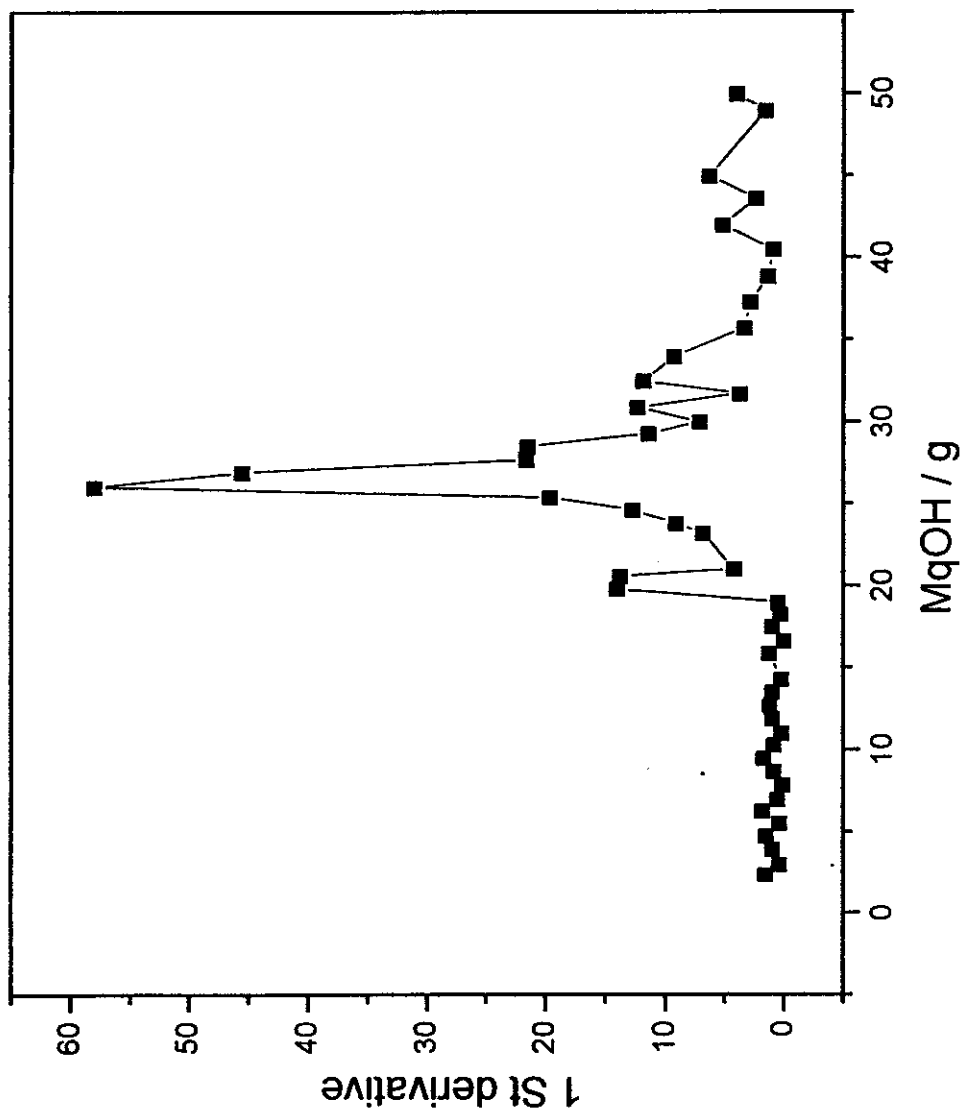


Fig. (3.28): Derivative curve of sample



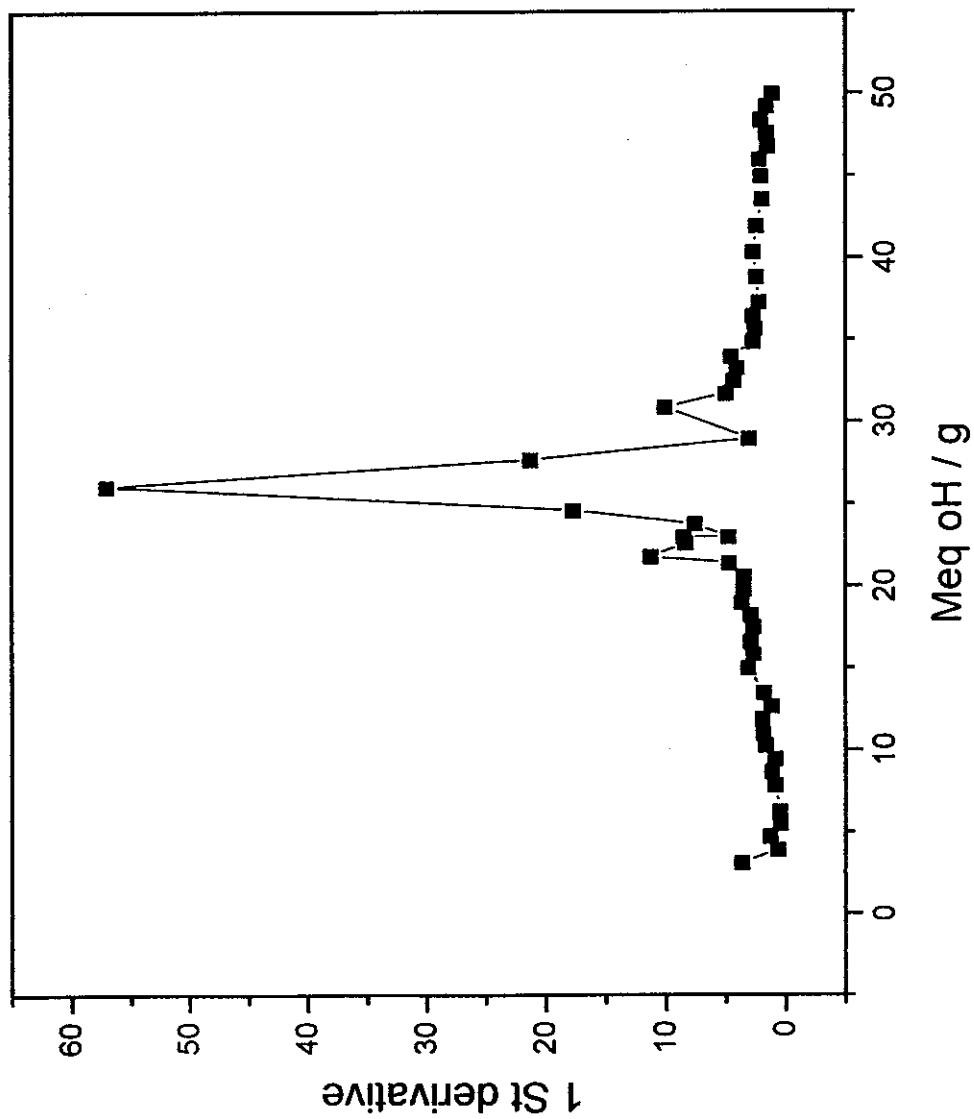


Fig.(3.29): Derivative curve of blank.

**Table (3.5):** The functional groups in Ismailia canal humic acid.

Functional group	(cmole/Kg)
Totat acidity	855.5
COOH	495
Total OH	676.5
Phenolic OH	360.5
Alcoholic OH	316
Carbonyl C=O	793

### **3.2 Interaction of humic materials with metal ions**

The trace element chemistry and the reactions in soil are related to the formation of stable complexes between metal ions and humic substances. As indicated by Stevenson <sup>[26]</sup>, the monovalent cations are held primarily by simple cation exchange through formation of salts with carboxyl groups, whereas multivalent cations have the potential for forming coordinate linkages with the humic molecules. A metal ion in aqueous solutions attached water molecules oriented in such a way that the negative (oxygen) end of the water dipole is directed towards the positively charged metal ion. A complex arises when water molecules surrounding the metal ion are replaced by other molecules or ions, with the formation of a coordinate compound. A chelate complex is formed when two or more coordinate positions about the metal ion are occupied by donor groups of a single ligand to form an internal ring structure.

The stability of a metal-chelate complex is determined by such factors as the number of atoms that form a bond with the metal ion, the number of rings that are formed, the nature and concentration of metal ions and pH.

The humic matter serves as a buffer in meliorating the adverse effects of heavy metals that are introduced into soil as contaminants. Lead and cadmium, for example, are highly toxic contaminants that have been added in large quantities to agricultural and forested ecosystems, much of Pb and Cd have been immobilized through complexation with humified organic matter of the forest floor with enrichment of the organic layer with these heavy metals.

In the present study, the metal-humate complex formation is confirmed by investigating the change in chemical behaviour and the absorption spectra. In this concern, the IR change is studied by comparing the IR spectra of humic acid and metal-humate complexes. Moreover, the chemical changes are investigated using ion-selective electrode and radiometrically.

### 3.2.1 IR investigations:

The results of IR measurements for free humic acid and a number of metal-humate complexes are illustrated in Figs.(3.30 - 3.32). The spectra have confirmed that COOH groups play a prominent role in the complexation of  $\text{Cs}^+$ ,  $\text{Pb}^{2+}$ ,  $\text{Hg}^{2+}$ ,  $\text{Cd}^{2+}$ ,  $\text{La}^{3+}$  and  $\text{Th}^{4+}$  by humic acid (ICHA, BHA) and in the sorption of  $\text{Pb}^{2+}$  by humin. The C=O absorption band for COOH at  $1720\text{ cm}^{-1}$  has disappeared upon reaction with metal ions and new bands for asymmetric and symmetric stretching vibrations of the carboxylic ion ( $\text{COO}^-$ ) have appeared near  $1600$  and  $1400\text{-}1380\text{ cm}^{-1}$ , respectively. As pointed out by Stevenson<sup>[26]</sup>, the position of the asymmetric  $\text{COO}^-$  stretching band near  $1600\text{ cm}^{-1}$  provides an indication as to whether the linkages are ionic or covalent. For ionic bonds, absorption occurs in the  $1630\text{-}1575\text{ cm}^{-1}$  region; when coordinate linkages are formed, absorption shifts to higher frequencies (i.e., between  $1650$  and  $1630\text{ cm}^{-1}$ ).

It is clear from the spectra that all the investigated metals are complexed with the ligand. The lead-humate complex appears to be stronger ionic linkage than the other complexes.  $\text{Cd}^{2+}$  and  $\text{Th}^{4+}$ -humate complexes reveal covalent linkages. In the spectrum of  $\text{Cs}^+$ -humate complex, the  $1380\text{ cm}^{-1}$  band is absent.

### 3.2.2 Cesium-humate complexation:

The complex formation is investigated radiometrically and by using ISE. A comparison between the two methods is illustrated in Figs. (3.33, 3.34 ). It is clear that the two methods are almost typical and ISE is a suitable technique for measuring the free metal ions remaining after formation of metal- humate complex.

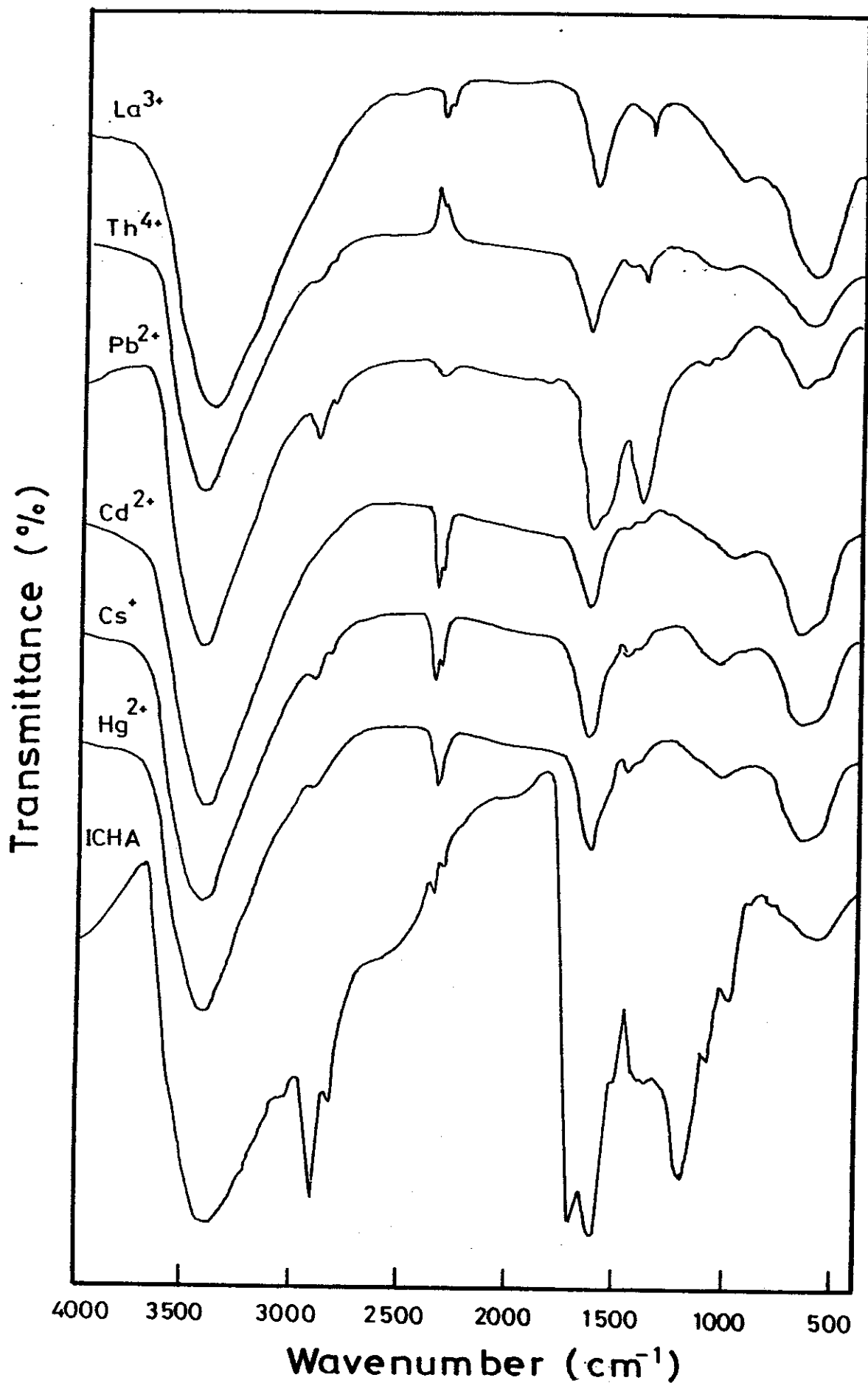


Fig.(3.30): The Infrared spectra of ICHA and Metal-Humate Complexes.

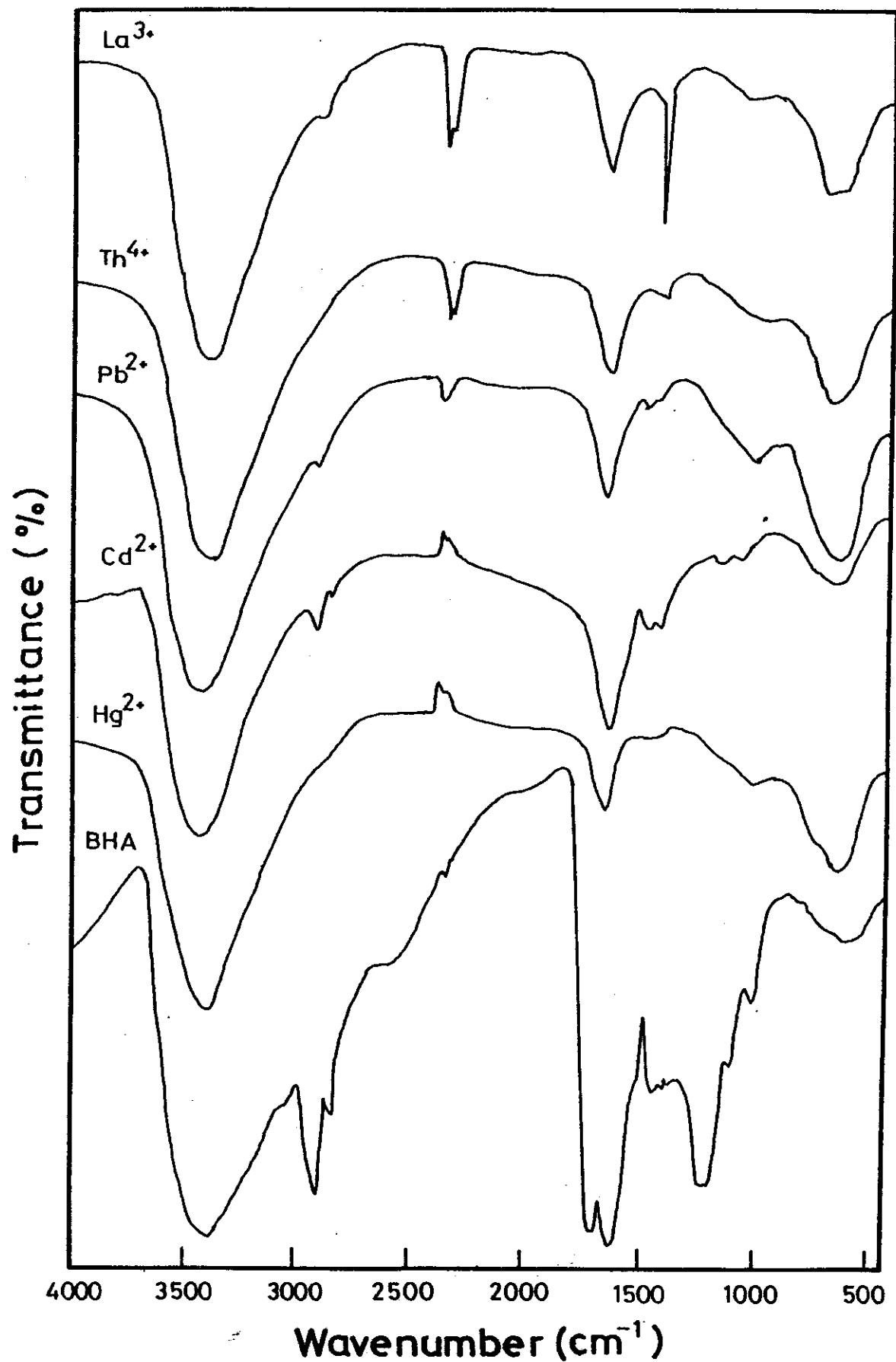


Fig.(3.31): The Infrared spectra of BHA and Metal -Humate Complexes.

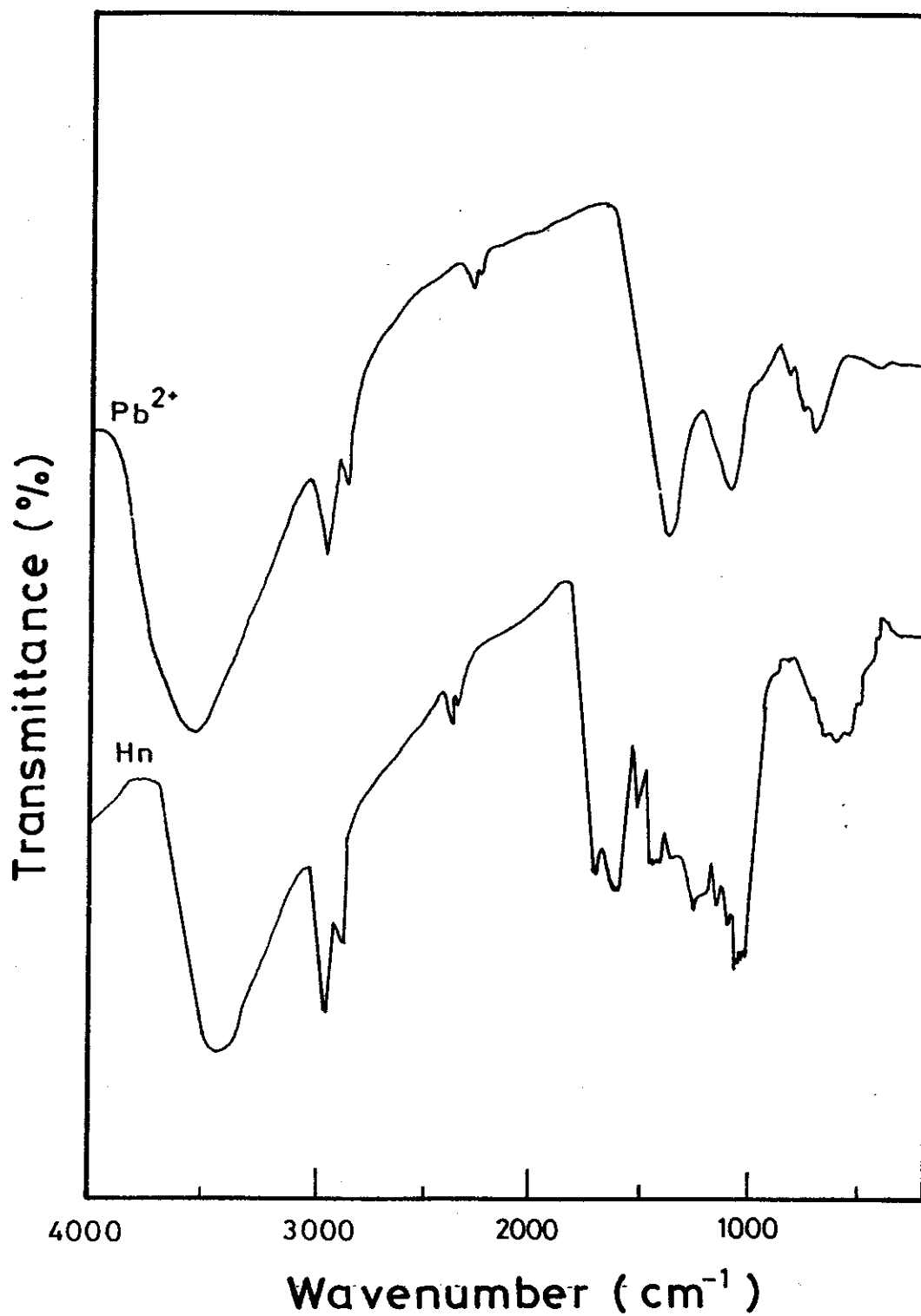


Fig. (3.32): Infrared spectra of humin singly and after sorption of Pb<sup>2+</sup>.

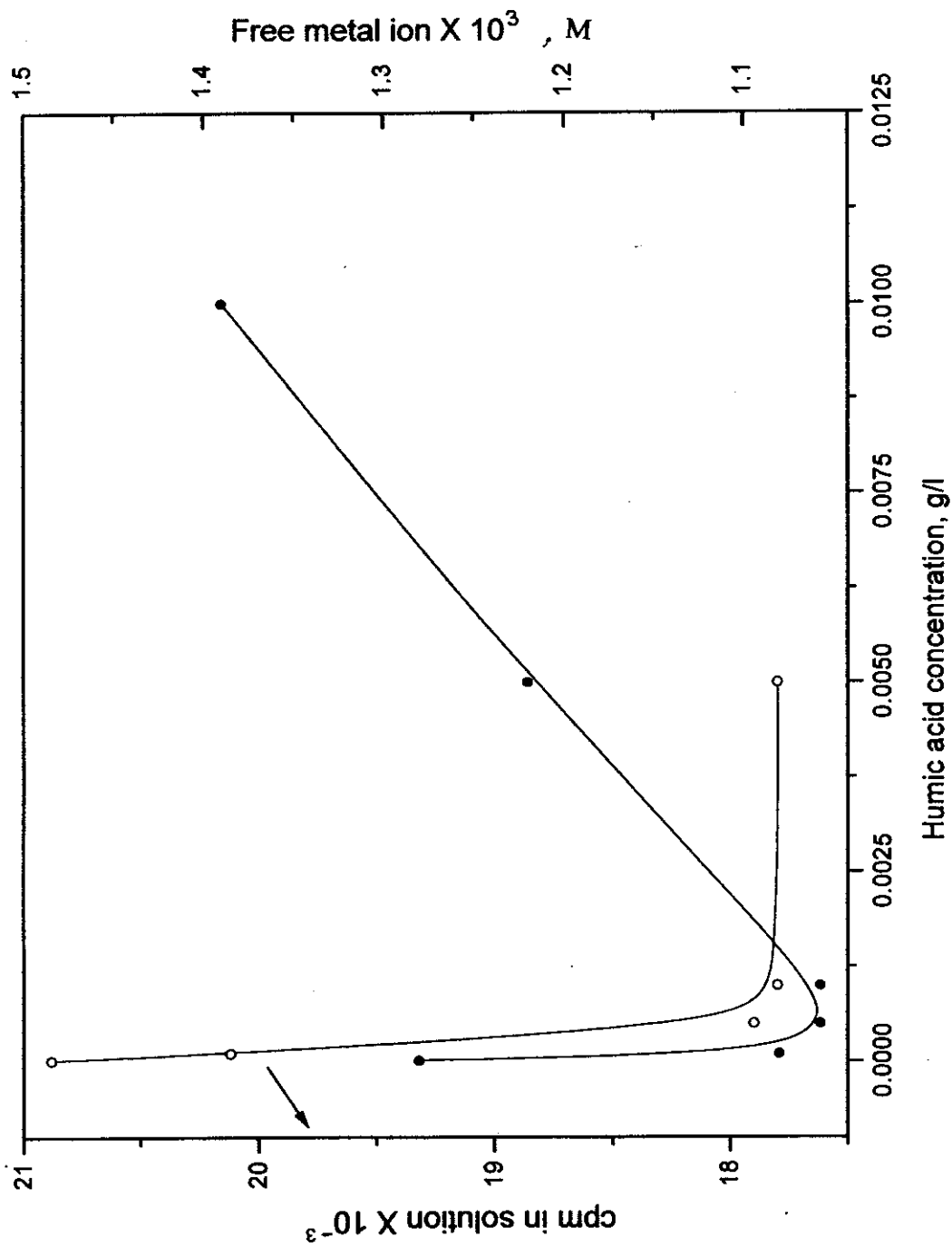


Fig. (3.33): Effect of humic acid concentration on the formation of Cs<sup>+</sup>-humate complex, radiometrically and by ISE.



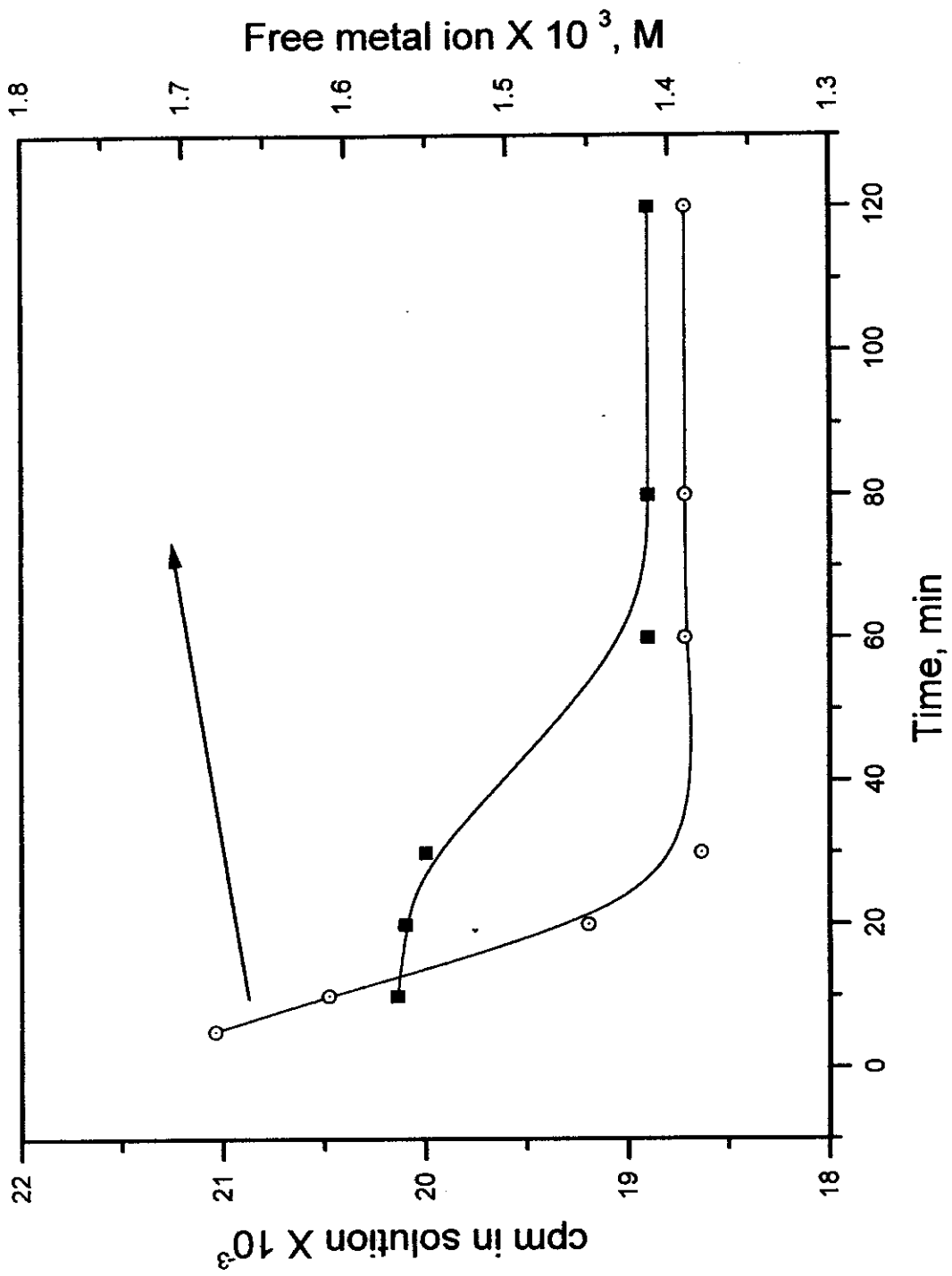


Fig. (3.34): Effect of shaking time on the formation of Cs-humat complex, radiometrically and by ISE.

### **3.2.2.1 Radioactive investigations:**

#### **a) Effect of shaking time:**

The formation of Cs-humate complex was studied radiometrically using  $^{137}\text{Cs}$ . The complex formation is based on the precipitation of humic acid with the metal ion. After separation of the complex by centrifugation, the supernate was studied radiometrically to evaluate the remaining metal ion as counts per minute (cpm). The reaction was carried out by shaking the system at different periods of time, as a preliminary test, to know the suitable time of equilibration. Fig.(3.35) show the effect of shaking time on the formation of Cs-humate complex. It is clear from the figure that the formation of complex increases with time and becomes constant at 60 minutes, which is the minimum time needed for the reaction.

#### **b) Effect of $\text{Cs}^+$ concentration :**

The effect of metal ion concentration is illustrated in Fig (3.36). The cpm decreases sharply with increasing the  $\text{Cs}^+$  concentration then becomes constant after consumption of the humic acid ( $10^{-3}$  g/l).

#### **c) Effect of humic acid concentration:**

Fig (3.37) indicates the effect of increasing the humic acid concentration on the formation of Cs-humate complex. In a similar behaviour to the previous item, the cpm decreased sharply by increasing the humic acid concentration and becomes constant after consumption of the  $\text{Cs}^+$  ( $10^{-3}$  M).

#### **d) Effect of pH:**

The effect of pH on the formation of Cs-humate complex is illustrated in Fig (3.38). The cpm decrease indicates that the complexation increases sharply by increasing pH. This behaviour is expected in the light of the exchange properties of the hydrogen ions and their effects on the complexation. The increase in pH of the solution results in additional ionization of the acidic groups of the humic acid.

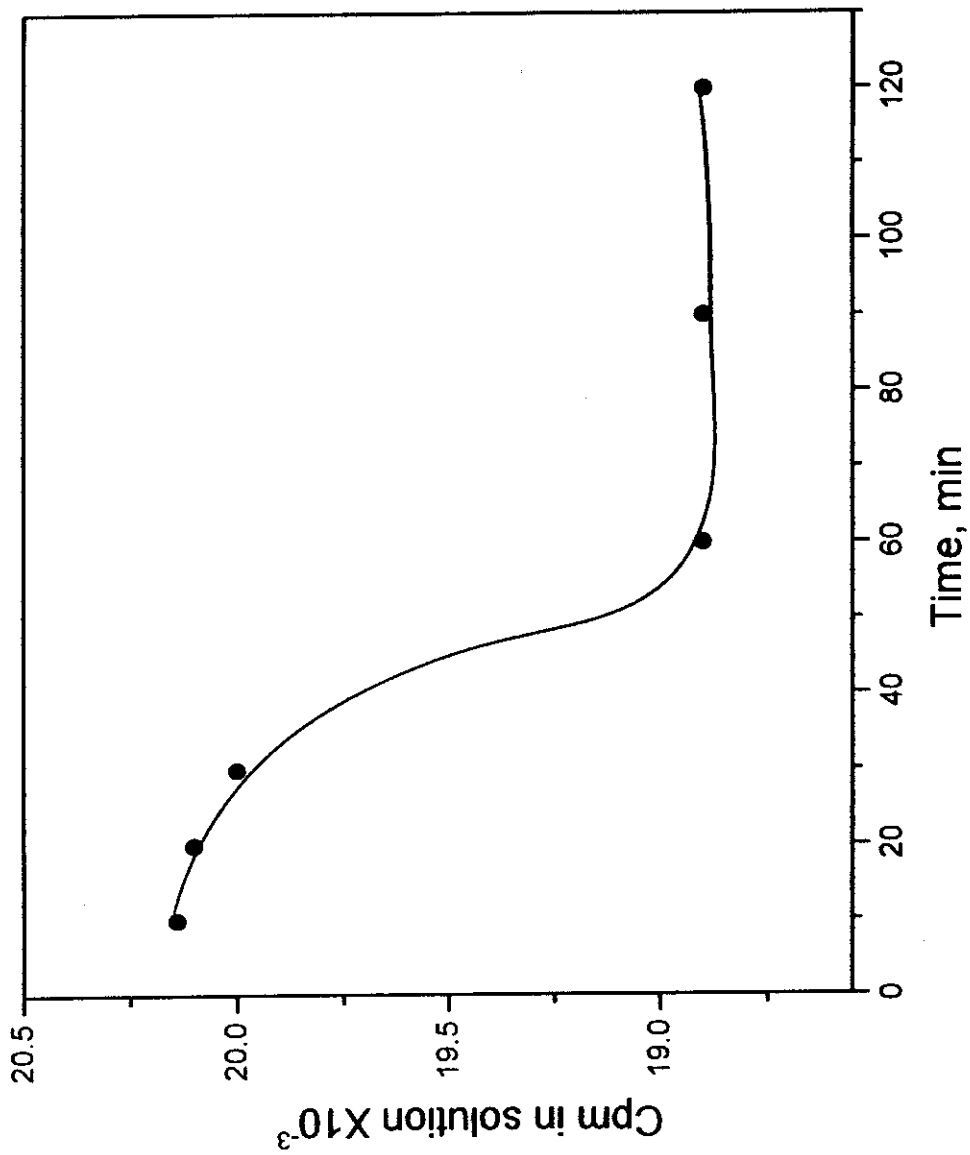
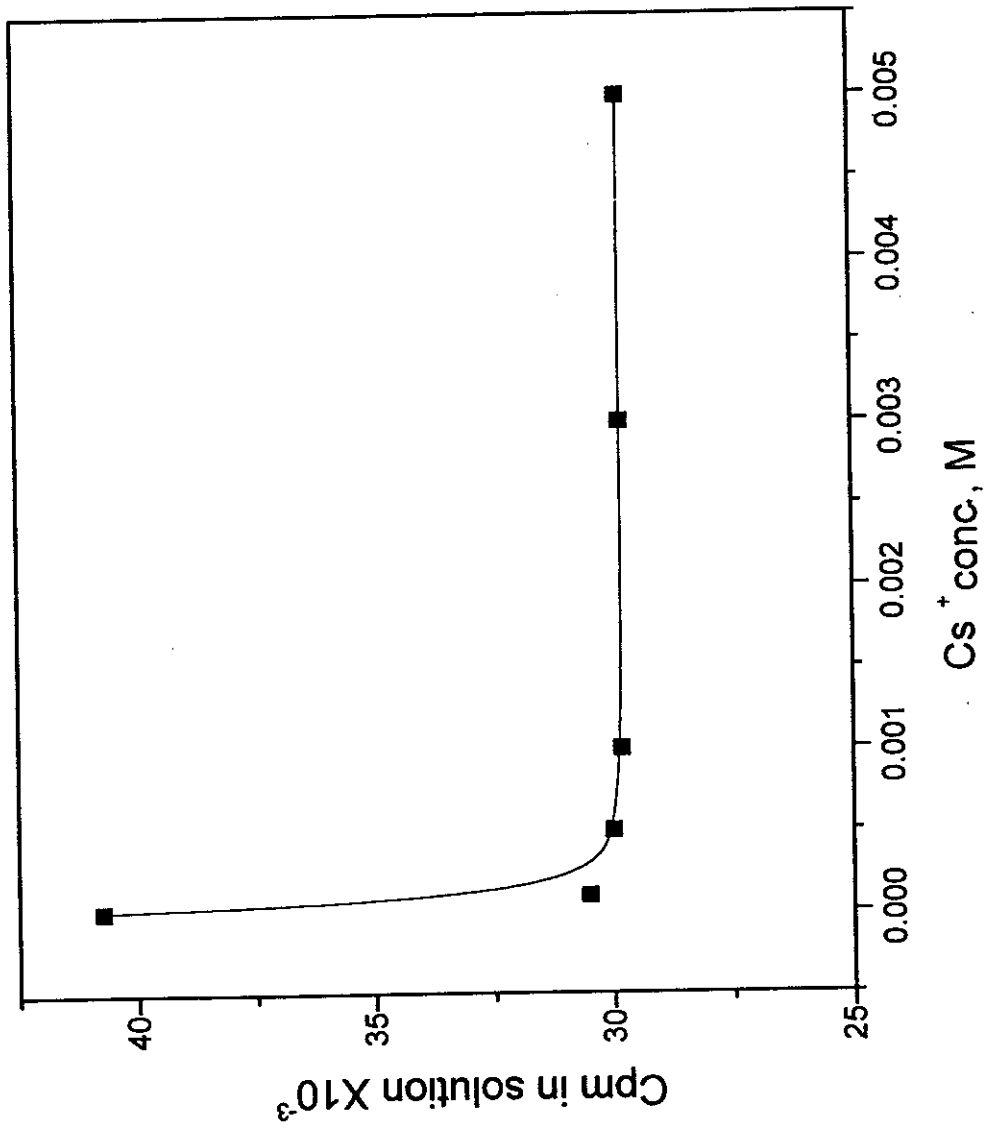
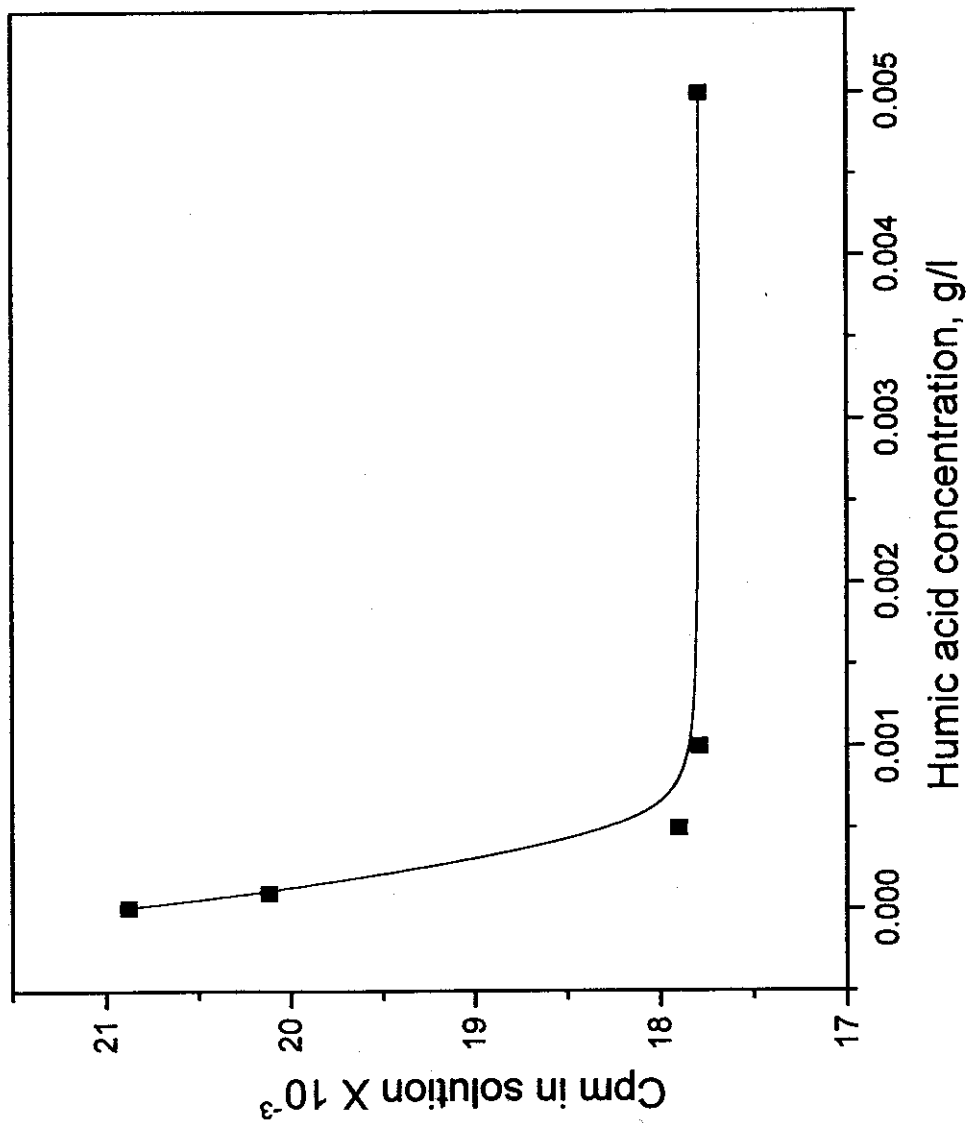


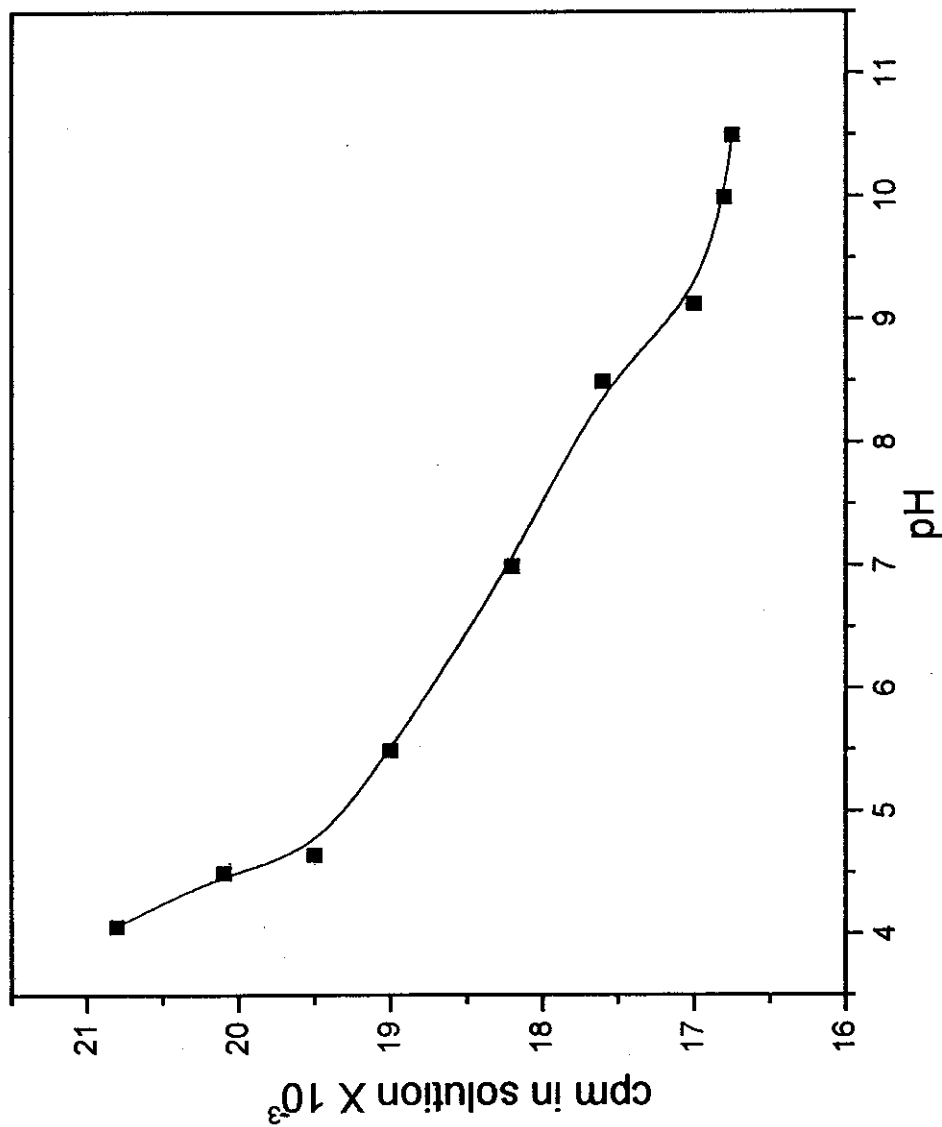
Fig.( 3.35): Effect of shaking time on the formation of Cs-humate complex.



Fig(3.36): Effect of cesium concentration on the formation of Cs-humate complex



Fig(3.37): Effect of humic acid concentration on the formation of Cs-humate complex.



Fig(3.38): Effect of pH on the formation of Cs-humate complex.

This can enhance the attraction of the  $\text{Cs}^+$  cations (i.e. binding of  $\text{Cs}^+$ ) on to the humic acid with subsequent formation of cesium-humate complex. At low pH, the competition effect of  $\text{H}^+$  ion with  $\text{Cs}^+$  ions for anionic binding sites on humic acid is high and causes a decrease in the binding process.

### 3.2.2.2 Ion-selective electrode investigations

Increasing use has been made of ion-selective electrode (ISE)) for determining the speciation of trace elements in the soil solution, as well as natural waters. A major limitation of ISE is its low sensitivity. The electrode response is affected by pH, ionic strength, and sorption of organics on the electrode surface.

To estimate the sensitivity of ISE, the investigations of Cs-humate complexation carried out radiometrically, as indicated above, were carried using ISE. The calibration curve for the sensor by  $\text{Cs}^+$  ion is shown in Fig.(3.39).

#### a) Effect of shaking time:

Fig.(3.40) illustrates the effect of shaking time on the complexation of  $\text{Cs}^+$  by humic acid. It is noted that the behaviour is almost similar to that obtained radiometrically where the time needed for equilibration is also 60 minutes.

#### b) Effect of $\text{Cs}^+$ concentration:

Fig. (3.41) shows the effect of metal ion concentration on the formation of the complex. The complexed  $\text{Cs}^+$  concentration is a measure of complexation. It is clear that the rate of formation of Cs-humate complex increase sharply, then gradually after the consumption of humic acid.

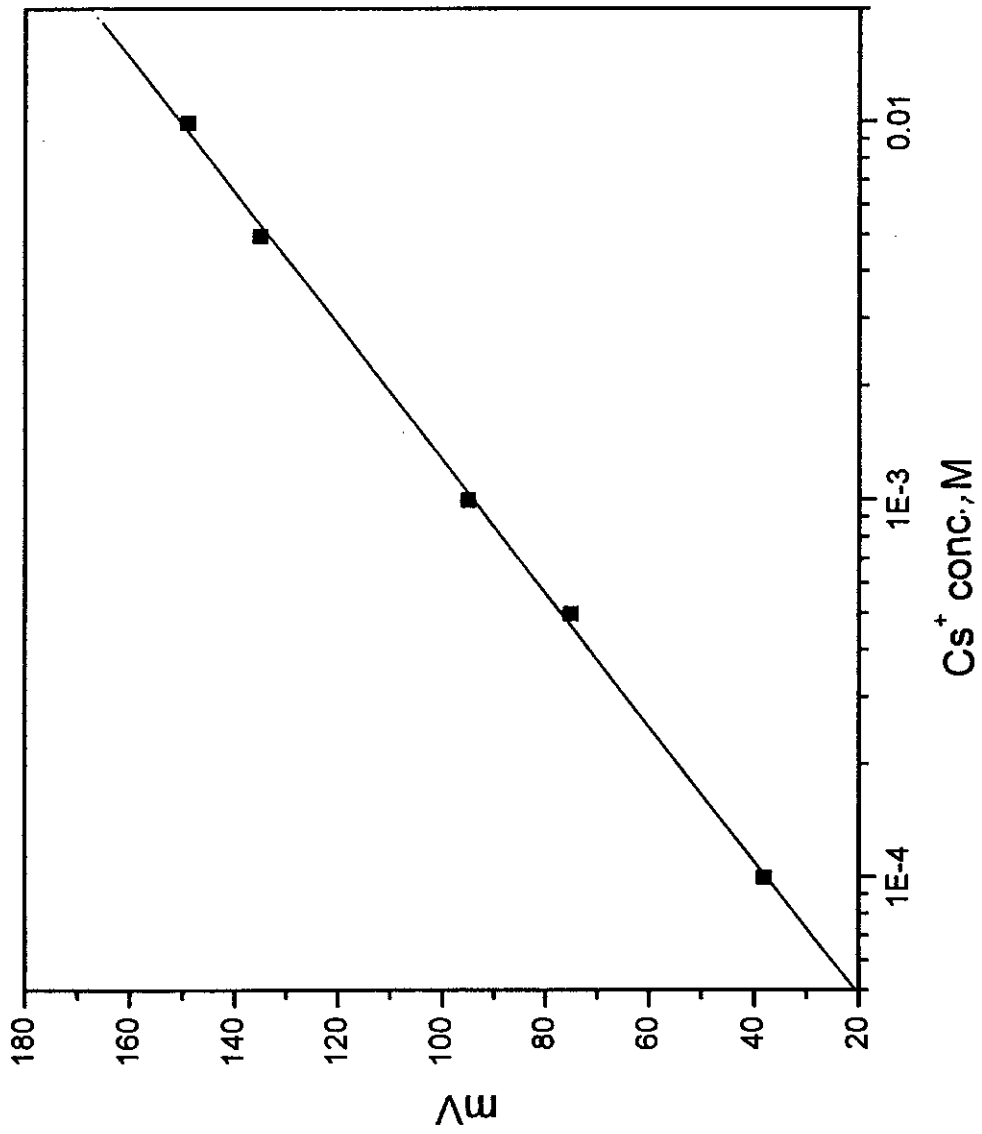


Fig.(3.39): Calibration curve of the sensor, using Cs<sup>+</sup>.



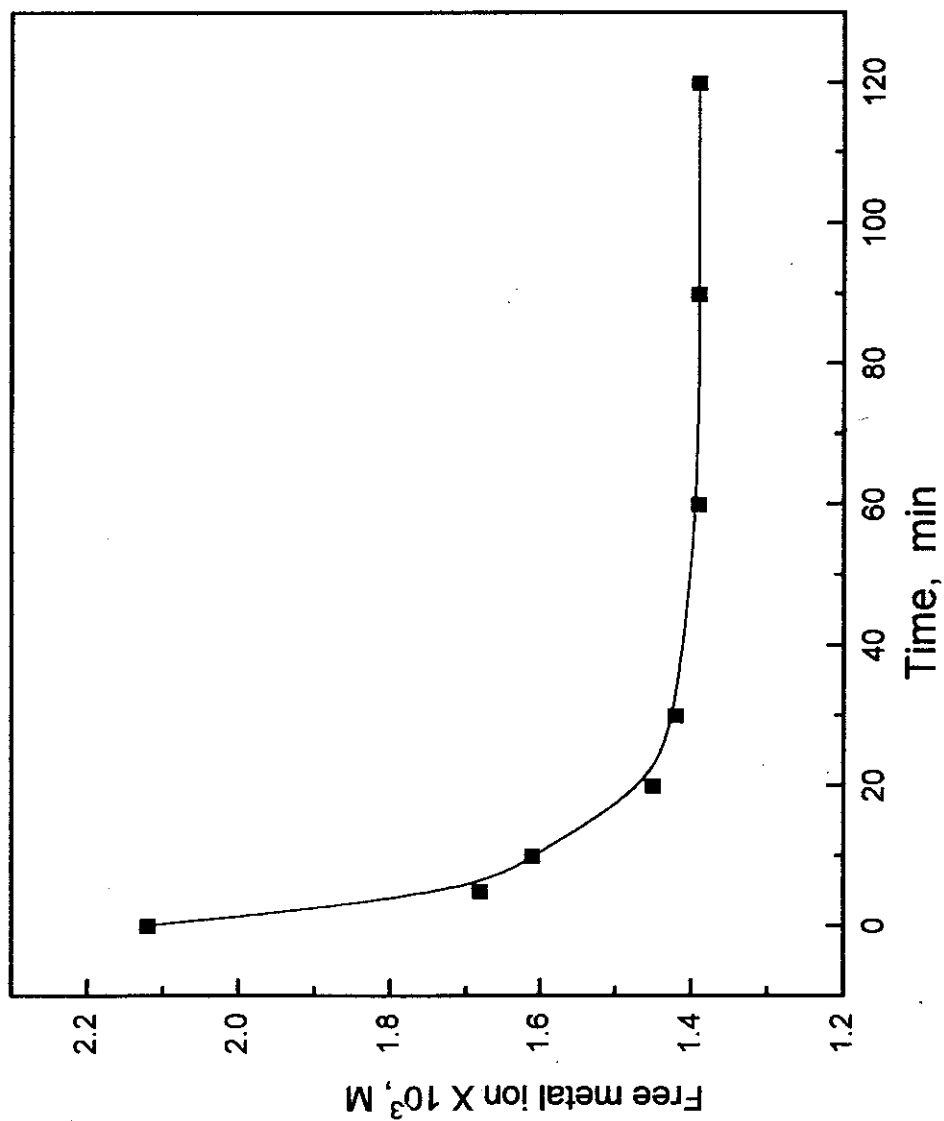


Fig. (3.40): Effect of shaking time on the formation of Cs - humate complex, at pH 5.8.

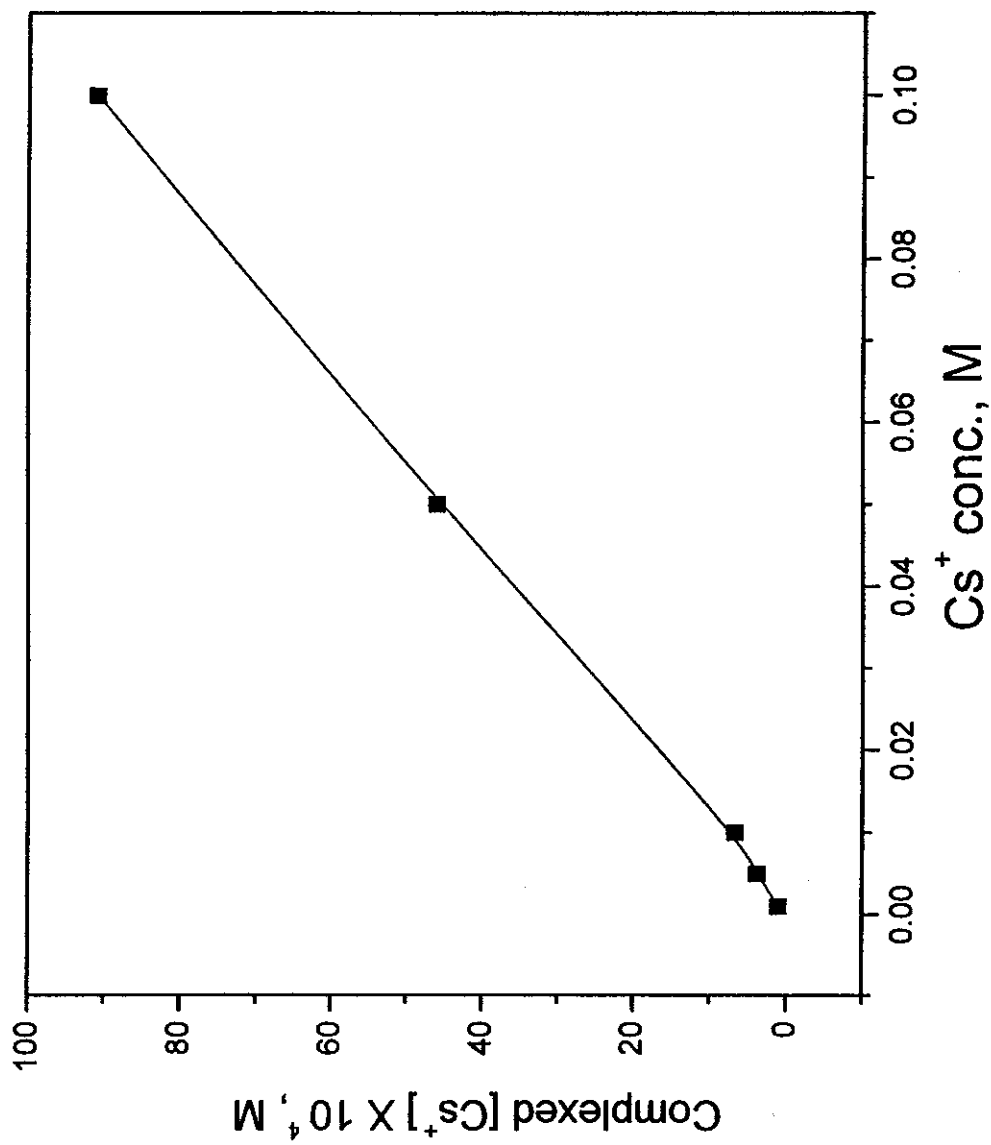


Fig. (3.41): Effect of Cs<sup>+</sup> concentration on the formation of Cs-humate complex at pH 5.8.

### **c) Effect of humic acid concentration**

Fig. (3.42) indicates the effect of increasing humic acid concentration on the formation of Cs-humate complex. The apparent increase in the free  $\text{Cs}^+$  after consumption of  $\text{Cs}^+$  ions is related to the increase in the ionic strength, since humic acid is dissolved in NaOH. The similarity of the two figures (3.36,3.37) confirms the formation of the complex. The amount of  $\text{Cs}^+$  suitable for complexation of  $5 \times 10^{-4}$  g/l of humic acid is found  $1.5 \times 10^{-3}$  M.

#### **3.2.2.1) Cs-Fulvate complexation**

The complexation of  $\text{Cs}^+$  with fulvic acid was investigated by ISE. As Figures (3.43, 3.44) show, fulvic acid has no ability to complex  $\text{Cs}^+$ . The free metal concentration was not affected by the presence of fulvic acid either by changing the metal ion concentration or the fulvic acid concentration.

#### **3.2.2.2) Sorption of $\text{Cs}^+$ by humin:**

The sorption of  $\text{Cs}^+$  by humin was studied by batch technique using ion selective electrode.

##### **a) Effect of humin weight:**

Figs. (3.45, 3.46) illustrate the sorption behavior of  $\text{Cs}^+$  by humin at different weights of the sorbent. The percentage of uptake (which is inversely proportional to the free metal ion) increases by increasing the weight of humin, then becomes constant at equilibration. The weight required to reach saturation was found (0.01) g. The maximum uptake was found 26 % which is agree with that obtained previously<sup>[105]</sup> for the sorption of  $^{137}\text{Cs}$  by humin, by radiometric measurements.

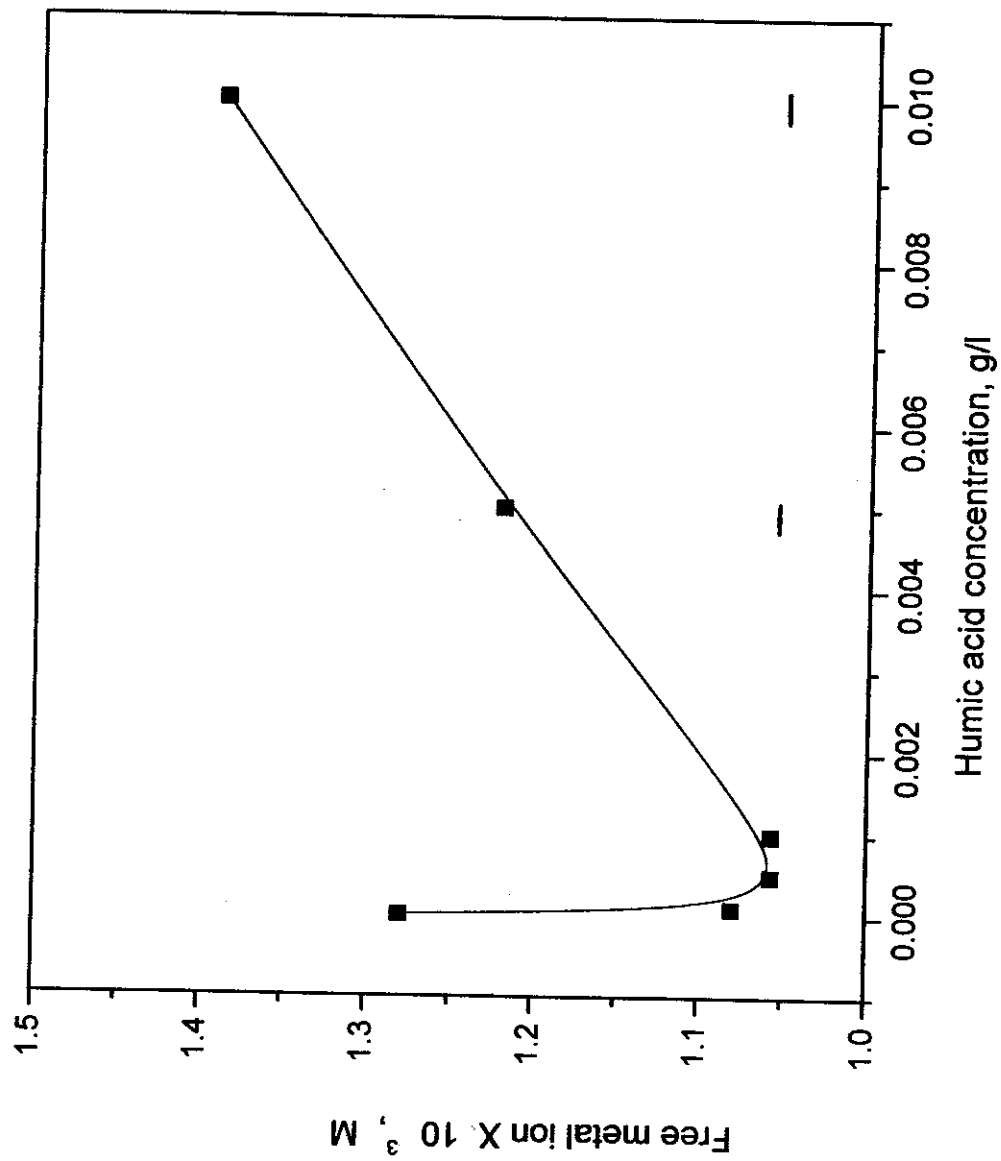


Fig. (3.42): Effect of humic acid concentration on the formation of Cs-humate complex, at pH 5.8.

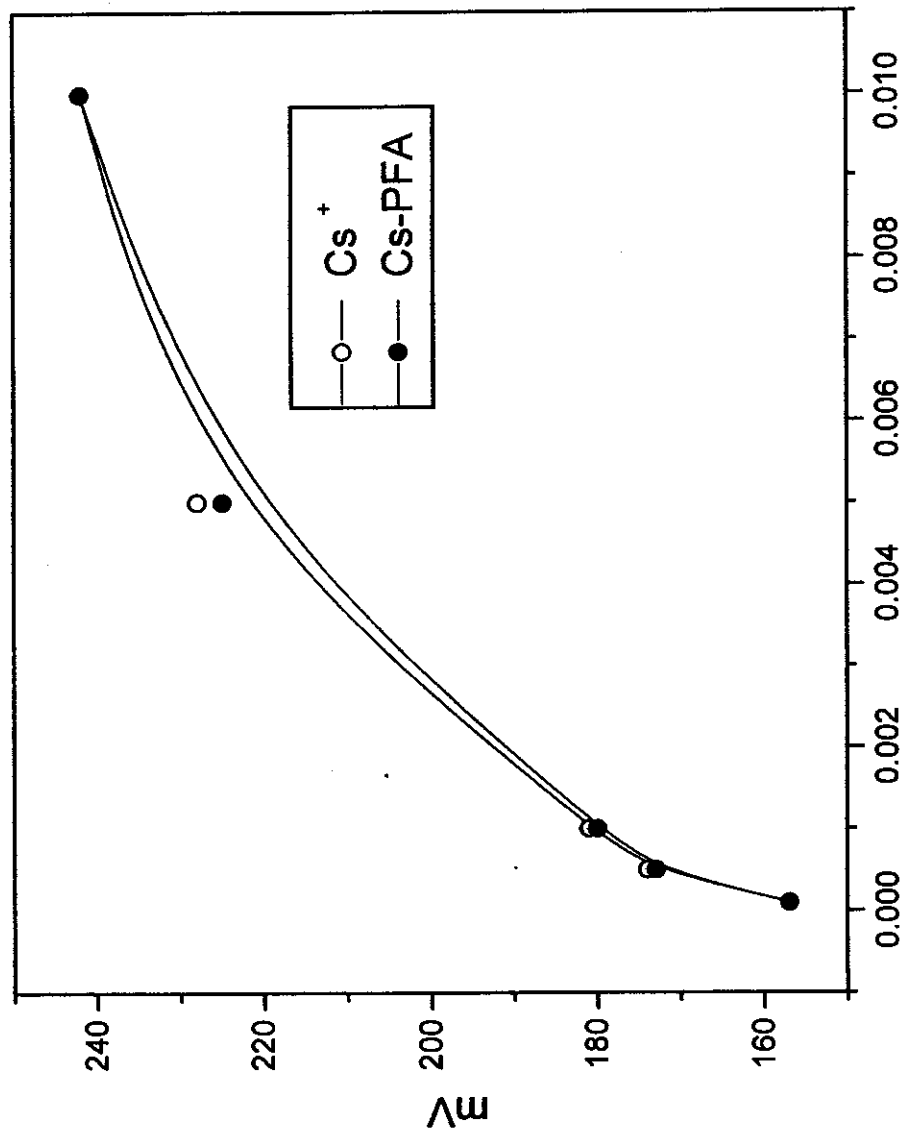


Fig (3.43): Effect of Cesium concentration on the formation of Cs-fulvate complex, at pH 5.8.

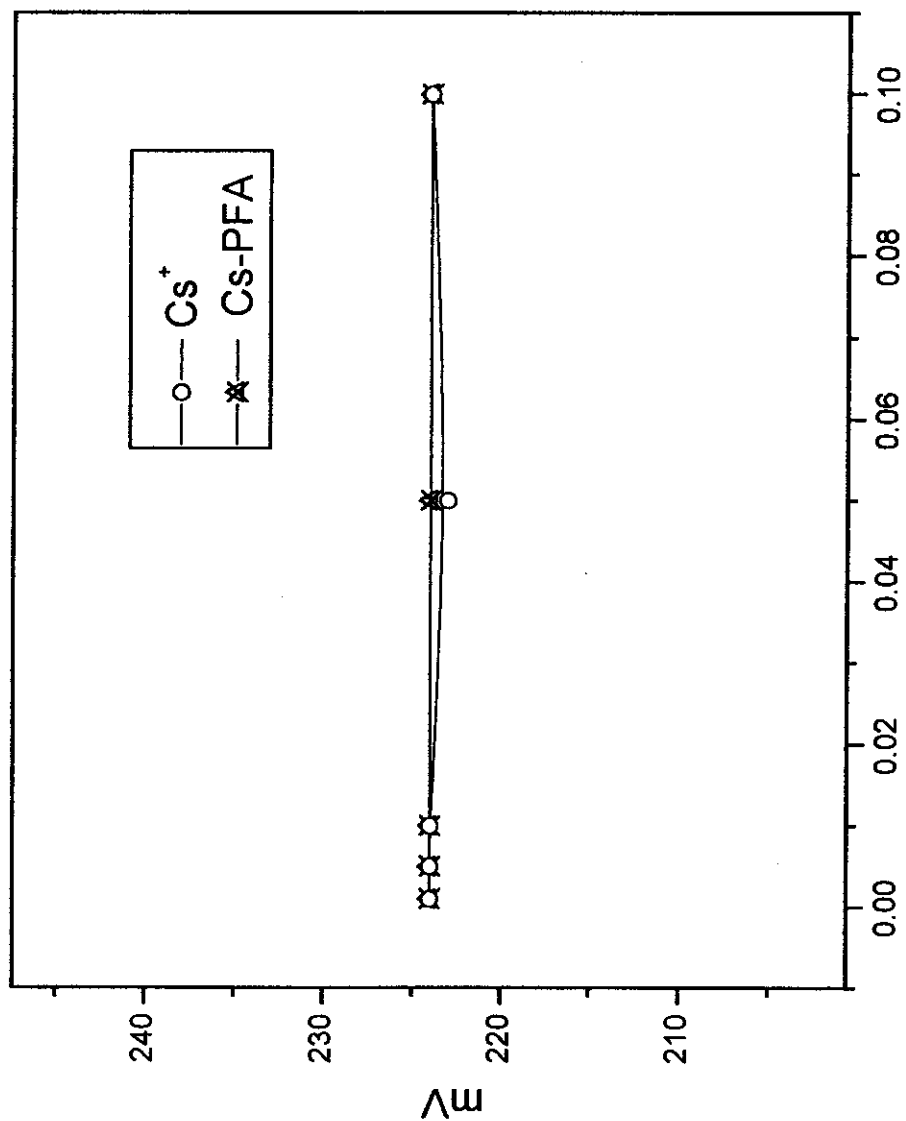


Fig.(3.44 ): Effect of peat fulvic acid on the formation of Cs-fulvate complex at pH 5.8.

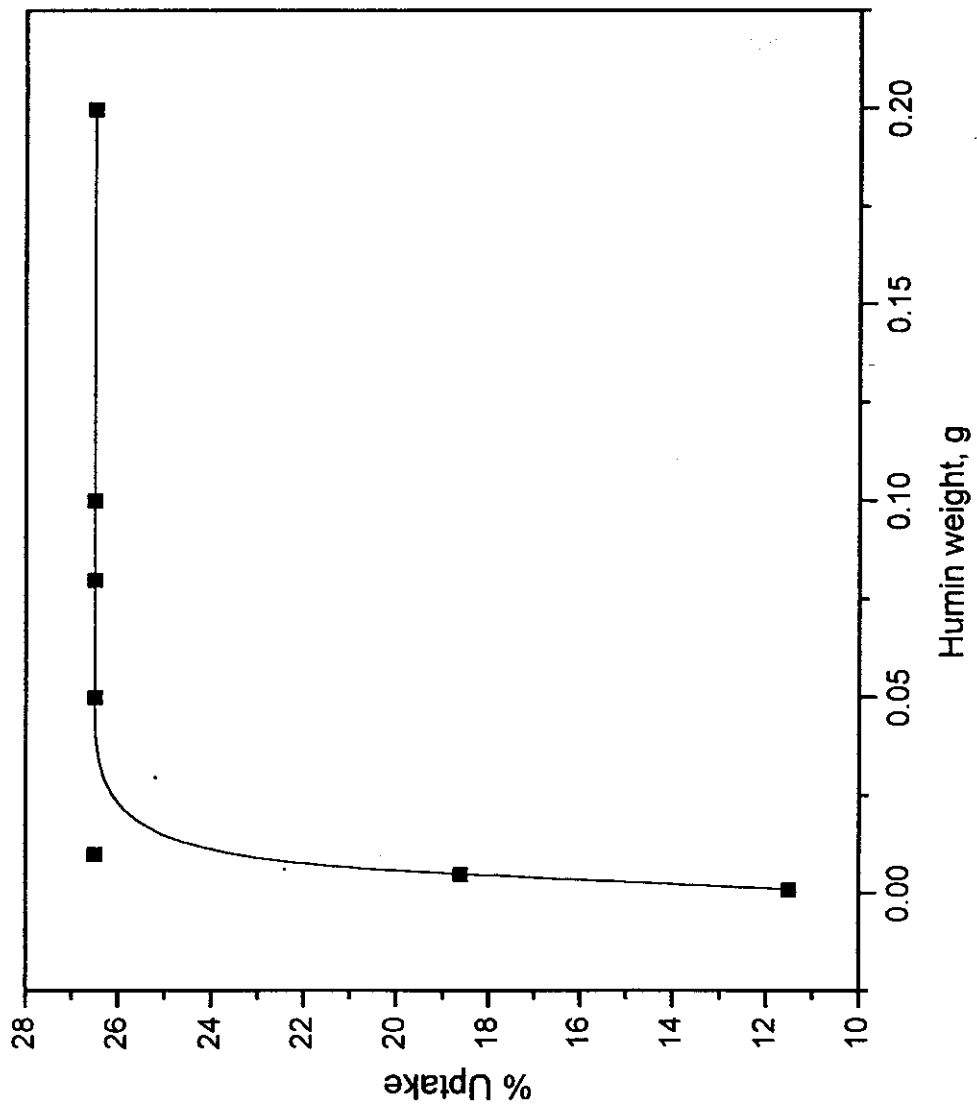


Fig.(3.45): Effect of humin weight on the sorption of Cs<sup>+</sup> by humin, at pH 5.8.

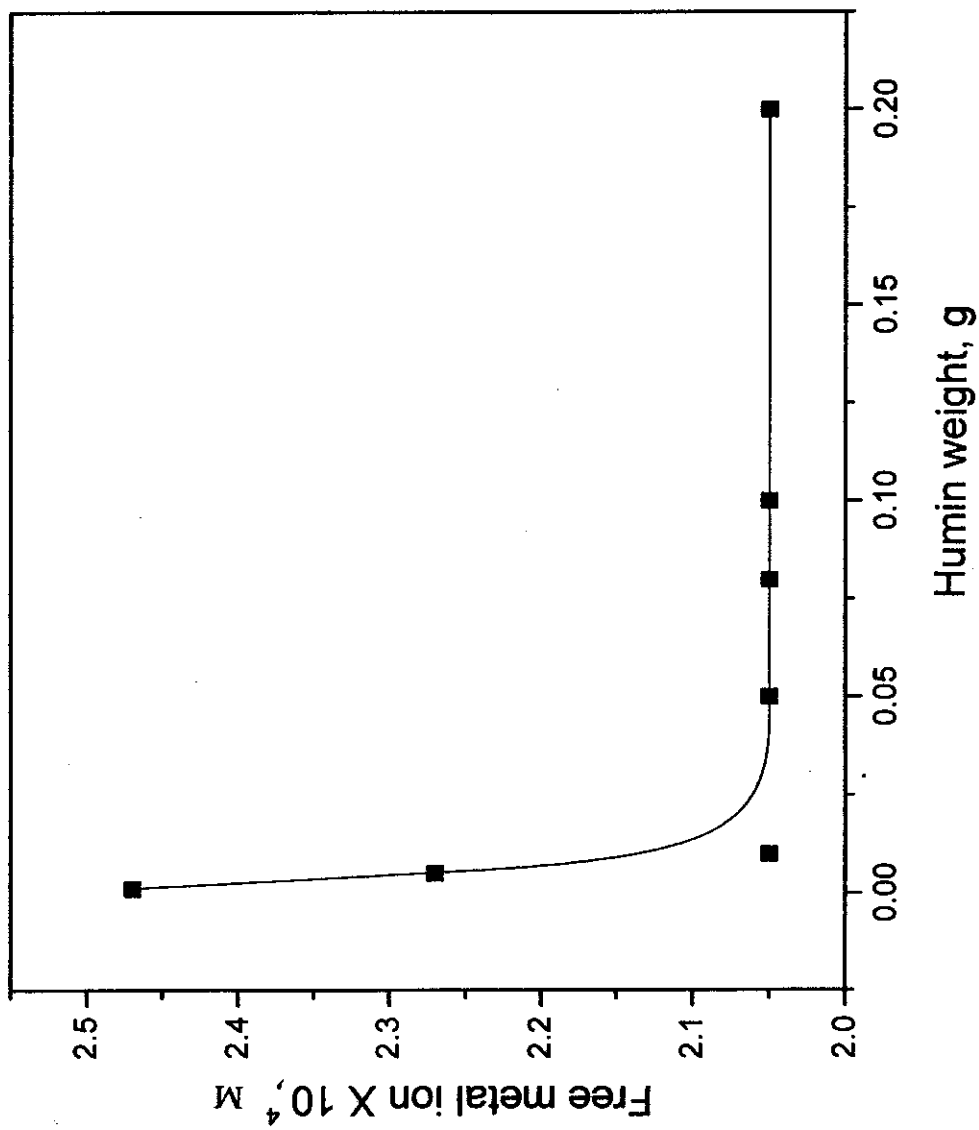


Fig.(3.46): Effect of humin weight on the sorption of  $\text{Cs}^+$  by humin, at pH 5.8.



**b) Rate of uptake:**

The effect of shaking time on the sorption of cesium by humin at pH 5.8 is indicated in Fig. (3.47). The rate of sorption is found to increase directly with the contact time to reach equilibrium at 60 minutes. This shows that the sorption process is of time dependence.

**c) Effect of metal ion concentration:**

Fig. (3.48) illustrates the variation of % uptake with  $\text{Cs}^+$  ion concentration. Fig. (3.49) shows the concentration of free metal ion as a function of the  $\text{Cs}^+$  ion concentration. It is clear that the free metal ion concentration increases with increasing the initial ion concentration, indicating that the humin is saturated and the additional ions remain in solution. By plotting the amount of metal retained by humin against the metal ion concentration (Fig. 3.49, 3.50), the behavior was found similar to that obtained above where the amount of metal retained increased sharply with increasing initial metal ion concentration to reach a maximum retention, then becomes constant at saturation. The maximum represents the saturation capacity of humin towards  $\text{Cs}^+$  ions. The amount of  $\text{Cs}^+$  required for saturation was calculated from the maximum in Fig.(3.48) and found 3.72 mg metal /g humin.

**3.2.3) Interaction of lead with humic materials:**

The interaction of  $\text{Pb}^{2+}$  with the different fractions of humic materials: humic acid, fulvic acid and humin was investigated using the ISE. Fig(3.51) illustrates the calibration curve of the used sensor at different concentrations of  $\text{Pb}^{2+}$ .

**3.2.3.1) Lead-humate complexation:**

Lead-humate complex is formed by adding  $\text{Pb}^{2+}$  ions to humic acid solution till complete precipitation. The investigation is carried out by shaking the humic acid with the  $\text{Pb}^{2+}$  solution. As a preliminary study, the system was shaken at different periods of time to know the

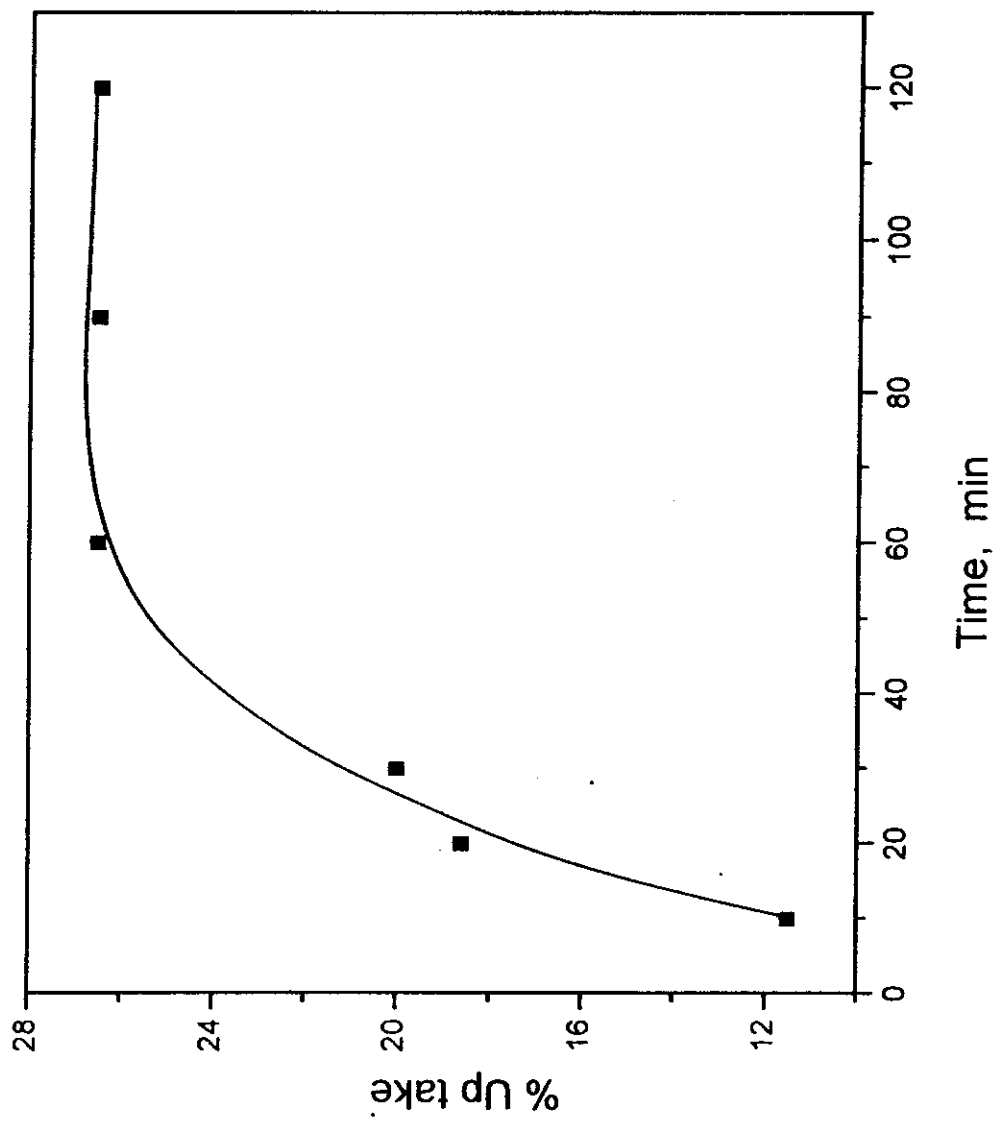
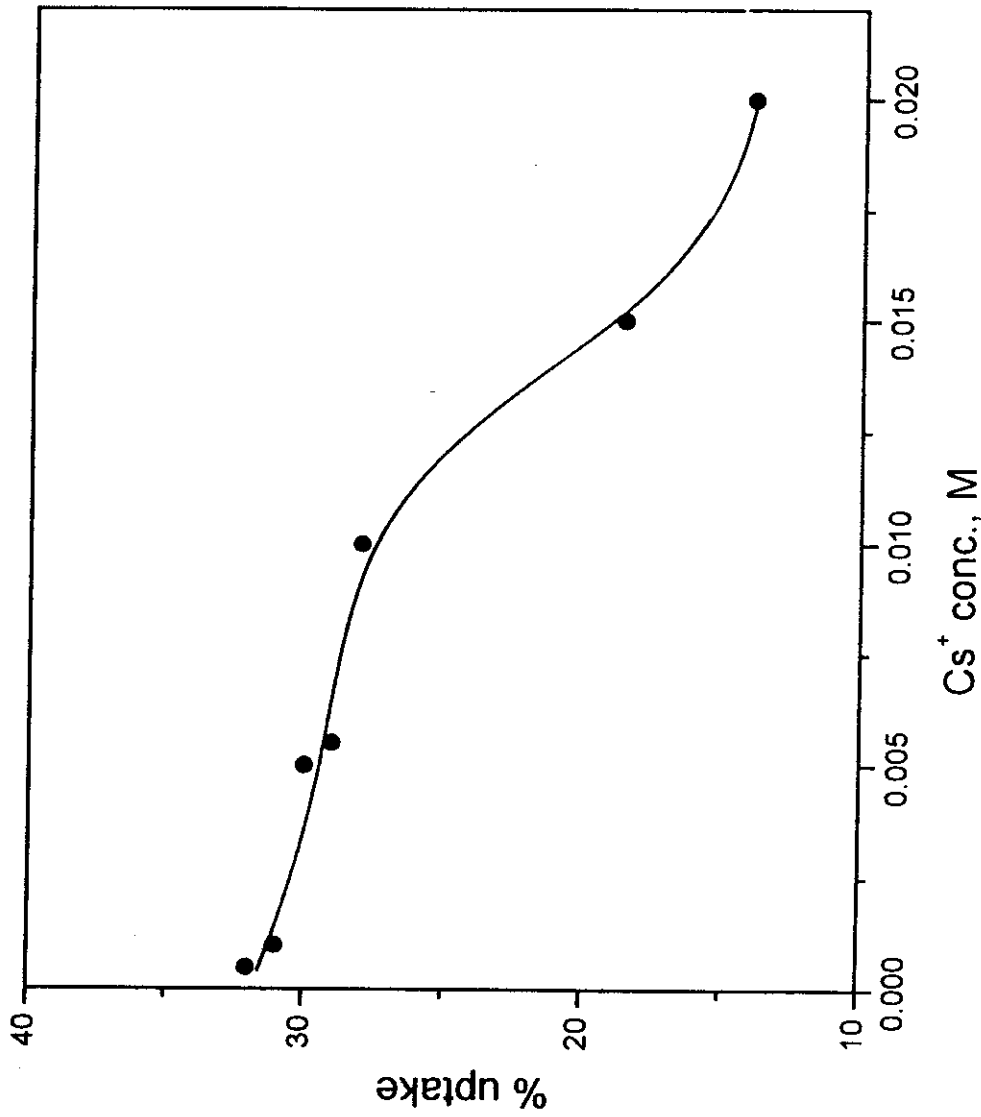


Fig. (3.47): Effect of shaking time on the sorption of Cs<sup>+</sup> by humin, at pH 5.8.



Fig( 3.48): Effect of metal coccentration on the sorption of Cs<sup>+</sup> by humin at pH 5.8..

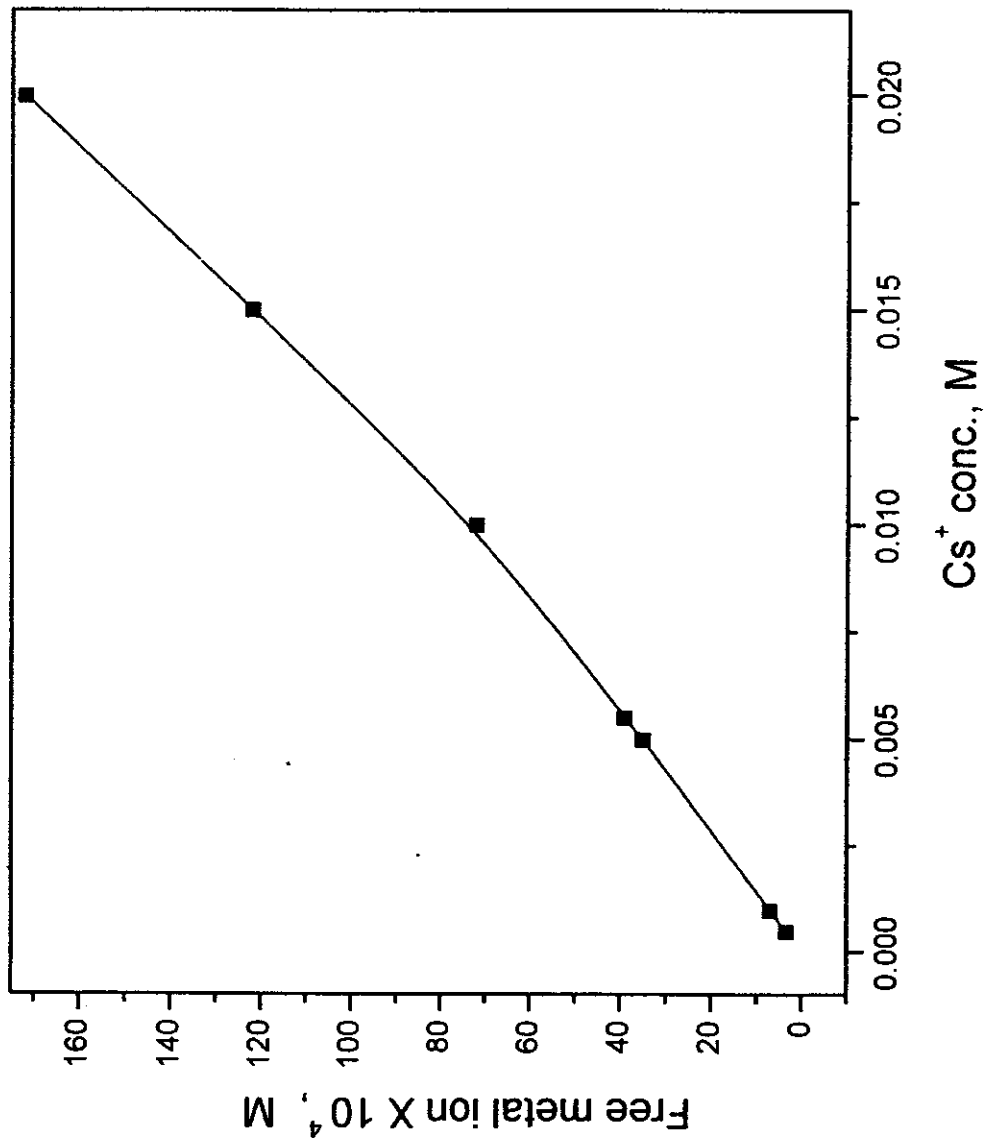


Fig. ( 3.49): Effect of metal concentration on the sorption of  $\text{Cs}^+$  by humin at pH 5.8.

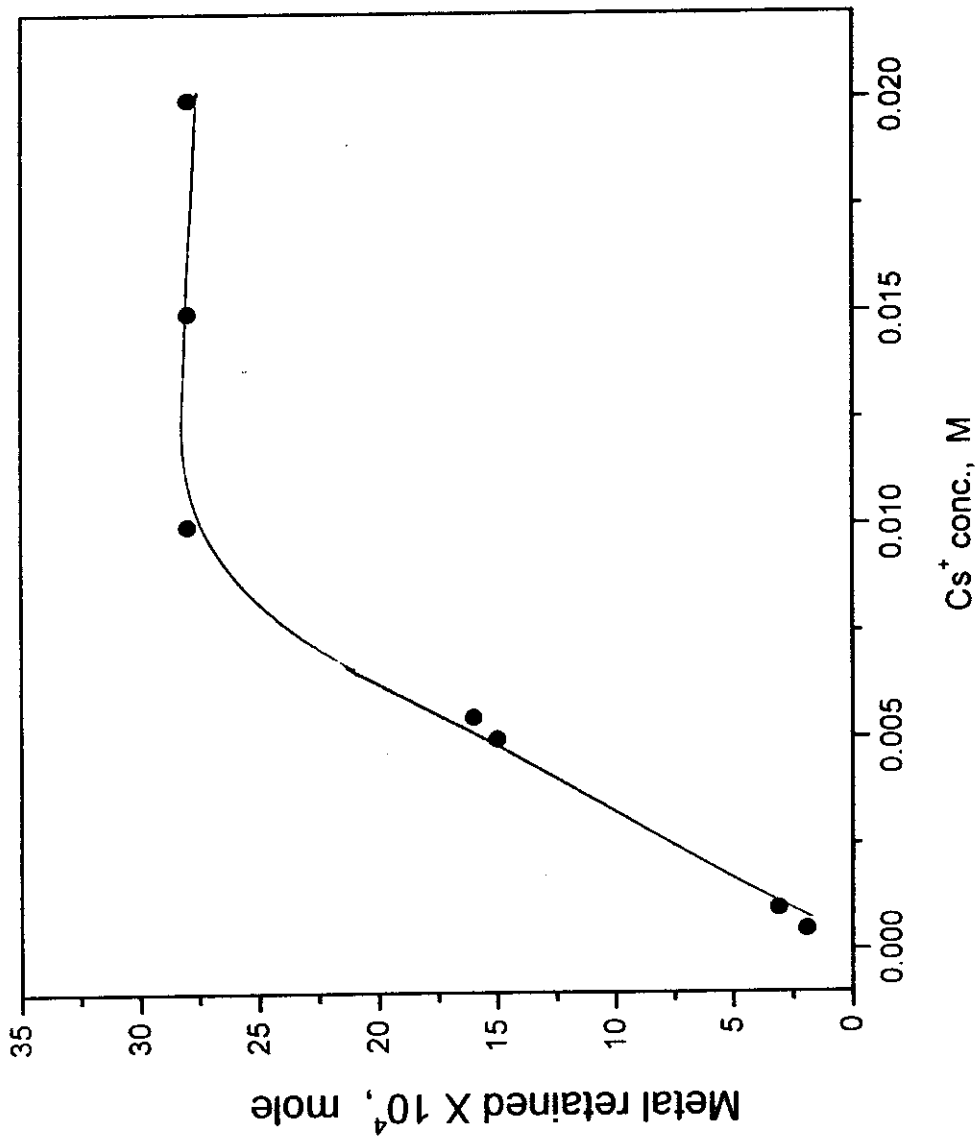


Fig.(3.50): Variation of metal retained on humin with  $\text{Cs}^+$  concentration, at pH 5.8.

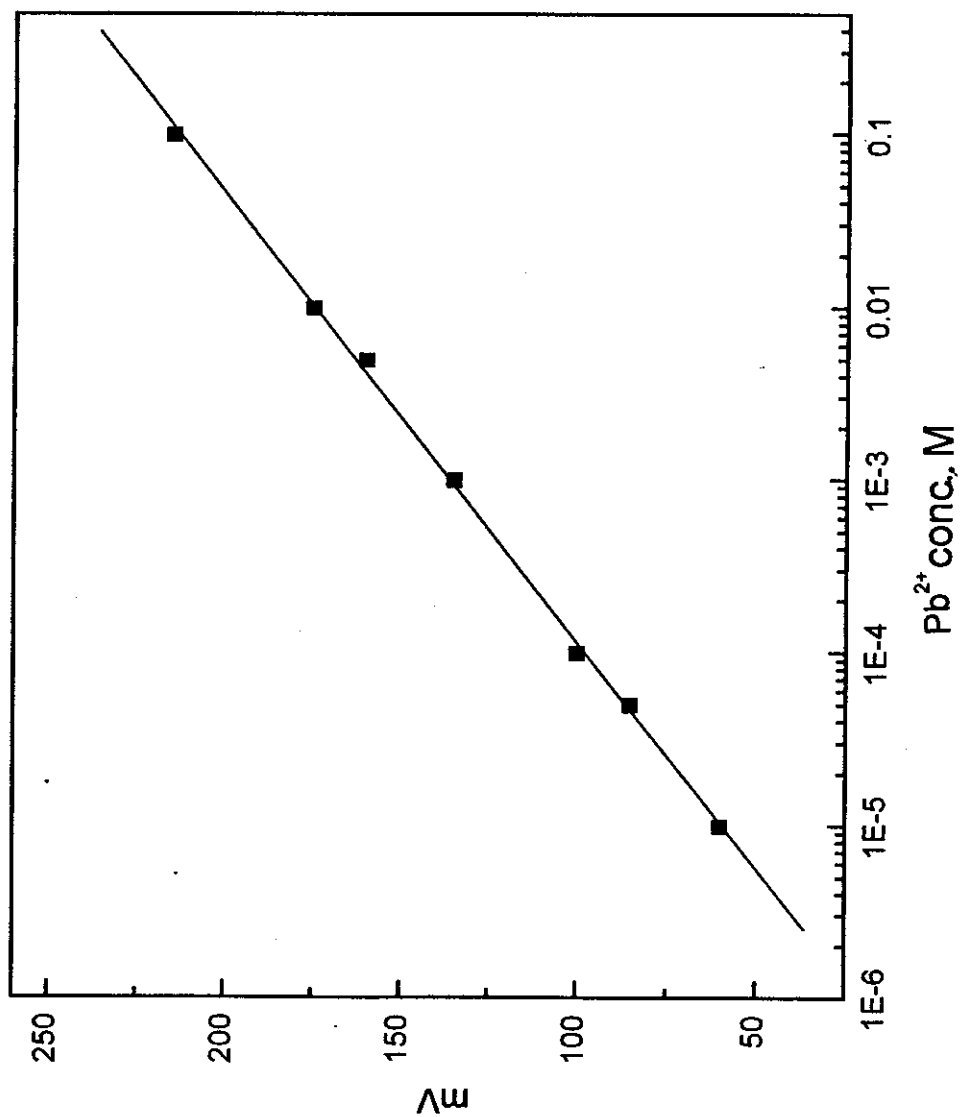


Fig.(3.51): Calibration curve for sensor of ZTP based electrode towards  $Pb^{2+}$  ion.

suitable time of equilibration. As Fig.(3.52) show, it is clear that the time required for complete equilibration is about 20 minutes. Fig. (3.53) shows the effect of metal ion concentration on the formation of the complex. The complexed  $Pb^{2+}$  concentration is a measure of complexation. It is clear that the rate of formation of Pb-humate complex increases sharply, then gradually after the consumption of humic acid.

Fig.(3.54) indicates the effect of increasing humic acid concentration on the formation of Pb-humate complex. The apparent increase in the free  $Pb^{2+}$  after consumption of lead ions is related to the increase in the ionic strength, since humic acid is dissolved in NaOH. The similarity of the two figures (3.48 and 3.49) confirms the formation of the complex.

#### **3.2.3.2) Lead-Fulvate complexation:**

The same procedure was applied for the formation of lead-fulvate complex, as illustrated above (in the lead-humate complexation). The time required for complexation of Pb-fulvate is longer than that for Pb-humate, as indicated in Fig.(3.55). The free metal concentration is decreased gradually with time showing an increase in the formation of Pb-fulvate complex, then the rate of formation becomes constant at saturation.

Fig. (3.56) illustrates the rate of formation of Pb-fulvate complex as a function of fulvic acid concentration. The amount of complex is increased sharply till the point of consumption of  $Pb^{2+}$  where the free metal becomes constant. The difference between this figure and that obtained for Pb-humate (Fig.3.54) is related to the constancy of ionic strength in case of Pb-fulvate complexation, where fulvic acid is dissolved in water.

The variation of the amount of complexed  $Pb^{2+}$  with the original lead concentration is shown in Fig.(3.57). It is clear that the rate of formation of Pb-fulvate complex increases gradually in a lower rate than that of humic acid (Fig(3.53)).

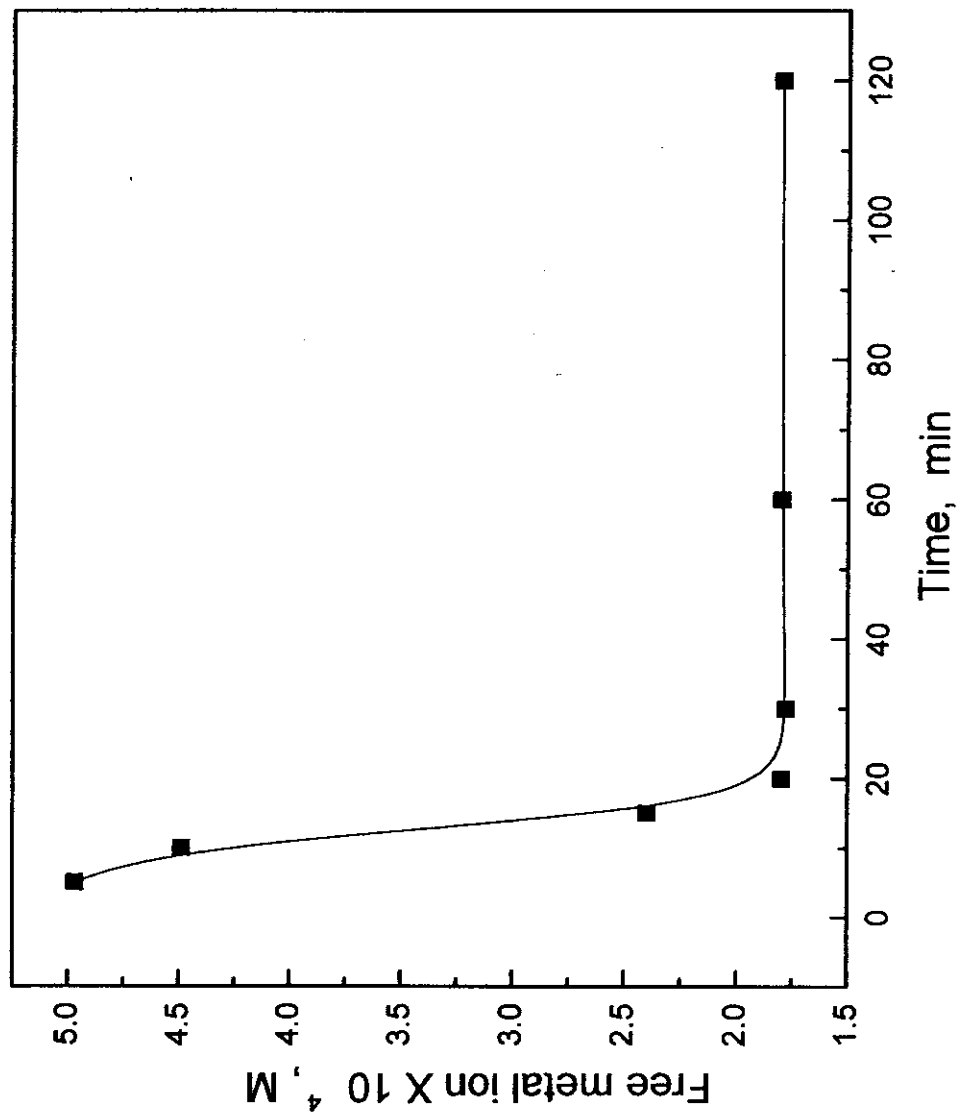


Fig. ( 3.52): Effect of shaking time on the formation of lead-humate complex, at pH 5.8.



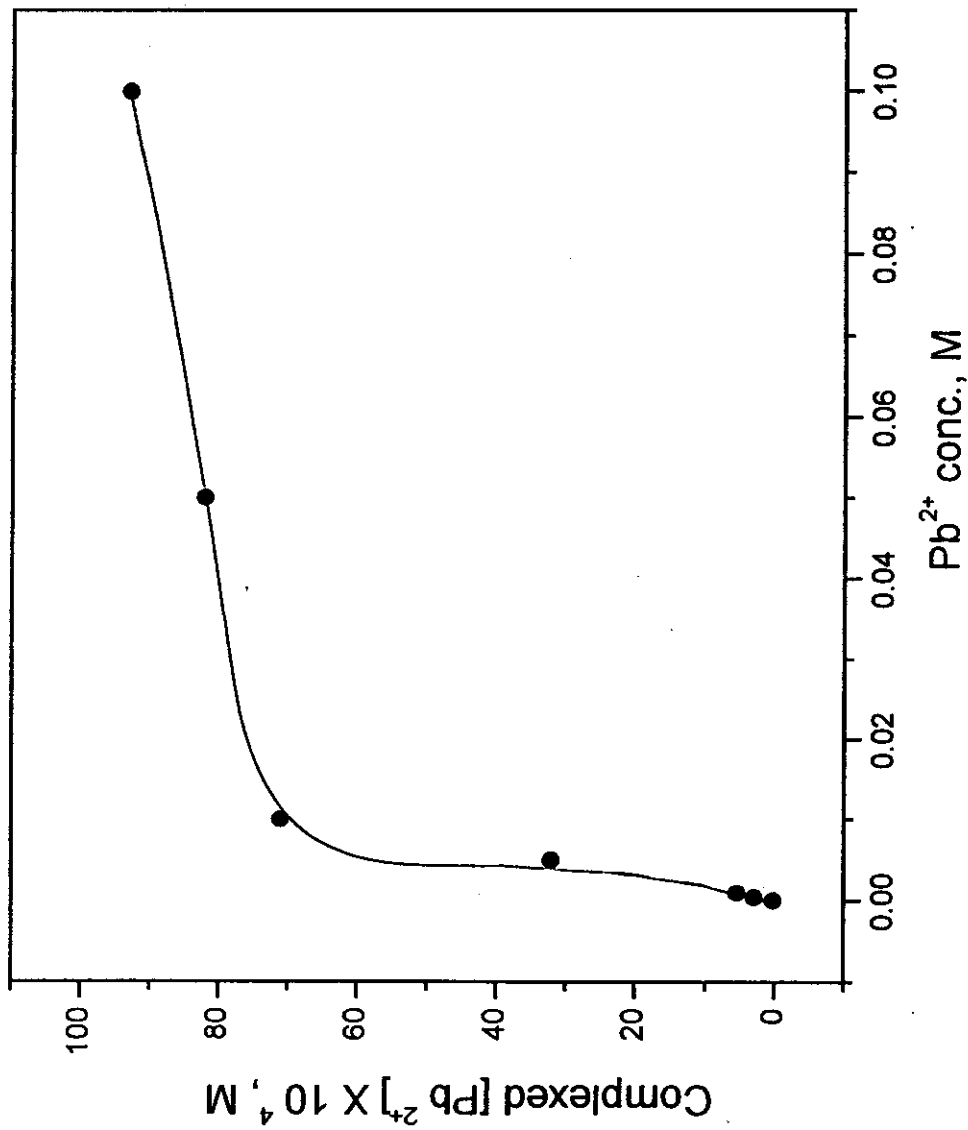


Fig. (3.53): Effect of  $\text{Pb}^{2+}$  concentration on the formation of lead-humate complex at pH 5.8.

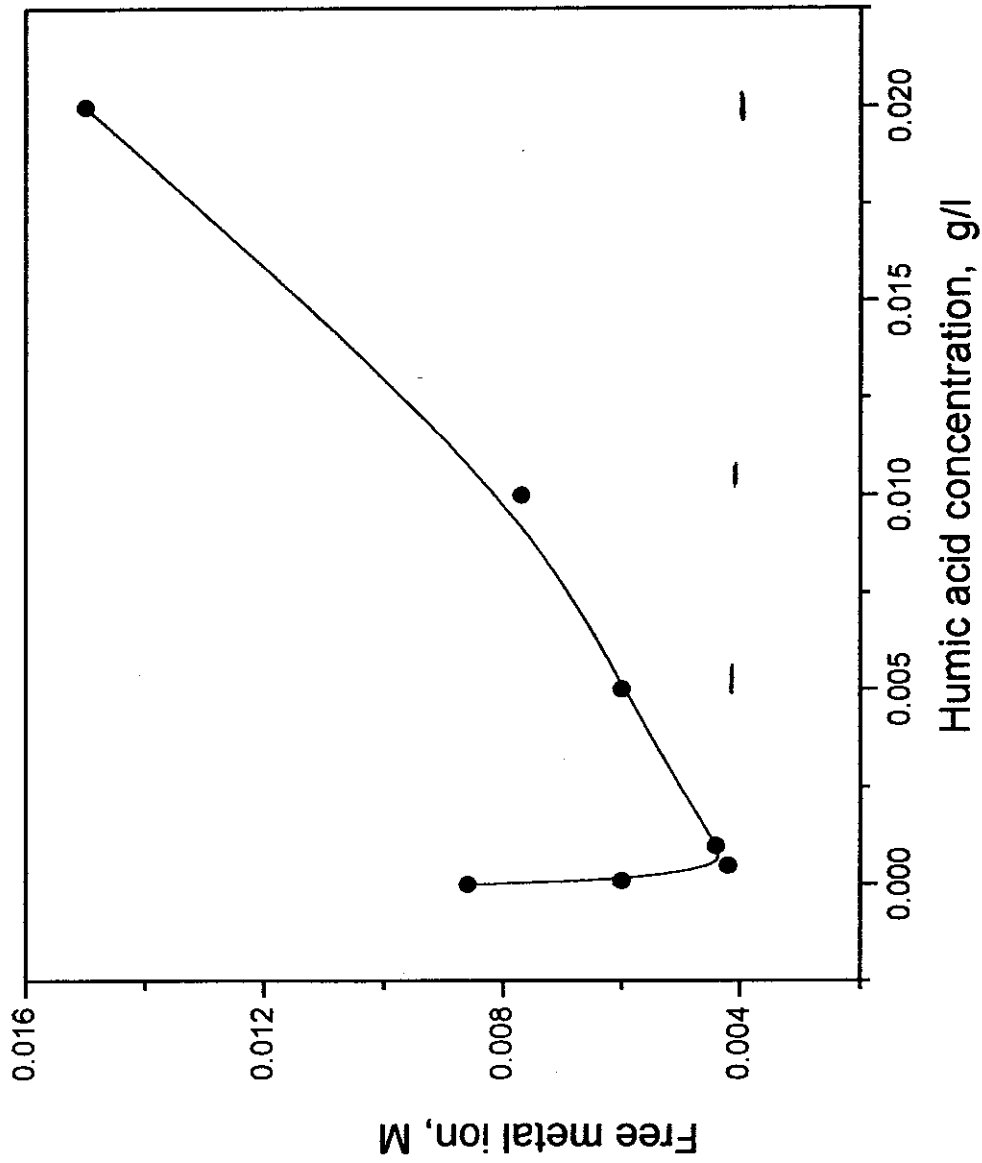
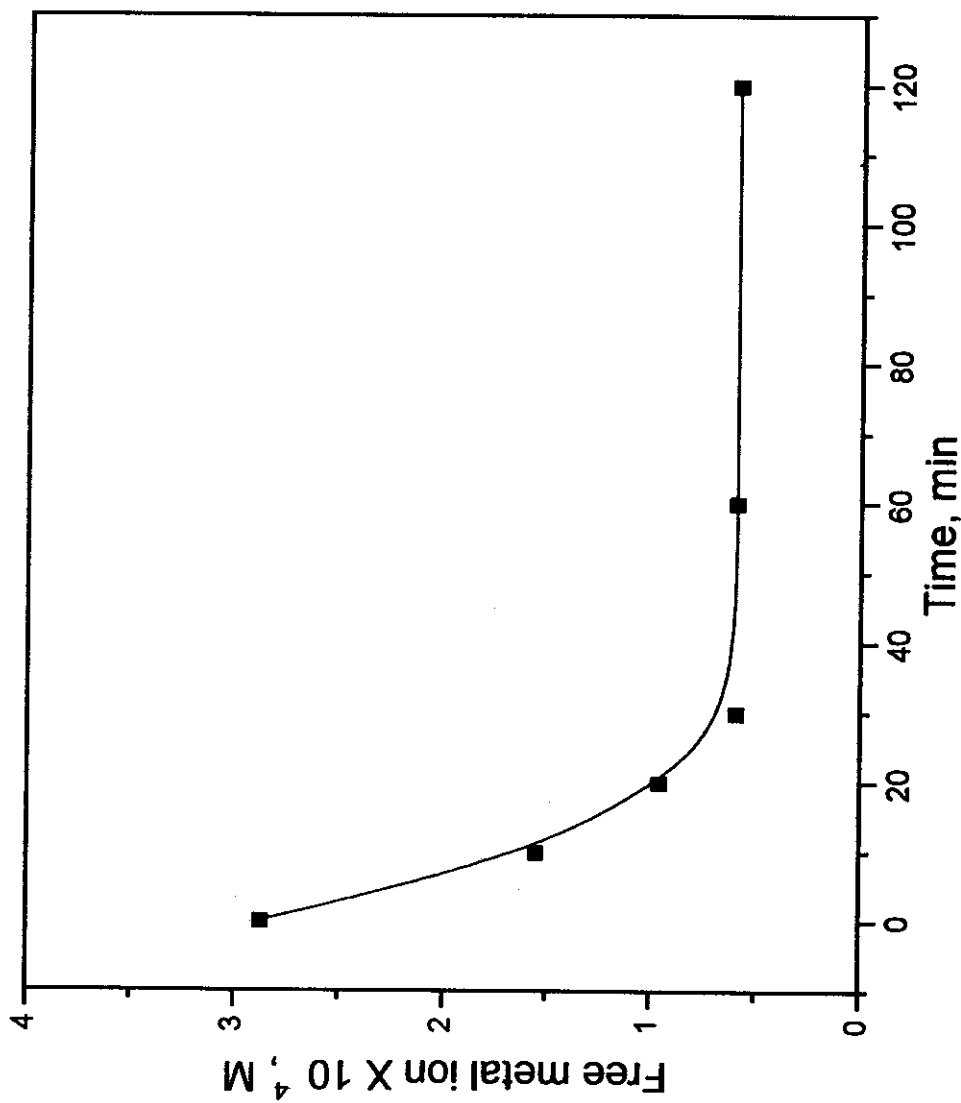
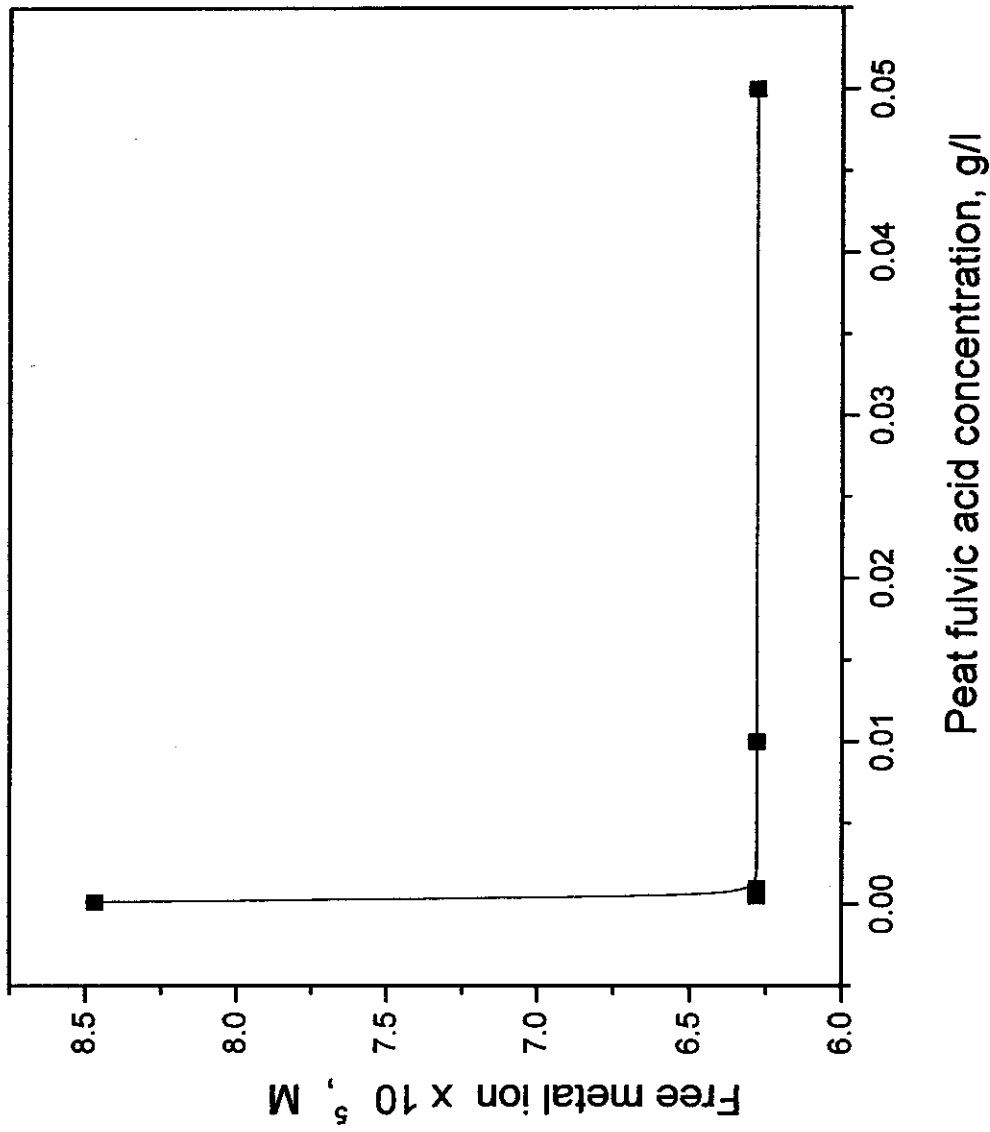


Fig (3.54): Effect of humic acid concentration on the formation of lead-humate complex at pH 5.8.



Fig(3.55): Effect of shaking time on the formation of Pb-Fulvate complex, at pH 5.8.



Fig(3.56) : Effect of PFA on the formation of Pb-fulvate complex, at pH 5.8.

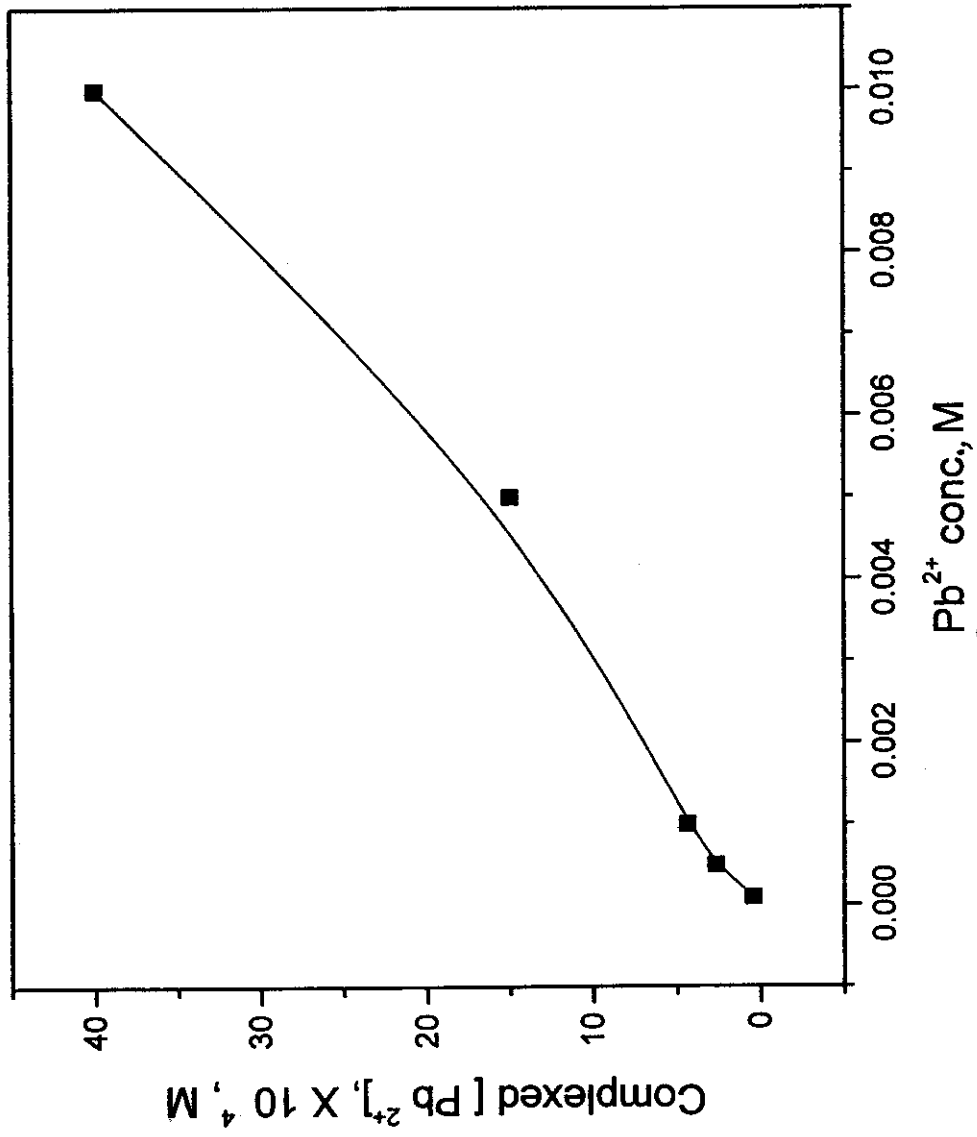


Fig. (3.57): Effect of Pb<sup>2+</sup> concentration on the formation of lead-fulvate complex, at pH 5.8.

### 3.2.3.3) Sorption of $Pb^{2+}$ by humin:

The sorption of lead by humin was studied by batch technique using ISE.

#### a) Effect of humin weight:

Fig (3.58, 3.59) illustrate the sorption behavior of  $Pb^{2+}$  by humin at different weights of the sorbent. The percentage of uptake increases by increasing the weight of humin then becomes constant at equilibration. The weight required to reach saturation was found (0.15) g. The maximum uptake was found (96.2)%.

#### b) Rate of uptake:

The effect of shaking time on the sorption of lead by humin at pH 5.8 is indicated in Fig. (3.60). The rate of sorption is found to increase directly with the contact time to reach equilibrium at 30 minutes. This shows that the sorption process is of time dependence.

#### c) Effect of metal ion concentration:

Fig. (3.61) shows the concentration of free metal ion as a function of the  $Pb^{2+}$  ion concentration. It is clear that the free metal ion concentration increases with increasing the initial ion concentration, indicating that the humin is saturated and the additional ion remains in solution. By plotting the amount of percentage of uptake and metal retained by humin against the metal ion concentration (Fig. (3.62, 63), the behavior was found similar to that obtained above where the amount of metal retained increased sharply with increasing initial metal ion concentration to reach a maximum retention, then becomes constant at saturation. The maximum represents the saturation capacity of humin towards  $Pb^{2+}$  ions. The amount of  $Pb^{2+}$  required for saturation was calculated from the maximum in Fig.(3.63) and found 19.3 mg metal /g humin.

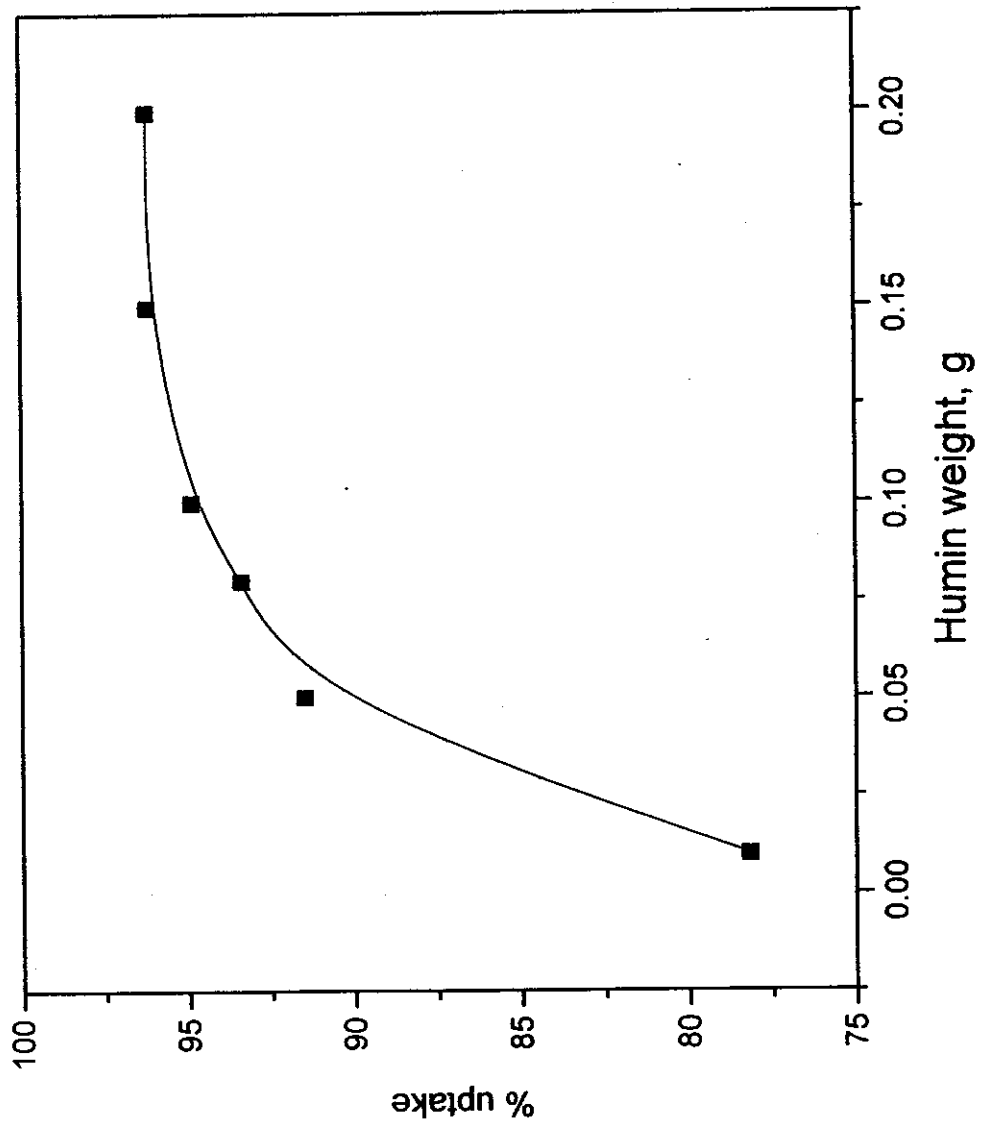


Fig.(3.58): Effect of humin weight on the sorption of  $Pb^{2+}$  by humin at pH 5.8.

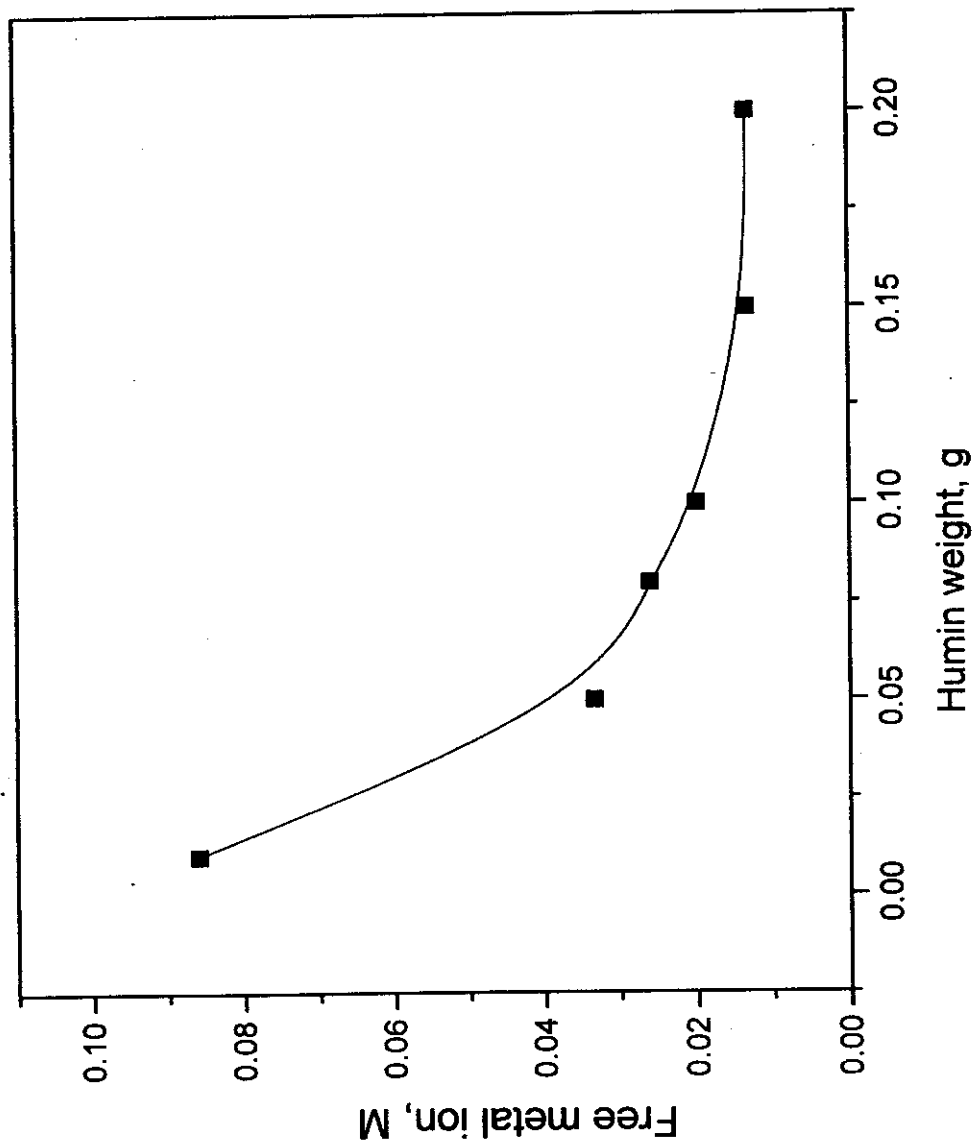


Fig. (3.59): Effect of humin weight on the sorption of  $Pb^{2+}$  by humin, at pH 5.8.



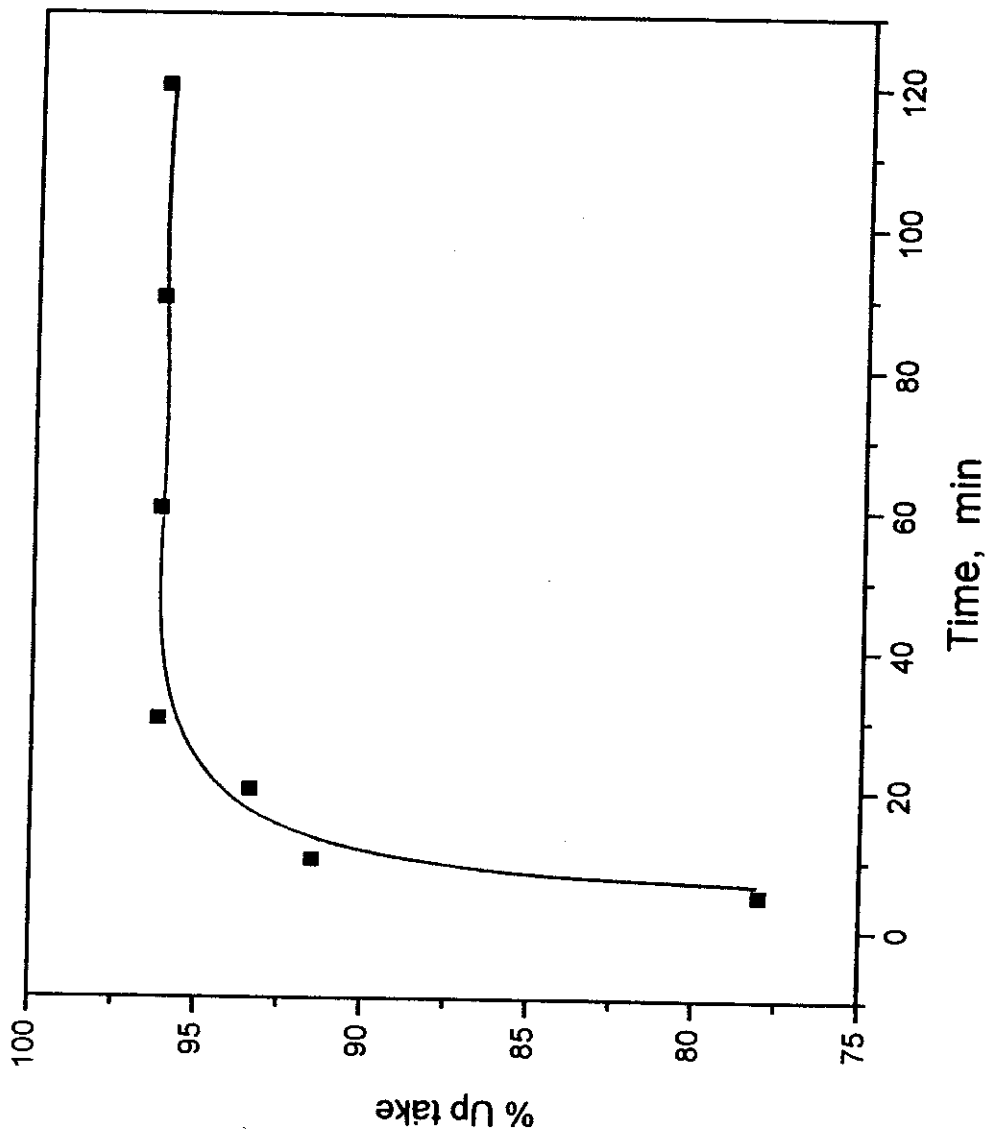
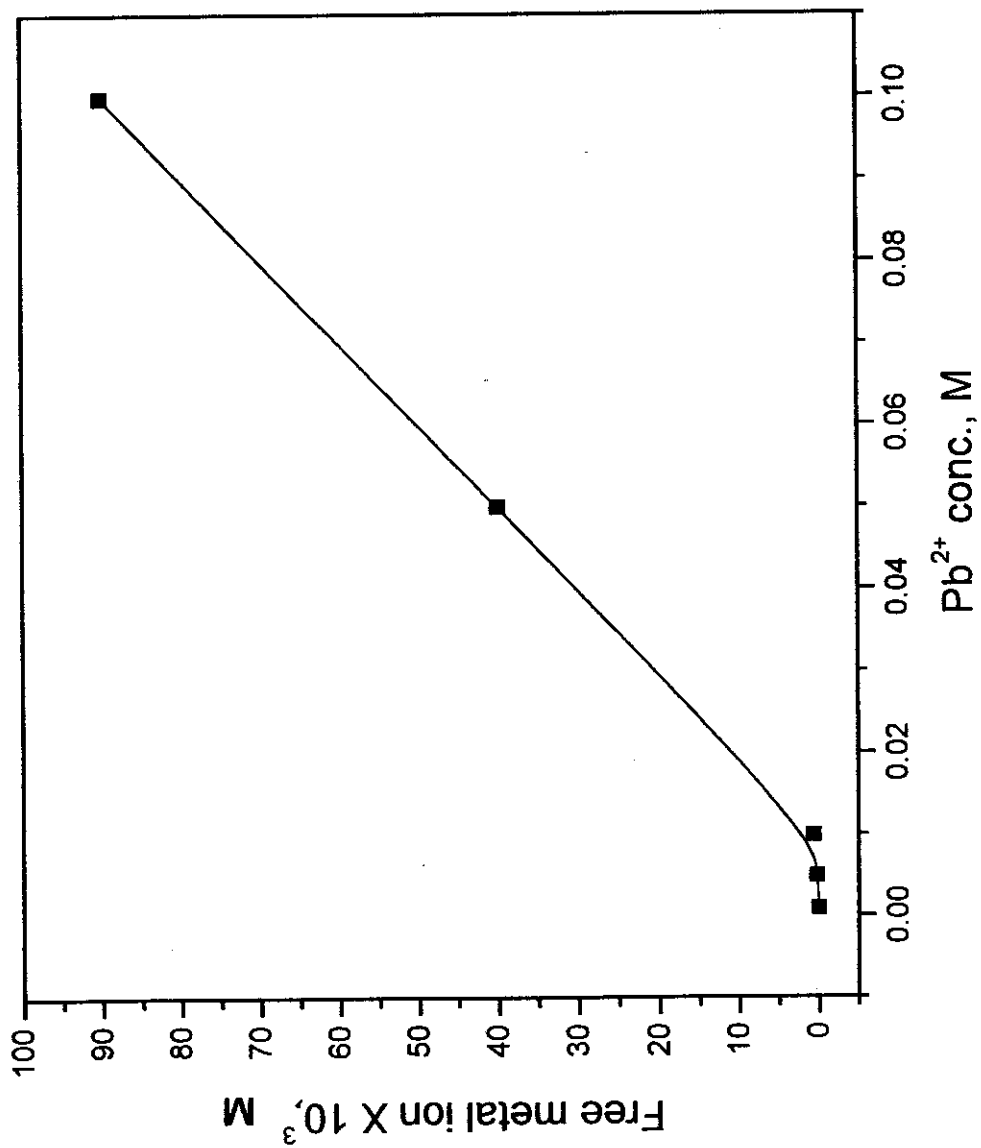


Fig.(3.60): Effect of shaking time on the sorption of  $Pb^{2+}$  by humin, at pH 5.8.



Fig(3.61): Effect of metal ion concentration on the sorption of  $Pb^{2+}$  by humin, at pH 5.8.

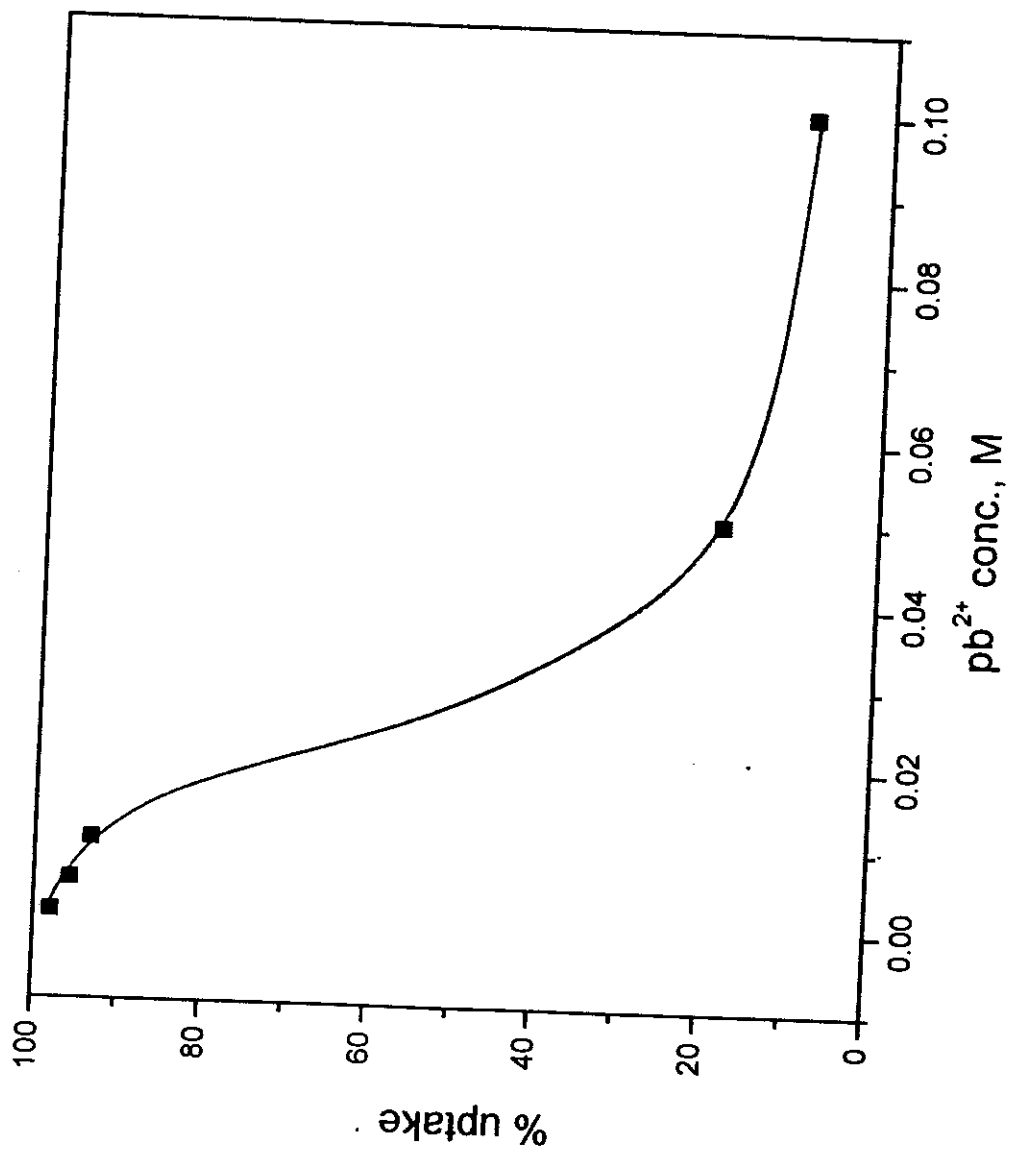


Fig.(3.62): Effect of lead concentration on the sorption of  $Pb^{2+}$  by humin at pH 5.8.

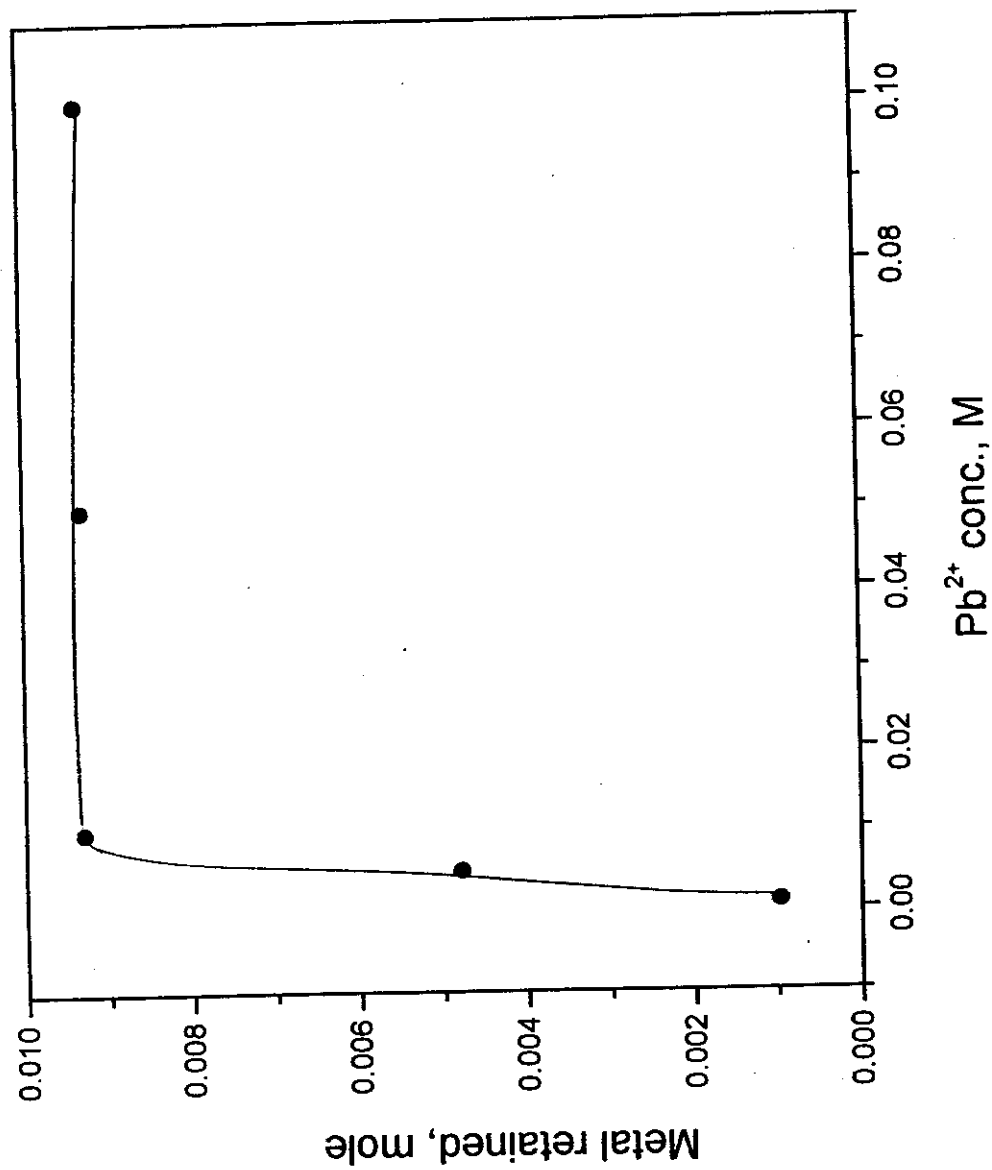


Fig.( 3.63): Variation of metal retained with Pb<sup>2+</sup> concentration, at pH 5.8.

#### 3.2.3.4) Effect of competing cations on lead-humate complex

The competition effect of  $^{137}\text{Cs}$ ,  $^{60}\text{Co}$  and  $^{(152,154)}\text{Eu}$  to  $\text{Pb}^{2+}$  on complexation with humic acid was investigated radiometrically after the formation of Pb-humate complex as carried out by ISE. As indicated in Figs.(3.64, 3.65),  $\text{Eu}^{3+}$  and  $\text{Co}^{2+}$ ,  $\text{Cs}^+$  have slightly competition effect on Pb-humate complex. As Fig. (3.64) shows, no competition effect at pH lower than 5 for  $\text{Cs}^+$  and  $\text{Co}^{2+}$ , and lower than 4 for  $\text{Eu}^{3+}$ .

#### 3.3) Disposal of radioactive waste by humic materials

Both humic acid and humin were used to evaluate the disposal of the radioisotopes  $^{137}\text{Cs}$ ,  $^{60}\text{Co}$  and  $^{(152,154)}\text{Eu}$  (as waste); either separately or in mixed form. The investigations were carried out at pH 6.5. It is clear from Figs. (3.66,3.67) that the addition of either humic acid or humin to the aqueous solution containing the radioisotopes decreases the radioactivity (cpm) by different values depending on the metal ion. The rate of decontamination is directly proportional to the valency of the investigated metal ion:  $\text{Cs}^+ < \text{Co}^{2+} < \text{Eu}^{3+}$ .

The solution is completely decontaminated from  $\text{Eu}^{3+}$  at a humic acid concentration of 0.3 g/l and at a humin weight of 0.4 g (in 10 ml solution). In case of  $\text{Co}^{2+}$ , the decontamination needed more ligands; 0.45 g/l for humic acid and 0.45 g for humin. However, the decontamination of  $\text{Cs}^+$  is weak in both cases.

The decontamination of mixed radioisotopes is illustrated in Figs.(3.68, 3.73). When humic acid was used for decontamination, the rate of decontamination, of  $\text{Cs}^+$  is increased in presence of  $\text{Eu}^{3+}$ , and to a lesser extent in presence of  $\text{Co}^{2+}$ , because of coprecipitation. In case of  $\text{Co}^{2+}$ , the presence of either  $\text{Cs}^+$  or  $\text{Eu}^{3+}$  slightly decreases the rate of decontamination. The same behaviour is noted in case of  $\text{Eu}^{3+}$ , but with higher extent than  $\text{Co}^{2+}$ . The use of mixture containing the three radioisotopes showed a retreating in the rate of decontamination, as compared to the mixtures of two nuclides only. This retreat is probably

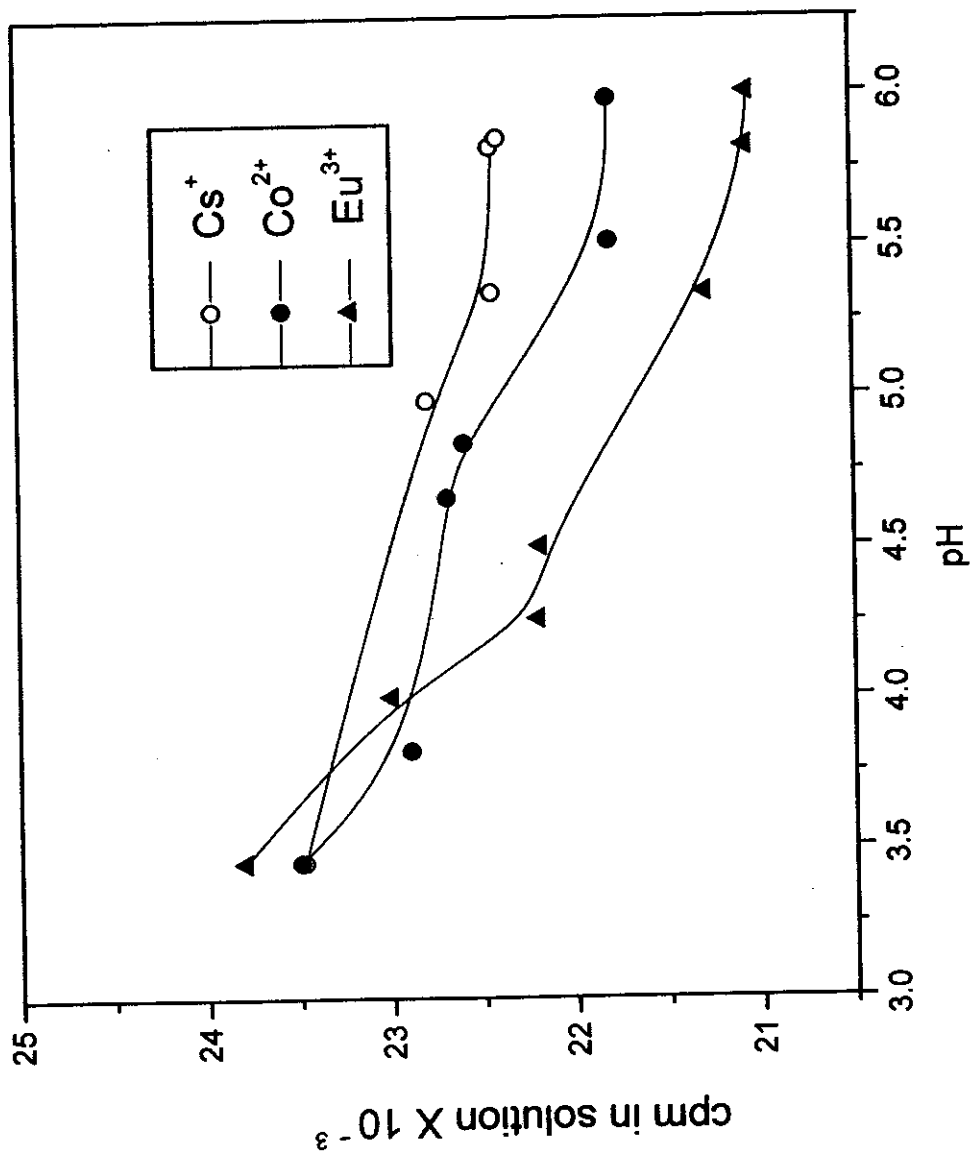


Fig (3.64): Effect of pH on the competition of  $\text{Cs}^+$ ,  $\text{Co}^{2+}$  and  $\text{Eu}^{3+}$  with  $\text{Pb}^{2+}$  on complexation with humic acid.

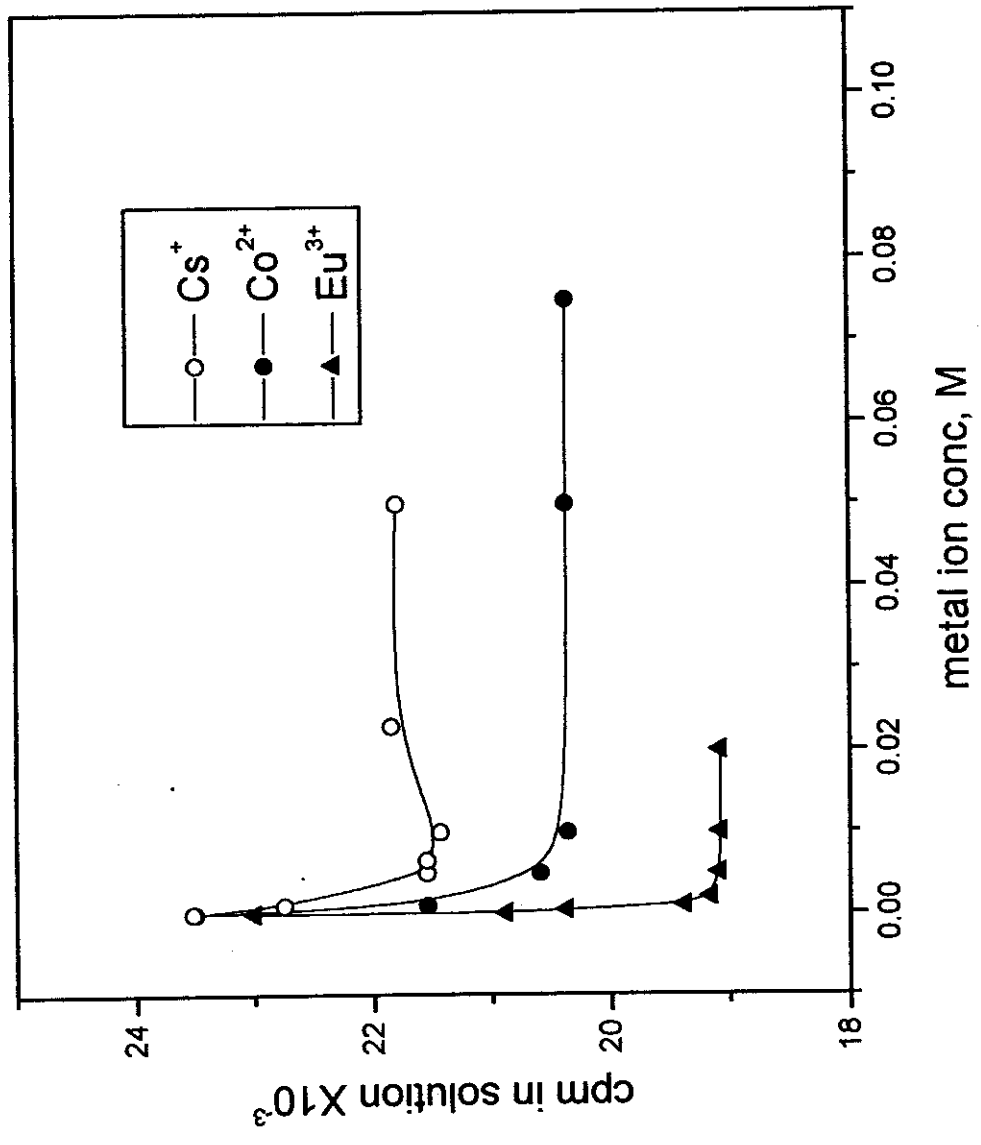


Fig (3.65): Effect of metal ion concentration on the competition of Cs<sup>+</sup>, Co<sup>2+</sup> and Eu<sup>3+</sup> with Pb<sup>2+</sup> on complexation with humic acid.

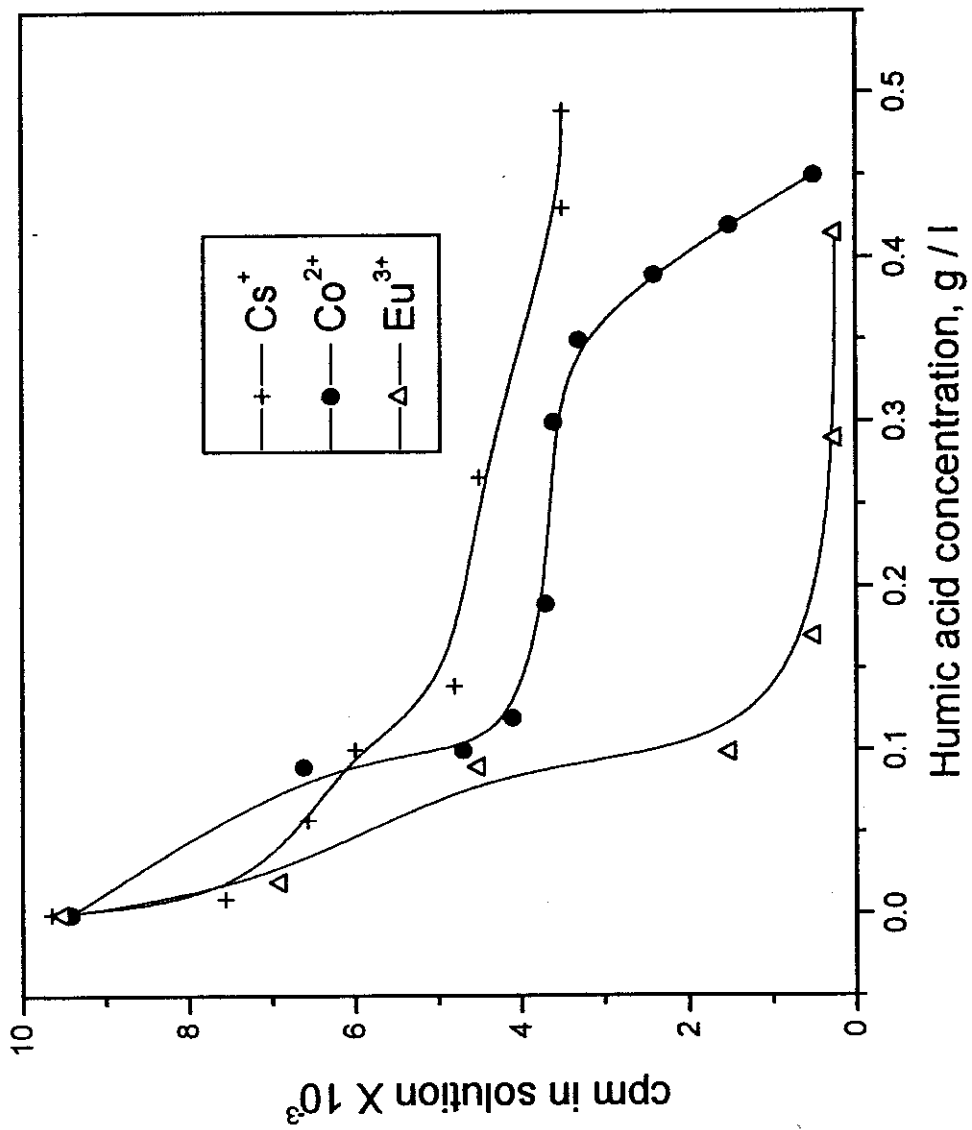


Fig (3.66): Effect of humic acid concentration on the decontamination of radioisotopes at pH 6.5.



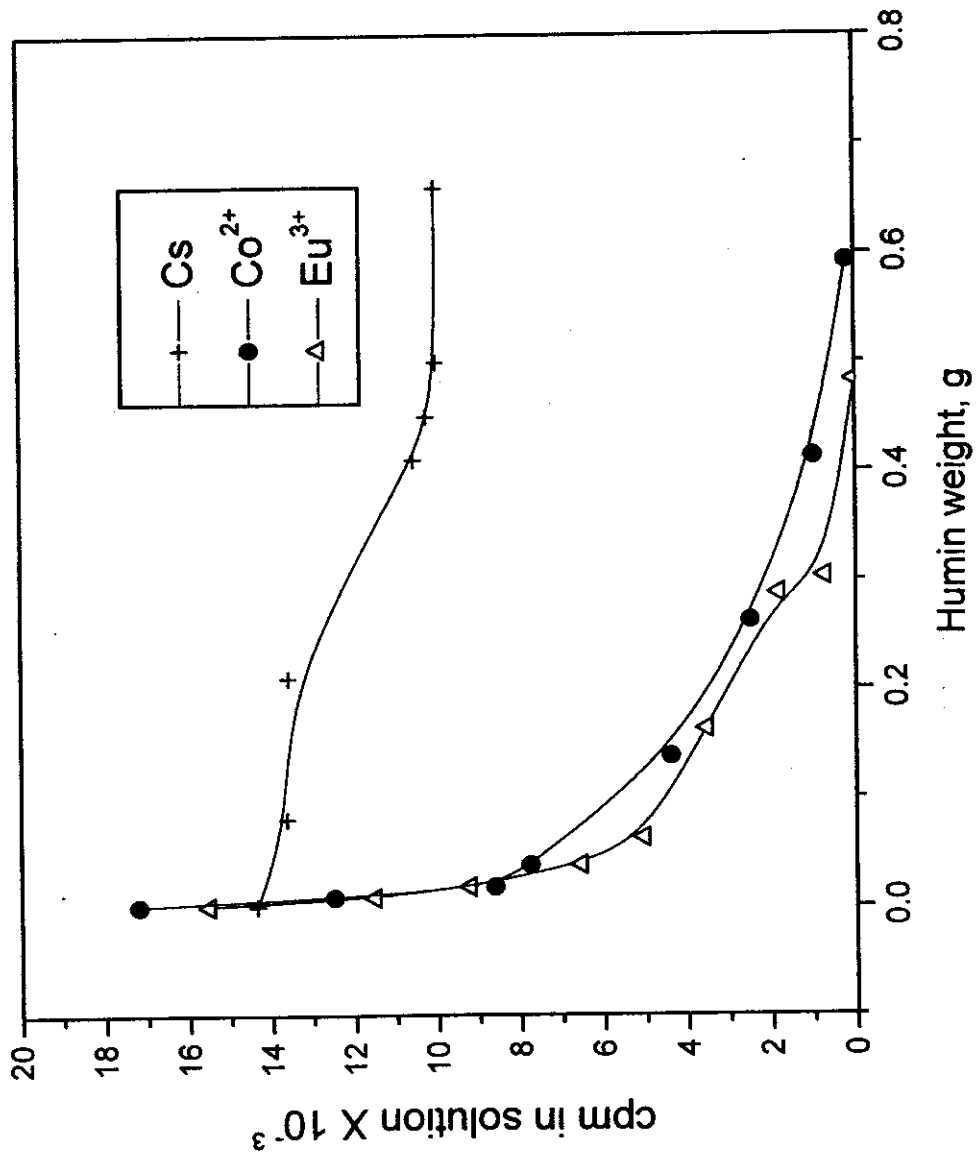


Fig (3.67): Effect of humin weight on the decontamination of radioisotopes at pH 6.5

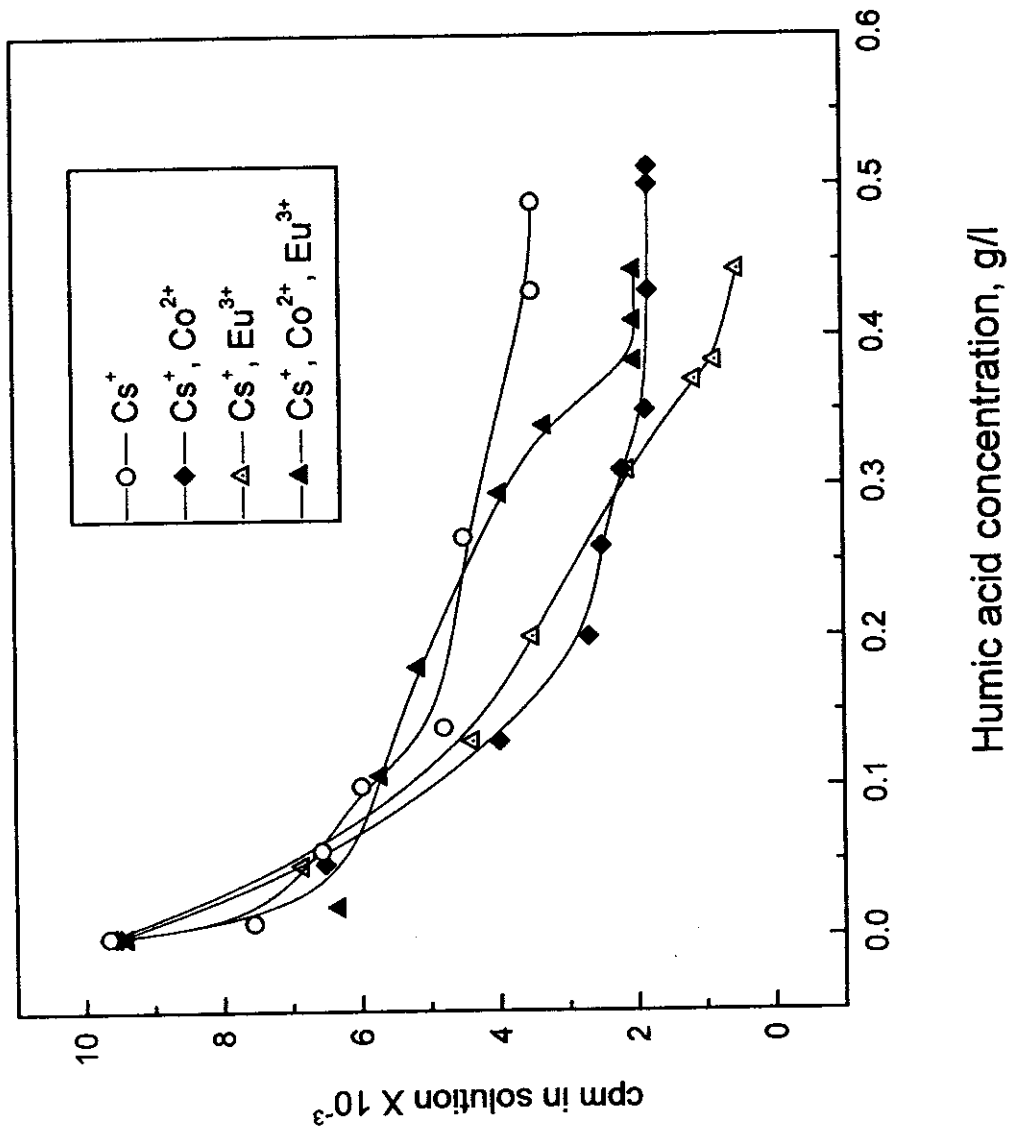


Fig (3.68): Effect of humic acid concentration on the decontamination of mixed radioisotopes at pH 6.5.

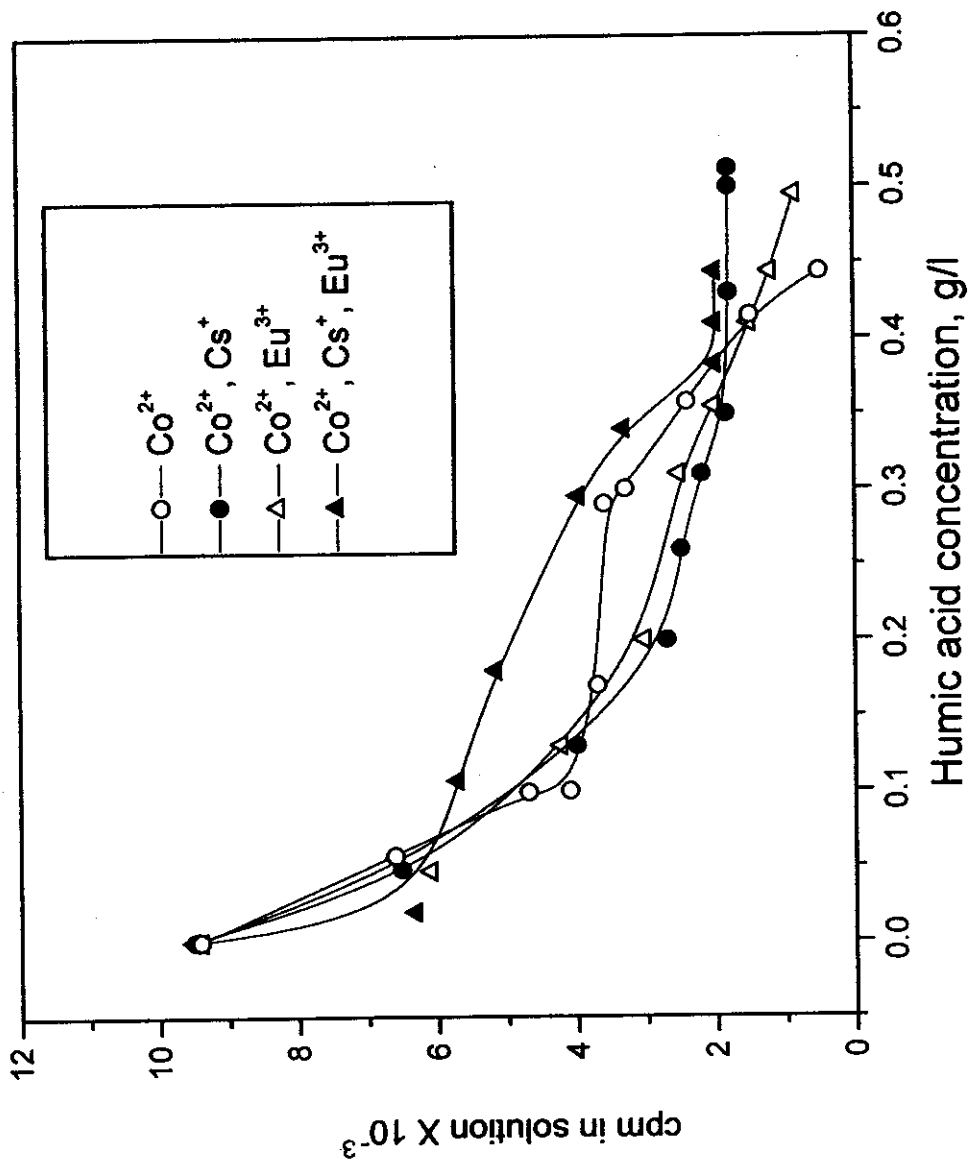


Fig (3.69): Effect of humic acid concentration on the decontamination of mixed radioisotopes, at pH 6.5.

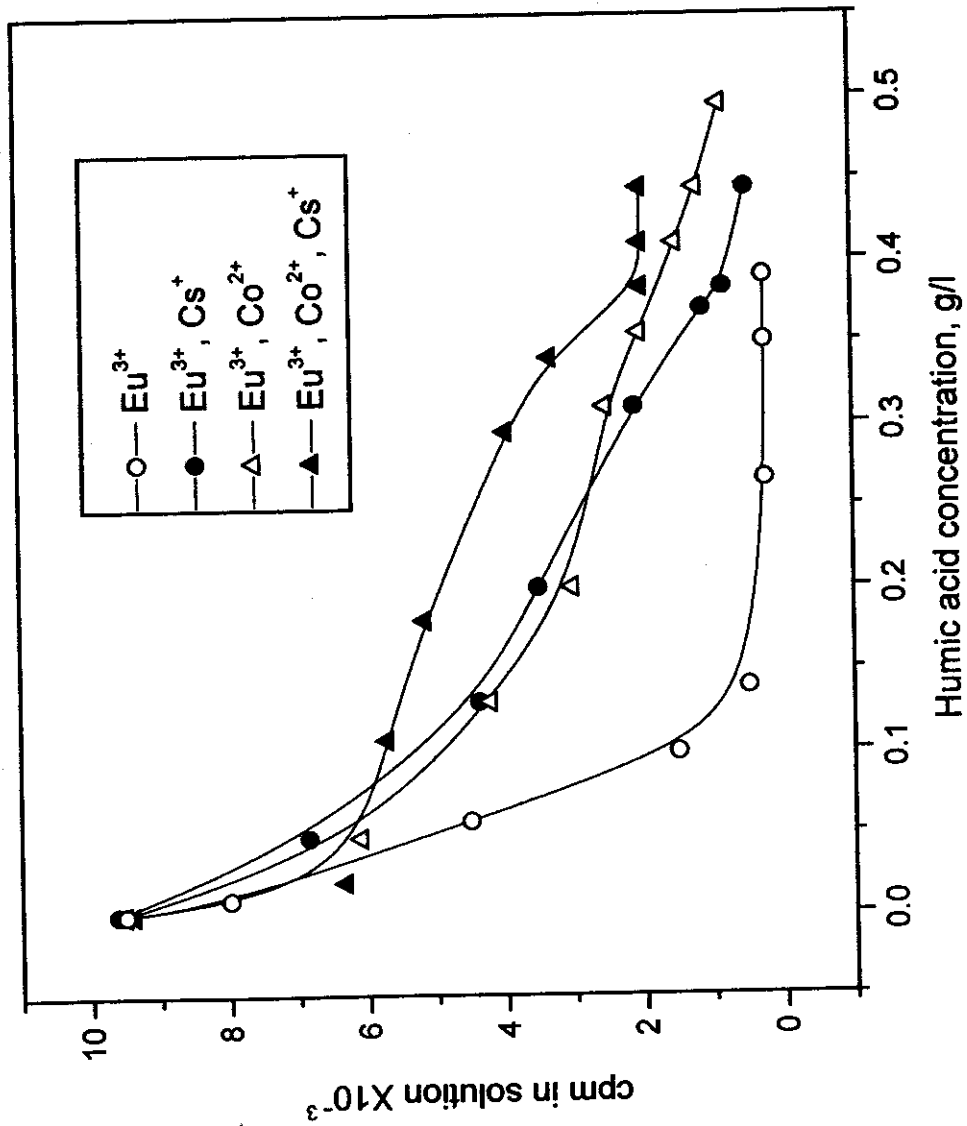


Fig (3.70): Effect of humic acid concentration on the decontamination of mixed radioisotopes, at pH 6.5.

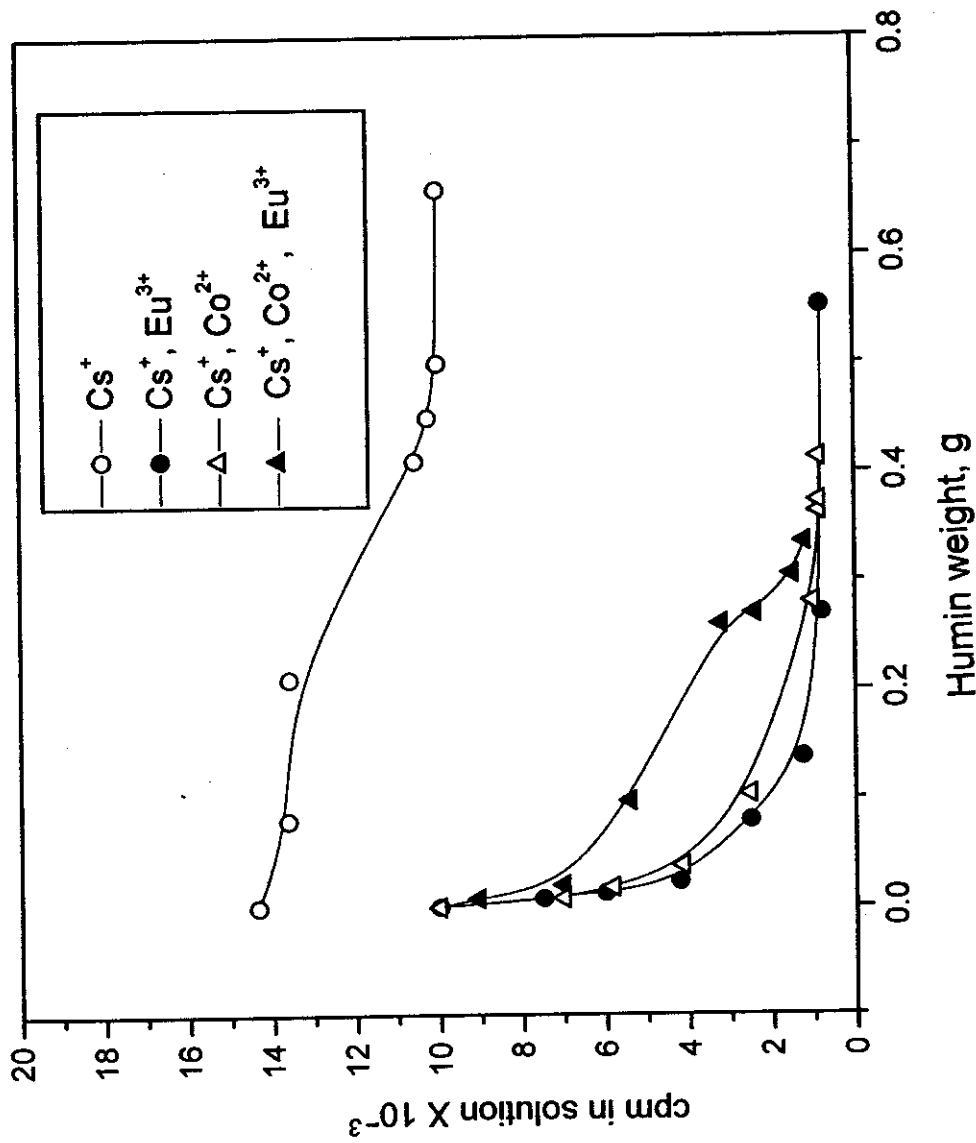


Fig. (3.71): Effect of humin weight on the decontamination of mixed radionuclides, at pH 6.5.

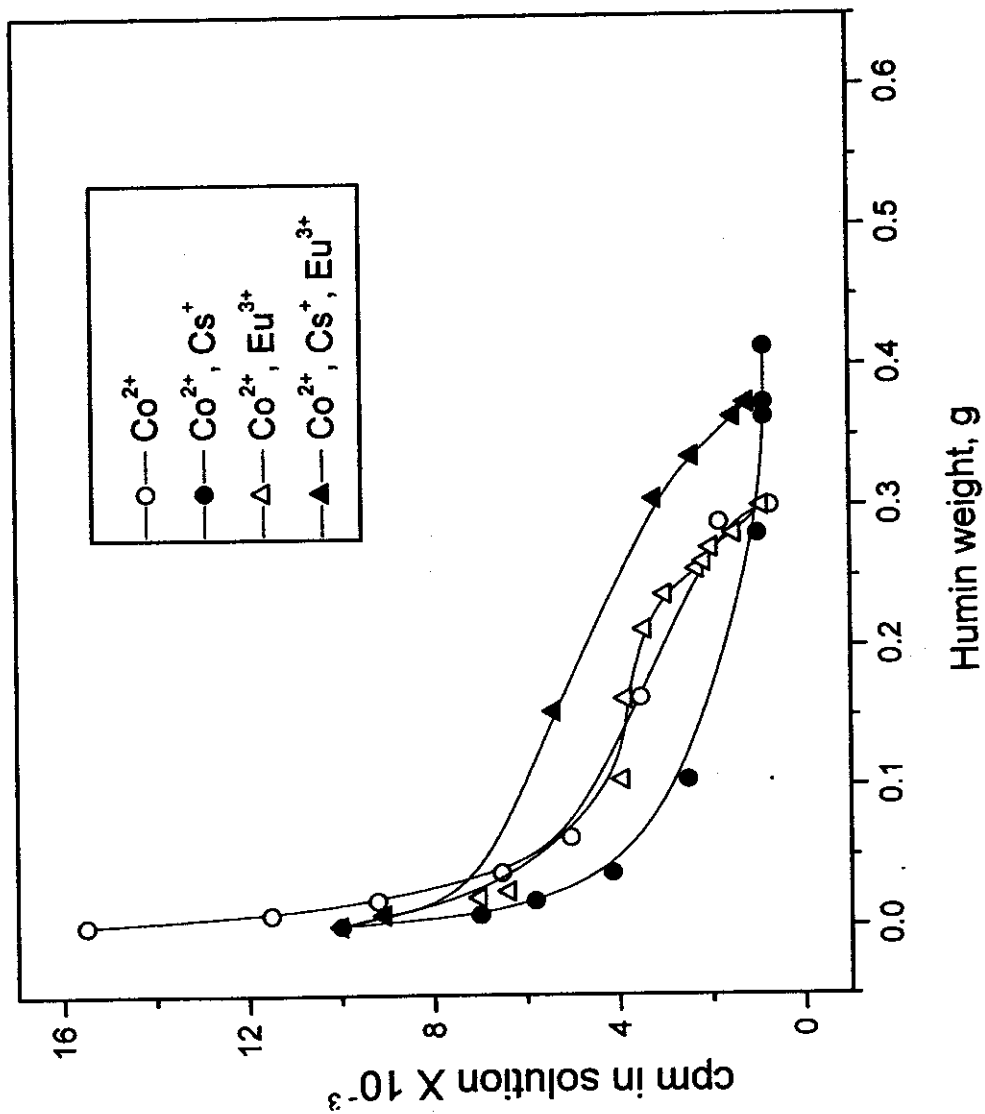


Fig (3.72): Effect of humin weight on the decontamination of mixed radioisotopes at pH 6.5.

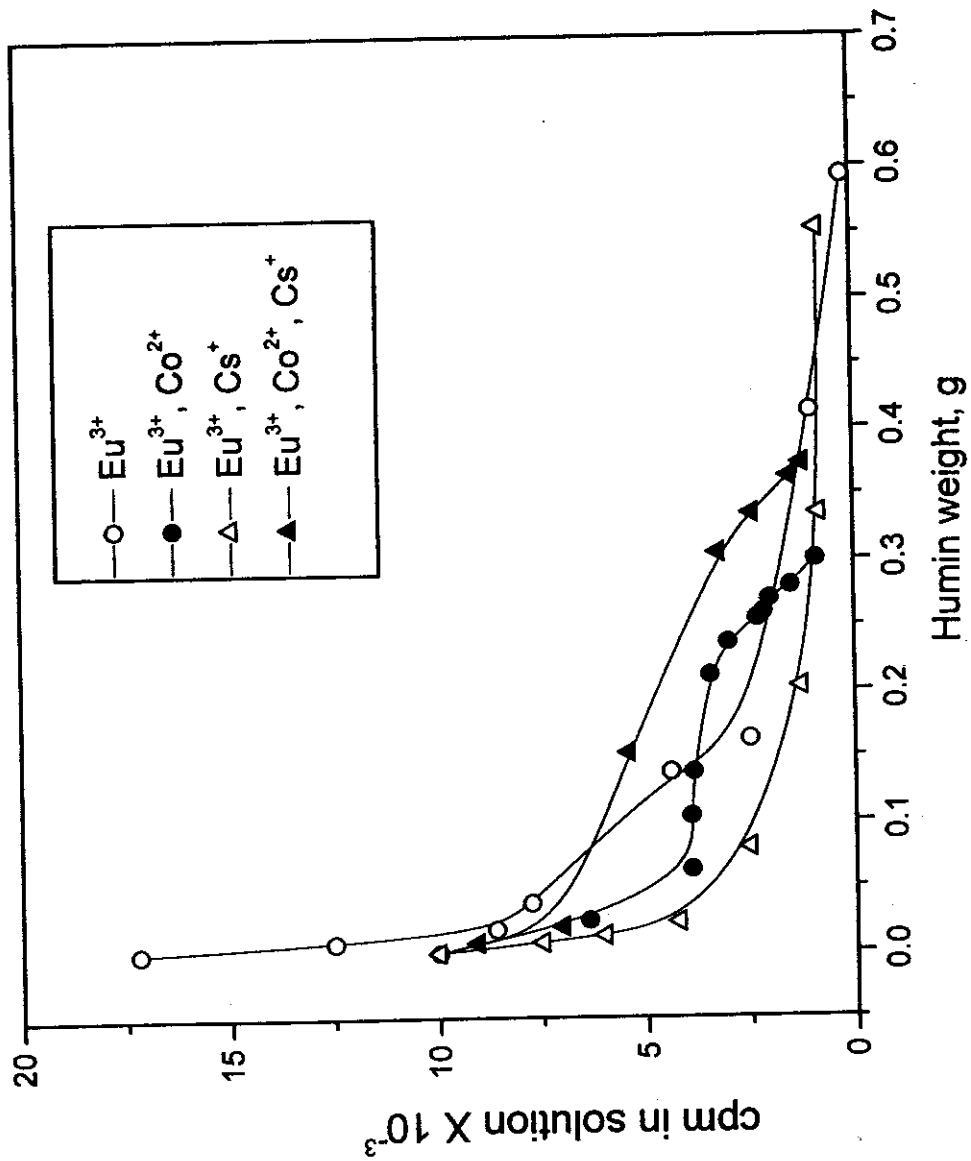


Fig (3.73): Effect of humin weight on the decontamination of mixed radioisotopes, at pH 6.5.

due to the competition effect for the active sites in the humic acid molecules; where  $\text{Cs}^+$  is driven away.

As the concentration of humic acid increases, the active sites increase and the rate of decontamination approaches that of the two nuclides. The use of humin for decontamination showed similar behaviour with higher rate of decontamination for the mixtures that containing two or three nuclides, as compared to humic acid. It is clear that humin is more competent for disposal of radioactive waste containing different nuclides, although humic acid has higher affinity for separate isotopes. A comparison between humic acid and humin for the affinity to each nuclide is illustrated in Figs. (3.74. 3.76).



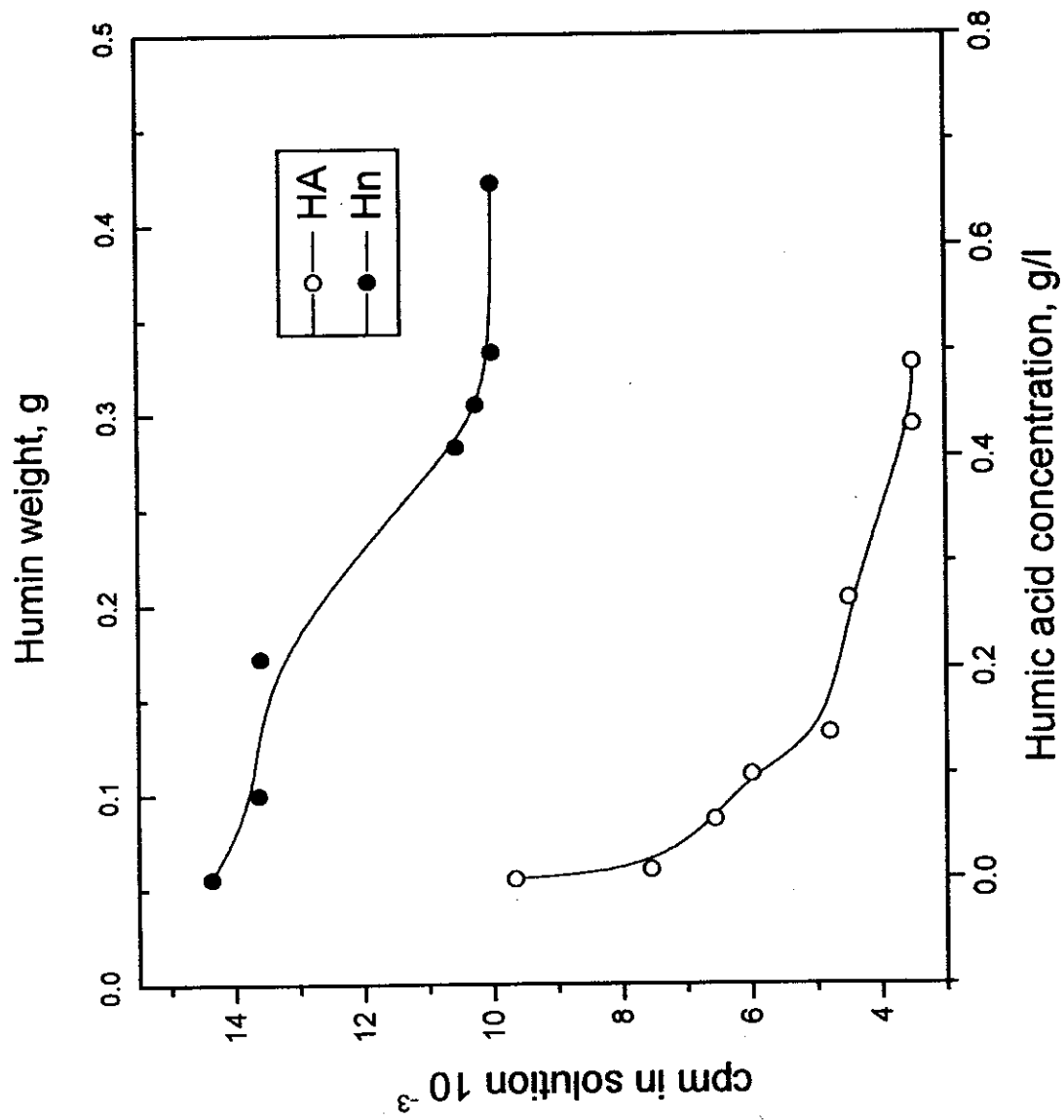


Fig. (3.74): Effect of ligand kind on the decontamination of radiocesium at pH 6.5.

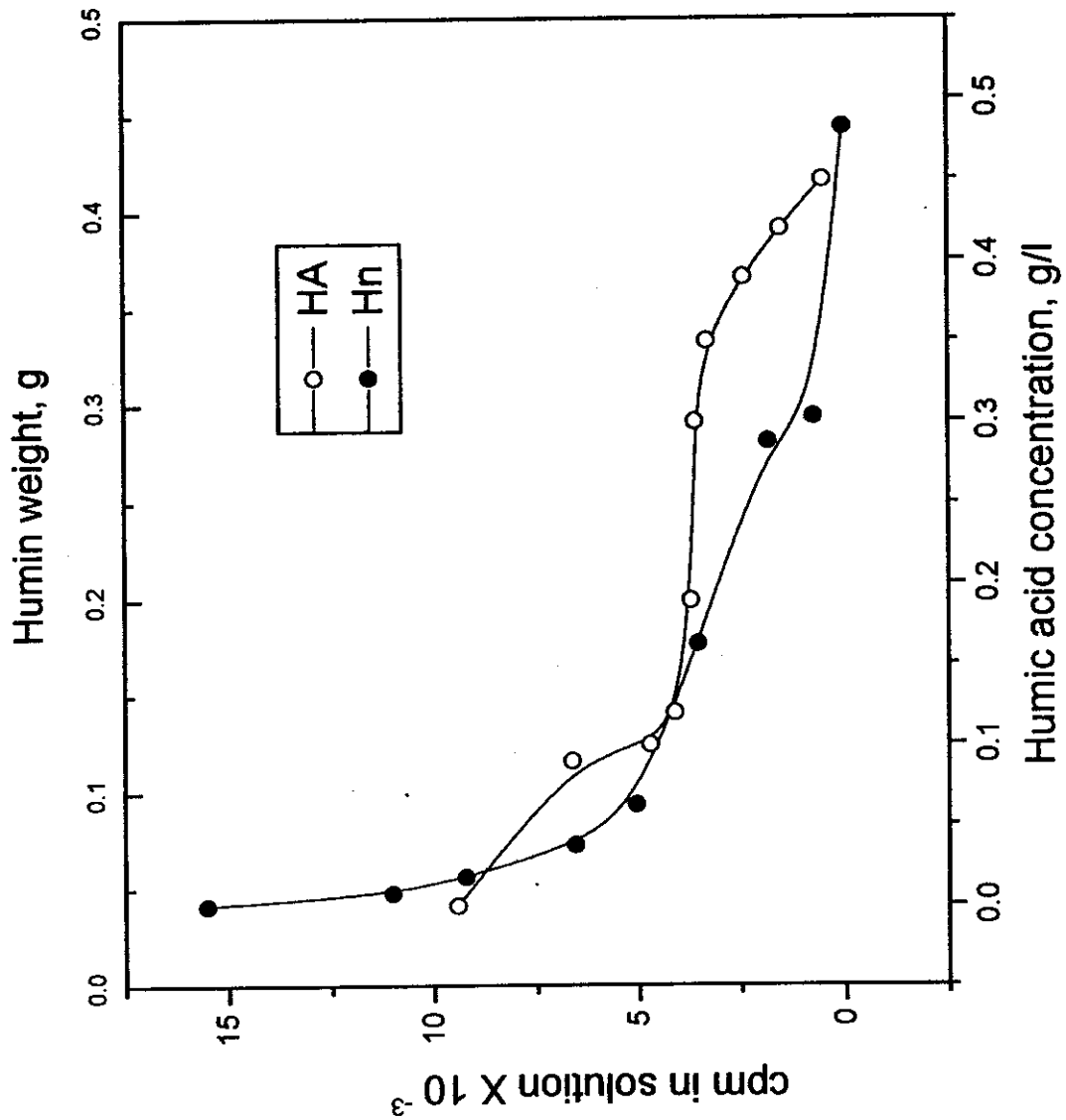


Fig. (3.75): Effect of ligand kind on the decontamination of radiocobalt at pH 6.5.

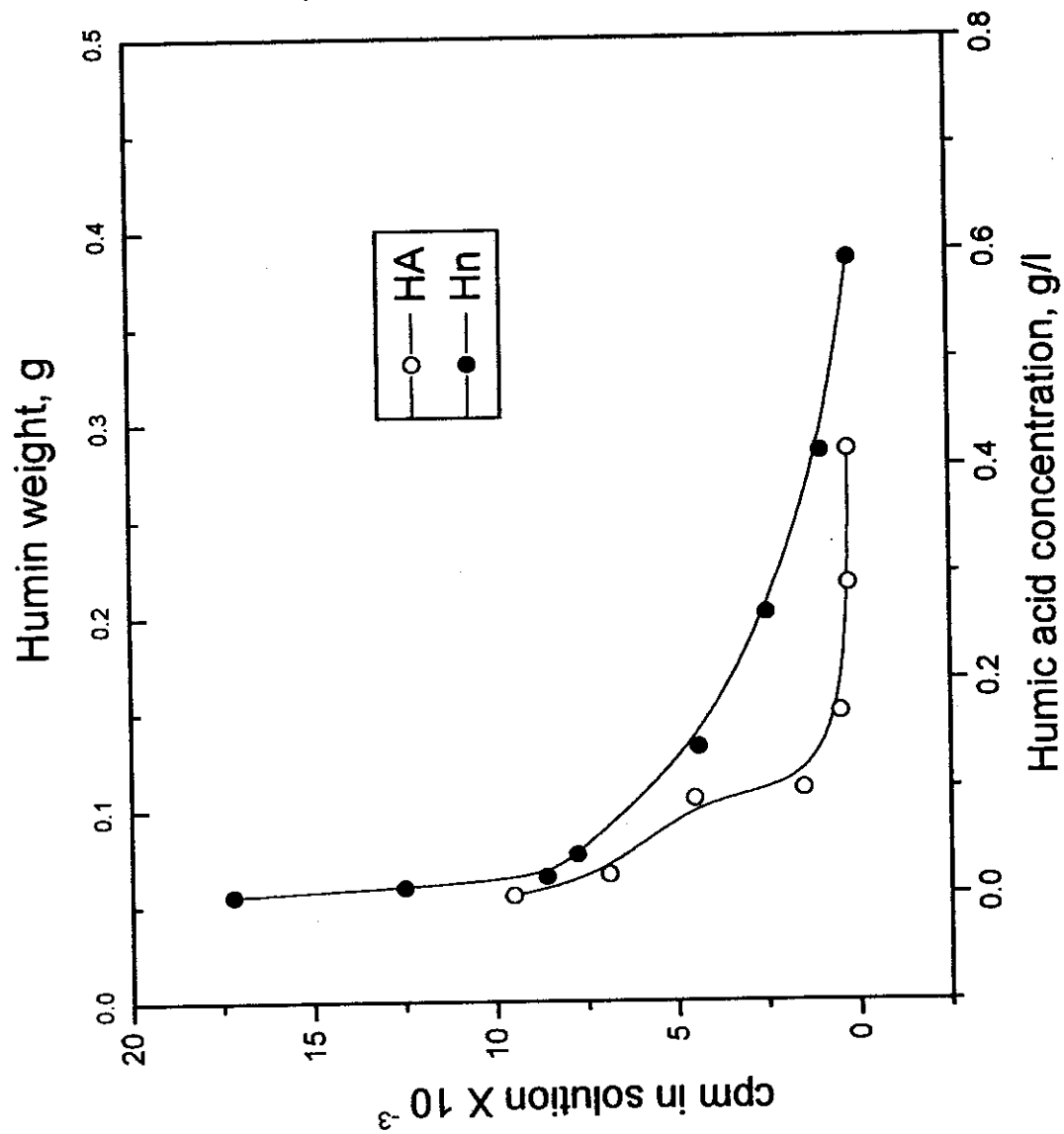


Fig. (3.76): Effect of ligand kind on the decontamination of radioeuropium at pH 6.5